MARKERS OF OXIDATIVE STRESS AND MATURE RED BLOOD CELL MIRNOME IN CATS WITH DIABETES MELLITUS

by

Deshuillers Pierre Lucien

A Dissertation

Submitted to the Faculty of Purdue University

In Partial Fulfillment of the Requirements for the degree of

Doctor of Philosophy

Department of Comparative Pathobiology

West Lafayette, Indiana

December 2018

THE PURDUE UNIVERSITY GRADUATE SCHOOL
STATEMENT OF COMMITTEE APPROVAL

Dr. Joanne B. Messick, Chair

Department of Comparative Pathobiology

Dr. Lynne F. Guptill

Department of Veterinary Clinical Sciences

Dr. Andrea Kasinski

Department of Biological Sciences

Dr. Harm HogenEsch

Department of Veterinary Administration / Department of Comparative Pathobiology

Approved by:

Dr. Narayanan

Head of the Graduate Program

A mes parents, Jacques et Jacqueline, ma grand-mère Simone, ma tante Jocelyne, ma sœur Marie-Anne et Fred pour leur patience et leur soutien. Sans vous je ne serai pas là où je suis aujourd'hui.

ACKNOWLEDGMENTS

To Dr. Joanne B. Messick, many thanks for your mentoring during my clinical pathology residency and during this PhD research. You have taught me so much during these years.
I would like to thank the rest of my PhD committee, Dr. Guptill, Dr. Kasinski and Dr. HogenEsch for their time, patience as well as for their insightful comments and suggestions.

This PhD would not have been possible without the help of the Morris Animal Foundation, the Purdue University Department of Comparative Pathobiology, Purdue University College of Veterinary Medicine and the Andrews Fellowship. Thank you for your support.

To the entire clinical pathology team at Purdue. My eternal thanks for being mentors, colleagues and friends during my residency and PhD. It has been a blast working with you all! (pun intended)

My sincere thanks also to my three surrogate mothers and friends at Purdue, Lisa, Barbara and Tammie who took care of me; my pottery friends for all the fun times playing with mud; and my friends, Kathy, Ellen and Katrina for their help.

TABLE OF CONTENTS

LIST OF TABLES

LIST OF FIGURES

ABSTRACT

Author: Deshuillers, Pierre L. PhD
Institution: Purdue University
Degree Received: December 2018
Title: Markers of Oxidative Stress and Mature Red Blood Cell miRNome in Cats with Diabetes Mellitus
Committee Chair: Joanne B. Messick

Despite previously accepted dogma, several recently published studies in humans and mice have shown that mature red blood cells (RBCs) contain a pool of microRNAs. Their role is currently uncertain; however, it has been suggested that microRNAs may play a role in cellular communications as they can be transferred from the RBC to endothelial cells or other cells. This thesis investigated the set of differentially abundant microRNAs found in mature RBCs of felines with oxidative stress, using diabetes mellitus as an oxidant stressor. We postulated that individual microRNAs identified in this study, might be valuable targets for future studies, investigating the role specific microRNAs play in the development or progression of diabetes and in the oxidative damage inflicted on the red cell and other cells by this disease.

The first specific objective of this thesis was to document oxidative stress in diabetic cats. In the absence of validated assays to document the presence of oxidative protein damage in felines, we first evaluated the performance of a commonly used colorimetric assay for measurement of protein carbonyls (PC) in serum and plasma. Although within run variation was acceptable and performed well over a wide range of PC content values, there were severe limitations related to excessive between run-variation, hemoglobin interference, and difficulty of assay performance. Therefore, we developed and validated a new method, using a fluorescent probe. This new assay had good within and between-run variations, a broad analytical range, and was easy and rapid to run. Hemoglobin and triglyceride only affected the results when present at moderate to higher

levels. To further evaluate their redox status, free-radical production and oxidative stress were measured in diabetic and healthy, control cats. The presence of oxidative stress was assessed by measurement of the resulting damage to biomolecules, and detection of antioxidant levels. Our data indicated the presence of protein and membrane lipid oxidation in diabetic individuals and suggest that the redox status of the mature RBC was shifted toward an oxidation state.

In the final chapter of this thesis, we document the presence of an abundant and diverse set of microRNAs in the mature erythrocytes of healthy and diabetic cats. While their function in the mature erythrocyte remains unknown, a difference was found in the microRNA expression patterns of diabetic and healthy cats. Our data uncovered severe bias in the microRNA sequencing such that the expression levels of some microRNAs appeared to be artificially increased and other diminished. The library construction kit used, appeared to be the cause of this bias. Among the 899 erythrocyte microRNAs sequenced, 12 differentially abundant microRNAs were identified in diabetic cats, however only 6 were differentially abundant by RT-qPCR. Let-7b, miR-1692, miR-339, miR-486 and a feline specific microRNA were increased in mature RBCs of diabetic cats, while miR-451 was decreased.

In conclusion, we have shown that diabetic cats have evidence of significant systemic protein and lipid oxidation as well as erythrocytic oxidative stress. The new, fluorescent PC content assay developed and validated herein could serve as useful tool to better understand the role and consequence of oxidative stress in feline diabetes or other diseases and to monitor antioxidant treatment. Further, this test could be readily adapted for use in other domestic species. Additionally, we have shown that a set of erythrocytic microRNAs are differently abundant in diabetic in comparison to healthy cats. The significance of such changes is currently uncertain. It could represent adaptation of erythroid precursors to changes in their environment during

erythropoiesis and as such, these microRNAs may be useful biomarkers for altered hematopoiesis. If microRNAs play a role in communication between circulating mature RBCs and cells in their surroundings such as endothelial cells, the possibility that changes in their expression in this host cells may result in pathology is an intriguing possibility that need to be further explored.

CHAPTER 1. INTRODUCTION

1.1 Diabetes in cats

1.1.1 Definition and classifications of diabetes mellitus in veterinary medicine

Diabetes mellitus (DM) has been recognized in antique Egypt and India for more than 3500 years. The Greek term diabetes means “to pass through” and was first used in antique Greece to describe the excessive emission of urine. Mellitus in turn comes from Latin and means honey-sweet. Hence, diabetes mellitus referred to polyuria associated with glycosuria as observed in affected patients. Nowadays, authors agree to define DM as a syndrome characterized by hyperglycemia resulting from either a defect in insulin secretion, a decreased sensitivity of target tissues to insulin or both[1]. During most of the 20th century, the classification of DM has been based on the age of onset (juvenile vs adult). In 1979, a new three tiers classification was suggested by the National Diabetes Data Group, based on clinical signs and insulin requirements to prevent ketosis. This classification included the insulin-dependent DM, the noninsulin-independent DM and a third, less defined category, encompassing DM secondary to pancreatitis, endocrinopathies, drug administration, and other causes. Gestational diabetes and impaired glucose tolerance were classified separately. Toward the end of the 20th century, this classification was abandoned and slowly replaced by the designation as type 1 and type 2 diabetes. Type 1 and type 2 diabetes mellitus corresponded to insulin-dependent and insulin-independent DM, respectively. Recently, the American Diabetes Association proposed a new classification system, which included type 1 DM, type 2 DM, in addition to other types of DM, gestational DM and prediabetes [2]. This system is based on the cause of DM as well as the stage of the disease. DM begins with a subclinical phase in which normal glycemia is maintained, but beta cell (β cell) mass and function anomalies are present. As the disease progresses, glucose intolerance can be detected, and a diagnosis of pre-

diabetes made. With further progression, glucose intolerance worsens until the criteria for DM diagnosis are met. In the diabetic state, insulin therapy can be needed permanently, transiently or recurrently. The need for insulin therapy does not define the disease category. For instance, patients with type 2 DM are usually, initially, insulin-independent, but can progress to being insulin-dependent. As in humans, animals can present type 1, type 2 or other type of DM, as well as gestational DM and prediabetes; however, these types of DM are not all found in all species. In cats, type 2 DM is considered by far the predominant type of DM[1] with only infrequent cases of type 1 DM reported in this species[3,4].

1.1.2 Epidemiology of type 2 diabetes mellitus in cats

Published epidemiologic data on feline DM indicate that the prevalence has increased from 0.08% to 1.2% over the last 30 years[5]. Aging is considered a risk factor as the incidence of DM onset increases with age[5-7]. In a population of Swedish cats, the incidence of type 2 DM has been shown to increase after the age of 6 years, reaching a peak at 13 years of age[7]. The predisposition of males to DM is often reported in the literature, [5,8] but some studies have failed to demonstrate it [7]. Burmese, Russian Blue, Norwegian Forest, European Shorthair and Abyssinian cats are more susceptible to develop DM[6-8], suggesting a genetic predisposition. However, the genes associated with DM have yet to be described in cats.

1.1.3 Pathogenesis feline type 2 DM

1.1.3.1 Insulin-resistance

The pathogenesis of type 2 DM in cats remains elusive. It involves insulin resistance and β cell failure to secrete adequate amounts of insulin to maintain euglycemia. Insulin is secreted by pancreatic β cells in response to increasing glycemia. Pancreatic β cells express GLUT2 glucose transporters, facilitate the rapid uptake of glucose in β cells, regardless of the extracellular glucose

concentration. Once intracellular, glucose is phosphorylated to glucose-6-phosphate (G6P) by the glucokinase. Increased G6P during hyperglycemia induces ATP synthesis, which depolarizes β cells and insulin is subsequently secreted. When insulin binds to its receptor, adaptor molecules (insulin receptor substrate, IRS) are recruited and in turn activate protein kinases, resulting in the translocation of insulin-dependent glucose transporters (GLUT-4) to the cell surface, facilitating glucose entrance[9,10]. Several mechanisms for peripheral insulin resistance have been proposed that may be pertinent to the development of type 2 diabetes. These include deactivation and degradation of IRS under the influence of adipokines, inflammatory cytokines or oxidative stress, accelerated insulin degradation, mitochondrial dysfunction and endoplasmic reticulum stress[9]. In cats, weight gain has been associated with insulin resistance[11,12] and attention has been focused on adipokines, cytokines secreted by adipose tissue. One of these secretory proteins, adiponectin, is postulated to play a critical role in glucose metabolism in insulin sensitive tissues. Low levels of circulating adiponectin in mouse models of obesity and correlation with the development of insulin resistance have been demonstrated. It has been reported in cats with type 2 DM that leptin is increased, whereas adiponectin is decreased in relation to the body fat mass. However, no direct relationship has been demonstrated between leptin, adiponectin and diabetes mellitus in felines[12,13]. The role of inflammation in insulin-resistance in obese cats remains uncertain[14,15]. Although not all obese cats with insulin-resistance will progress to a diabetic state, obesity is a major risk factor accounting for a 4-fold increased risk of developing DM[16].

1.1.3.2 Diabetic mellitus state

When insulin-resistance is present, pancreatic islets β cells become hypertrophic and hyperplastic, and insulin secretion increases, in an attempt to achieve normoglycemia. A diabetic state is reached when β cells fail to secrete enough insulin to attain euglycemia resulting in chronic

hyperglycemia[17]. Several mechanisms leading to β cell failure have been considered: islet cell damage by glucose, lipids, reactive oxygen species (ROS), inflammatory cytokines or abnormal protein accumulation. In contrast to other cell types, β cells, have no protective mechanism against an excess uptake of nutrients, including glucose, as these cells must sense plasma glucose concentration to adapt the insulin secretion[10]. This can result in glucotoxicity and lipotoxicity, which refer to the harmful effects of high intracellular glucose and lipids on insulin secretion and β cell viability, an effect demonstrated *in vitro*[18]. A natural model of type 2 diabetes in cats failed to confirm lipotoxicity *in vivo*, whereas chronic glucose infusion induced decreased insulin secretion and β cell apoptosis, confirming the role of hyperglycemia in the development of this disease in cats[19]. This effect of glucose is likely linked to hyperglycemia-induced reticulum endoplasmic stress and misfolded protein response[20]. It is also suggested that oxidative stress may plays a pivotal role in decreased insulin secretion and β cell viability. Increased intracellular glucose accelerates glycolysis and oxidative phosphorylation, which in turn enhances mitochondrial membrane potential and ROS production. These ROS are responsible for cell damage and the superoxide anion generated by mitochondria activates uncoupling proteins (UCPs) to decrease mitochondria membrane potential. Under hyperglycemic conditions, ATP production by mitochondria is augmented and ATP opens a potassium ATP dependent calcium channel, resulting in β cell membrane depolarization and insulin secretion. When excess reactive oxygen species are produced, and UCPs are activated, glucose-stimulated β cell secretion of insulin is impaired[21]. Additionally, β cells are more susceptible than other cells to oxidative stress as they contain low levels of antioxidants and are more inclined to non-specific attacks of cellular components by ROS or production of advanced glycation end-products (AGE)[10,22].

Accumulation of the peptide hormone, amylin, also has been associated with β cell cytotoxicity. Amylin is synthesized, stored and co-secreted with insulin[23]. Within cells, amylin forms β sheets that are resistant to degradation and thus, it accumulates in islets cells, triggering the unfolded protein response of the endoplasmic reticulum. Although the first function of the unfolded protein response is to protect cells from further damages, it can also lead to cell membrane disruption and apoptosis, decreasing the insulin secretion capacity[24,25]. An increase in amyloid secretion and aggregation into fibrils also has been implicated in progressive destruction of β-cells. The implication of amyloid in the development of diabetes is still debated in cats. Amyloid deposits are observed in pancreas of diabetic cats and a relationship between the presence of amyloid and diabetes has been described[22]. However, other studies failed to show such correlation and did not find a significant difference between the amount of amyloid in pancreas of diabetic and healthy controls cats[26,27].

Finally, inflammation could play a role in the development of type 2 diabetes in cats. Increased fat mass changes the adipokine plasma profile. Leptin is a proinflammatory hormone while adiponectin is anti-inflammatory and in obesity, changes result in a pro-inflammatory state[28]. One human study has reported an improvement in β cell function when interleukin (IL) 1β receptor agonists were administered. In these patients, decreased doses of insulin were needed to achieve normoglycemia. In cats, no direct link has been established between adipokines and endocrine pancreas inflammation yet[29]. In addition to adipokines, AGE induce the secretion of inflammatory cytokines such as IL-1β, IL-6 and tumor necrosis factor α (TNF-α), which accelerate cell damages[30]. In felines, increased islet cell IL-1β expression and infiltration by lymphocytes has been reported as well as evidence of oxidative-related damage to β cells[22,27].

Decreased glucose intake by cells harboring insulin-dependent glucose transporters arise from the combination of insulin-resistance and decreased insulin secretion. The metabolism in these cells shifts from a glucose-based to an amino-acid and lipid-based metabolism through gluconeogenesis and lipolysis. Glycogenolysis and gluconeogenesis are simultaneously accelerated by the liver[31,32], which further exacerbates the accumulation of glucose in plasma and hyperglycemia. When glycemia exceeds the renal tubular glucose reabsorption, glucosuria is observed. The presence of excessive glucose in the renal tubules creates an osmotic diuresis and polyuria, compensated by polydipsia [33].

In contrast to humans, ketoacidosis in the cat is a relatively frequent complication of type 2 DM. It is recognized that the insulin-mediated suppression of lipolysis in adipose tissue is blunted in type 2 DM, which may represent an important mechanism in the progression to ketosis in diabetic cats. Free fatty acids are mobilized and used as a source of energy instead of glucose and degraded through β oxidation, which produces high quantities of ATP and NADH as well as acetyl-CoA. Acetyl-CoA utilization in the citric acid cycle is reduced because of decreased oxaloacetate, the Acetyl-CoA acceptor, and inhibition of the reactions by ATP and NADH. Therefore, Acetyl-CoA is directed towards ketogenesis and the formation of ketones, acetoacetate, acetone and/or β-hydroxybutyrate. These ketone bodies are freely filtered by glomeruli[33] and appear in the urine.

1.1.4 Clinical signs of diabetes mellitus in cats

In almost all diabetic individuals, clinical signs are similar. They include polyuria, polydipsia, polyphagia and weight loss. Lethargy, decreased interactions, and poor coat grooming can also be observed. Progression from onset of diabetes to ketoacidosis is unpredictable and can appear in days to months when diabetes remains untreated [33].

In cats, a plantigrade posture can be observed and indicates a diabetic polyneuropathy from decreased nerve conduction. Less frequently, a palmigrade stance, posterior paresis and postural reaction deficits or decreased patellar reflexes can also point to a diabetic neuropathy [34]. Similar neuropathies are identified in 30 to 50% of all human diabetic patients, and animal models of diabetic neuropathies are lacking [34]. Although the origin of this neuropathy is unknown in cats, AGE and oxidative stress have been implicated in people and animal models[35].

Diabetic retinopathy is described in cats and people with a poorly controlled glycemia. Lesions include microaneurysms, intraretinal hemorrhages, capillary plugging and neovascularization [34]. Again, the mechanisms in cats are not well documented. However, advanced glycation signaling through the AGE receptor (RAGE), along with reactive oxygen species, are likely the cause of microvascular changes seen in the eyes and other organs of diabetic patients[35].

1.1.5 Diagnosis of diabetes mellitus in cats

Diabetes mellitus is diagnosed in cats based on the presence of clinical signs (polyuria, polydipsia, polyphagia, weight loss) in addition to persistent fasting hyperglycemia, and glycosuria. Detection of ketones in urines confirms a ketoacidotic state. A transient hyperglycemia and glucosuria can occur in cats if the animal is stressed. Hence, documenting persistent hyperglycemia and glucosuria can be challenging. The presence of an increased serum fructosamine concentration can be used to support a sustained hyperglycemia [33,36]. Since fructosamine formation results from the non-enzymatic linking of glucose to plasma proteins, principally albumin, serum fructosamine concentration is correlated with the magnitude and duration of hyperglycemia[37]. Fructosamine half-life is considered to be two to three weeks and is thought to represent the mean plasma glucose from the previous two to three weeks[36,37].

On a peripheral blood smear, evidence of oxidative damage to red blood cell hemoglobin and membrane (Heinz bodies) may be detected in diabetic cats, especially when there is a concurrent ketoacidosis [38-40]. The mechanisms involved in the formation of Heinz bodies in diabetic cats is not well understood, however several mechanisms have been suggested. They might result from the total body depletion in phosphorus, which is often seen in diabetes. The decreased availability of intra-erythrocytic phosphate results in reduced formation of glucose-6-phosphate and subsequently, decreased NADPH production. NADPH is necessary to maintain glutathione in its antioxidant, reduced form (GSH) [38]. On the other hand, it could be due to increased ROS formation, possibly by induction of the liver cytochrome P450 2E1 by ketosis [41]. Another possibility is the production of increased ROS by other tissues, which could then leak into the extracellular fluid, bathing red blood cells in an oxidant rich milieu.

The pathogenesis of feline diabetes, as we currently understand it, is very similar to the pathogenesis of type 2 diabetes and complications of this disease in people. Hence, feline could be considered as a natural model for human type 2 diabetes. Oxidative stress appears to play a major role in the pathogenesis of diabetes mellitus in people and is also a likely culprit in the cat. The mechanisms for increased ROS formation and the methods to test the presence of oxidative stress are reviewed below.

1.2 Oxidative stress in cats with type 2 diabetes mellitus

1.2.1 Discovery of reactive oxygen species, antioxidants and definitions

Free radicals are uncharged molecules that are electron deficient, having an unpaired electron in its outermost orbital. They were first described by Moses Gomberg in 1900 [42], but descriptions in biological materials, animal and plant tissues was not found until 1954 [43]. In the latter study, Commoners *et al*. compared etiolated and normal leaves, showing that the quantity of

free radicals was proportional to the tissue metabolism. Thereafter, free radicals were recognized as potentially deleterious molecules and because of their high potential to react with a variety of other biological molecules, they were linked to the development and progression of various diseases. Free radicals were subsequently shown also to be involved in antibacterial defense by inflammatory cells [44,45], relaxation signaling of the endothelium [46] and mitochondrial energy production [47].

Following the discovery of free radicals in biological materials, mechanisms to defend against their deleterious effects were identified. The first enzymes described with anti-free radical activity were isolated from bovine red blood cells and liver [48] and later from human red blood cells [49,50]. They were named, hemocuprein and erythrocuprein, respectively. Sharing a similar function, they catalyzed the dismutation of superoxide ions in the presence of protons, into dioxygen and hydrogen peroxide. Based on its anti-radical activity, this enzyme was named superoxide dismutase (SOD) [51].

Although the term "free radical" has been used since their first discovery, this is not the most appropriate term to designate the family of compounds responsible for oxidative damage to biological elements. In fact, all molecules causing oxidative damage are not free radical and a more appropriate term, now widely accepted is reactive oxygen species (ROS). ROS are unstable oxygen containing compounds, either free radicals, unstable non-radical compounds (such as hydrogen peroxide) or compounds containing an oxygen atom in an excited state (singlet molecular oxygen or excited carbonyl). They share a short lifespan due to high reactivity with other molecules[52].

The concept of oxidative stress was first introduced in biology in 1985 by Sies [52]. Its definition relies on the concept that ROS are produced during cell metabolism and most of them are neutralized by antioxidant mechanisms. However, when there is a disturbance in the pro-

oxidant-antioxidant balance in the favor of the pro-oxidant state, ROS escape antioxidant mechanisms and can react with cellular components. These cellular components can then be repaired or removed.

1.2.2 Oxidative stress in diabetes

1.2.2.1 Increased generation of ROS

A multitude of cellular processes, resulting in increased production of ROS, have been described in diabetes. One of the most important and best understood is the production of ROS by mitochondria. Physiologically, reduced dinucleotide carriers, NADH and $FADH_2$ transfer electrons from the citric acid cycle to the electron transfer complexes I and II located in the inner membrane of the mitochondria. The transfer of electrons along the mitochondrial membrane complexes creates a proton gradient and a membrane potential across the inner membrane used for the generation of ATP by the ATP synthase. This electron transfer is driven by the final electron acceptor, dioxygen which is normally reduced to two molecules of water[53,54]. Although superoxide anions can be generated at almost every step of the electron transfer chain if dioxygen is available, two sites are more susceptible to inadequate dioxygen reduction: the NADH reductase and the ubiquinone complex[54]. These mechanisms have been demonstrated *in vitro* in a variety of cell types under hyperglycemic conditions, including β cells and endothelial cells which are both unable to regulate intracellular glucose concentration [55,56].

Glucose autoxidation has also been suggested has a major source of ROS in diabetes; yet limited evidence have been published. Autoxidation occurs in the presence of transition metals such as iron, particularly abundant in red blood cells, manganese or copper and result in the production of superoxide anions, hydrogen peroxide and hydroxyl radical. This mechanism has been documented *in vitro* only, in endothelial cells[57,58].

Advanced glycation end-products have also emerged as a major cause of ROS and are suspected of being major contributors to diabetic complications. Glycation is a non-enzymatic reaction occurring between a reducing sugar, such as glucose or fructose, and a free amino group of proteins. It first forms an unstable intermediate, Schiff base which undergoes rearrangement to a more stable compound called amadori product. The amadori product is then degraded into a reactive dicarbonyl compound which yields advanced glycation end-products (AGE) after oxidation, dehydration or cyclization[35]. AGE can react with proteins to forms proteinase resistance protein aggregates, potentially triggering endoplasmic reticulum stress and the unfolded protein response. They are also involved in cell signaling and recognized by a receptor for advanced glycation end products (RAGE), a member of the immunoglobin superfamily, found on the cell surface. Upon ligand binding, RAGE can signal through different pathways, including JAK/STAT, PKC/PI3K/Akt, MAPK/Erk and Src/RhoA/Cdc42, which activate a variety of transcription factor such as NFκB[59]. In turn, NFκB induces the expression of NADPH oxidases (Nox) that are capable of generating ROS. Nox proteins are transmembrane proteins, first described in leukocytes, but subsequently reported in a variety of other cell types, including β cells and endothelial cells[60-63]. They are able to transfer electrons from FAD to molecular oxygen, generating superoxide anion[64], which can in turn activate NFκB in a positive feedback loop[65]. The involvement of RAGE signaling and Nox in diabetes has been reported in animal models of diabetes and in diabetic complications including neuropathies, retinopathies, nephropathies and cardiovascular disease[59,66]. To the best of our knowledge, AGE and RAGE signaling has not been studied in felines.

Other cellular processes that may result in increased production of ROS in diabetic patients have begun to emerge. These include the production of ROS by xanthine oxidoreductase and cytochrome p450 monooxygenases. In endothelial cells, xanthine oxidoreductase assumes several

roles. In its reduced state, it exhibits a dehydrogenase activity and oxidizes hypoxanthine to uric acid while reducing NAD^+ to $NDAH_2$. However, in its oxidized state, it exhibits an oxidase activity using dioxygen as electron acceptor and producing superoxide anion. This shift in the oxidoreduction activity of xanthine oxidoreductase increased ROS production under oxidative conditions[54,67,68]. Cytochrome p450 monooxygenases are a family of enzymes that catalyze the transfer of electrons from a variety of donors to a variety of substrates, using superoxide anion as an intermediate, which can lead to the release of ROS. In the presence of ketones, an increase in hepatic cytochrome 2B, 4A and 2E1 expression in diabetic patients, is speculated to be involved in the production of increased ROS[69-71].

1.2.2.2 Decreased antioxidant defenses

1.2.2.2.1 The glutathione system

To neutralize ROS, organisms and cells have evolved a multitude of antioxidant mechanisms. The actors of the antioxidant defenses either directly scavenge ROS or catalyze the formation of less reactive oxygen species from highly reactive ROS. In cells, the main antioxidant is the glutathione.

Glutathione is a tripeptide (γ-glutamyl-L-cysteine-L-glycine) synthesized *de novo* intracellularly or imported from plasma when synthesized by liver[72,73]. Additionally, red blood cells can export reduced glutathione (GSH) to plasma, contributing to the systemic antioxidant capacity of plasma[72-74]. GSH has a highly reactive sulfhydryl group that may act non-enzymatically as a free radical acceptor to counteract oxidant damage[73]. GSH can also reduce peroxides and modulate protein sulfhydryl group oxidation states. These reactions are catalyzed by a group of enzymes consisting of glutathione peroxidase (GPx), peroxiredoxine (Prx) and glutaredoxin (Grx). GSH can also react with electrophiles to yield glutathione conjugates and

temporarily protecting protein moieties most susceptible to oxidation. This reaction may be reversed under reducing conditions, restoring the protein function. These reactions are catalyzed by glutathione-S-transferase. Finally, GSH can regenerate reduced vitamin C, another antioxidant. This reaction is catalyzed by the dihydroascorbate reductase[75,76]. Physiologically, less than 1% of the intracellular glutathione is found in its oxidized form (GSSG) while the remaining is found in its reduced form (GSH). Reduction of GSSG to GSH is catalyzed by the glutathione reductase with NADPH as the electron donor[76]. In the red blood cells, GSH is constantly being oxidized but most GSH is maintained in its reduced form by the glutathione reductase reaction. RBC can increase metabolism through the pentose phosphate pathway (PPP) to provide the NADPH necessary for the regeneration of GSH[73]. RBC membranes are not permeable to GSH, but they are permeable to GSSG or glutathione-S-conjugates, which are exported from RBC using an ATP-dependent multidrug resistance proteins transporter. Transport of glutathione-S-conjugates happens at low concentration, whereas transport of GSSG outside of the red blood cells happens at high intraerythrocytic concentration. Regardless, the end result is that a pool of intracellular glutathione can be maintained for antioxidant defense and detoxification[77,78].

Being at the crossroads of antioxidant defenses, glutathione has received much attention in DM. In vitro studies have showed decreased GSH concentration in various cells under hyperglycemic condition. These included β cells, endothelial cells, renal cells, hepatocytes, as well as mature red blood cells and reticulocytes[79-86]. The cause for decreased cellular glutathione is not well understood, however it has been suggested that decreased synthesis or accumulation of the oxidized form of glutathione[80] may play a role. In cats, limited information is available. One previous study described a correlation between the presence of Heinz bodies (indicating systemic

oxidative stress in the red blood cells and increased plasma β-hydroxybutyrate with a decrease in the erythrocyte glutathione concentration[41].

1.2.2.2.2 Antioxidant enzymes

In addition to the glutathione antioxidant system, superoxide dismutase and catalase are two major effectors of cellular antioxidant defense. These two enzymes work conjointly to reduce superoxide to water. Superoxide dismutase (SOD) can be found in the cytoplasm (copper-zinc-SOD) and in mitochondria (manganese-SOD). Both types are also present in extracellular fluids, including plasma. [87]. While the manganese-SOD limits the amount of superoxide anion produced in the mitochondria, copper-zinc-SOD catalyzes the dismutation of superoxides that have leaked from the mitochondria or that have produced in the cytoplasm by other mechanisms. Both SODs function to dismutate two superoxide anions into one dioxygen molecule, available for oxidative phosphorylation, and hydrogen peroxide, which are less reactive than superoxide[73]. Hydrogen peroxide is then converted by catalase into water and dioxygen. The function of catalase is maintained by NADPH. Decreased cellular NADPH concentration and binding of $NADP^+$ to catalase results in the enzyme inactivation[73]. Conflicting data are reported for SOD and catalase in diabetes mellitus and thus, the role of both enzymes in this disease remains unclear[79,81,83,84,86,88-92]. Interestingly, one research team has reported an association between decreased catalase activity in red blood cells related to inherited hypocatalasemia or acatalasemia and diabetes mellitus[93-95]. SOD and catalase activity or expression has not been studied in diabetic cats.

1.2.2.2.3 Thioredoxin, glutaredoxins and peroxiredoxins

Thioredoxins (Trx), glutaredoxins (Grx) and peroxiredoxins (Prx) are three electron donors which have a similar active site containing two cysteines. These cysteines can be reduced (thiols) or oxidized (disulfide bond). With a high redox potential, Trx reduces protein sulfhydryl groups,

oxidized under oxidative conditions and can also regenerate oxidized Grx and Prx. The regeneration of Trx necessitates an electron transfer from NAPDH which is catalyzed by a Trx reductase. Under oxidative conditions, antioxidant enzymes can be damaged by ROS. Trx is able to reduce these enzymes and restore their antioxidant functions. Meanwhile, Grx are specialized in the deglutathionylation of protein-glutathione mixed disulfides, restoring protein functions[96,97]. Prx are also involved in ROS scavenging and are in comparison to Trx and Grx more easily oxidized. New functions have emerged for Trx and Prx. Both are oxidized at different levels of cellular oxidative stress, and they are involved in sensing, signaling and regulating the response of the cells to oxidative stress. [96,98]. Trxs, Grx and Prx have a protective role, as ROS scavengers. In β cells in diabetes, they improve insulin secretion and decreased β cell apoptosis[99-101]. The role of Trx in signaling in β cells has emerged only recently. In its reduced state, Trx binds to a Trx-interacting protein (TXNIP) and sequesters it to the cytoplasm or the mitochondria. When oxidative stress is present in β cells, TXNIP inhibits the reducing capacity of Trx, and the role of Trx in the antioxidant defense may not be as essential as first thought. It also induces apoptosis through activation of mitochondrial cytochrome c and caspase-3 cleavage and thus, may provide a link between glucotoxicity and β cell apoptosis. In β cells, TXNIP expression is strongly up-regulated in response to increased intracellular glucose and endoplasmic reticulum stress while FOXO transcription factors decrease its expression. [102]. TXNIP induces miR-204 expression which targets the 3' untranslated transcribed region (3'-UTR) of MafA, a transcription factor participating in insulin synthesis, resulting in decreased insulin synthesis and secretion[102]. In a murine model of type 2 diabetes, TXNIP-deficient mice were able to maintain adequate plasma glucose while reducing β cell apoptosis[103]. Recent data suggest that inhibition of β cell TXNIP

expression results in enhanced β cell survival and function and may prevent or improve overt diabetes. The role of Trx, Grx and Prx in feline diabetes or other conditions has not been studied.

1.2.2.2.4 Alpha tocopherol and ascorbate

Vitamin E (α-tocopherol) is a lipophilic electron donor able to reduce lipid peroxyl, resulting from ROS damage to cellular membranes. When ROS encounter cell membrane lipids containing one or several carbon-carbon double bonds, ROS capture a hydrogen atom forming a carbon centered lipid radical, which in turn initiates the generation of other radicals. Thus, lipid radicals may react with oxygen to form a lipid peroxyl radical, which then capture a hydrogen atom from a neighboring lipid, starting a chain reaction that will end when vitamin E donates a hydrogen, forming a non-radical product.

The oxidation of lipids or lipid peroxidation is believed to play a crucial role in the pathogenesis of diabetes and many other diseases. Two main products of lipid peroxidation, malondialdehyde (MDA), 4-hydrozynonenal (4-HNE) or isoprostanes[104,105], have been extensively studied. While these products may function as signaling molecules to stimulate gene expression and cell survival, they may also play a cytotoxic role and promote cell death. The cellular response evoked appears to depend on the cellular level of these molecules and the pathway activated by them[104].

Ascorbic acid or vitamin C is also an antioxidant and red blood cells play an important role in preserving plasma levels of ascorbate. Erythrocytes have a high capacity to regenerate ascorbate from its oxidized form and slowly release it into the plasma. Further, intracellular ascorbate can facilitate the recycling of alpha-tocopherol in the erythrocyte membrane, which in turn helps to protect the cell membrane from lipid peroxidation[106,107]. Thus, both vitamin C and E are potentially important mechanisms for preventing lipid peroxidative damage. The link between diabetes and

these antioxidants remains unclear. Nevertheless, several studies have shown that vitamin E and C were decreased in models of diabetes or in diabetic patients[79,84,108-111]. No studies have been performed in diabetic cats looking at levels of these vitamins.

1.2.3 Markers of oxidative stress

ROS are continually produced during metabolic processes. Their lifetime in biological systems is fleeting and depends on their reactivity and the level of cellular antioxidants. In light of their high reactivity and short lifespan, they exist in very low concentrations *in vivo* and their detection requires probes that very rapidly react with ROS to compete with antioxidants and produce stable products that can be quantified. Two methods have been developed to directly measure the production of ROS. The first technique depends on measuring the presence of ROS by electron paramagnetic resonance, while method 2 relies on measuring the change in a detector compound reacting with ROS[112-114]. Because these techniques have significant limitations, which hamper their use in biological systems, other approaches have been developed for detecting ROS in intact cells.

1.2.3.1 Detection of oxidative stress related damage to nucleic acids

Other methods for assessing the injury inflicted by ROS involve either measuring the amount of oxidative stress damage to cellular compounds or assessing the antioxidant defenses. Targets of ROS with biological importance are nucleic acids, lipids and proteins. The most common biomarkers of ROS attack on nucleic acids are strand breaks, 8-hydroxy-2'-deoxyguanosine (8OH-2dG) or 2'-7,8-dihydro-2'-deoxyadenosine (7,8OH-2dA). In the comet assay, nucleic acid breaks are detected by gel electrophoresis with or without additional strand break by repairing enzymes[115]. The limitations of this assay are its lack of sensitivity and repeatability[115,116]. Detection of 8OH-2dG and 7,8OH is done by ELISA or by

immunohistochemistry using antibodies developed to bind to these targets. However, the antibodies are often not appropriately validated, and their binding may not be as specific as expected[116,117].

1.2.3.2 Detection of lipid peroxidation

The most commonly used technique for measurement of lipid peroxidation is the measure of thiobarbituric reactive species (TBARS) to assess malondihaldehyde (MDA) one of the final degradation product of lipid peroxides [112]. This method, despite its wide use is neither sensitive nor specific with up to 98% of MDA produced after sample collection, during the incubation time of the assay. Additionally, MDA can form when platelets are activated such as during collection [118]. Nevertheless, one study reported the detection of increased TBARS in RBC lysate in diabetic cats without ketoacidosis when compared to healthy controls[41].

The importance of F_2-isoprostanes (F_2-IsoPs) as a measure of lipid peroxidation have grown over the last few years. F_2-IsoPs are a family of molecules initially derived from *in situ* peroxidation of arachidonic acid. They are released from the phospholipid backbone as free acids by the action of phospholipases or platelet activating factor [119]. Free F_2-IsoPs are found in most biological fluids, including plasma and urine after filtration by the kidneys[120,121]. In urine, F_2-IsoPs are conjugated to glucuronide and require hydrolysis before they are measured. They are reliable, sensitive and specific markers of lipid peroxidation. Yet, their assessment can be challenging, and gas chromatography coupled with mass spectrometry, the reference method, is preferred to ELISA. Several reports suggest that the results from the two techniques may not correlate well[122,123]. Assessment is commonly performed on plasma and urine; however, in urine, measurement of both free and conjugated F2-IsoPs is recommended [124]. Increased isoprostanes have been reported in diabetic human patients[119,121] but have not been documented in diabetic cats. A single study has

looked at the urine F_2-IsoPs in feline with kidney disease and showed a decreased concentration with progression of kidney disease[122].

1.2.3.3 Detection of protein oxidation

The most commonly used methods to document oxidative stress related damage to proteins consists of measuring the amount of PC. The identity of the oxidant responsible for carbonyl formation as well as the targeted protein structure determine which amino acids may be oxidized. For instance, lysine, arginine, proline or threonine residues can by oxidized directly by ROS while carbonyl can be introduced in histidine, cysteine or lysine by reactive carbonyl species from advanced glycation end products or in serine, lysine, arginine, threonine and proline by reaction with hypochlorous acid.[125,126]. Historically, protein carbonyls have been measured by colorimetry after reaction with 2,4-dinitrophenylhydrazine (DNPH) yielding a protein-dinitrophenylhydrazone conjugate[127] (**Figure 1.1**). Commercial assays using this method are available, but they have not been validated and scarce information is available regarding their performances. One of the advantages of this method is the possibility to determine protein carbonyl content without standards, using the Beer-Lambert law. Yet, this technique is labor intensive and time consuming due to the extensive washing of proteins needed to remove unreacted DNPH[127]. In addition to this colorimetric method, several ELISA assays have also been developed. After protein carbonyl have reacted with DNPH, an anti-DNPH antibody is added for detection[128]. ELISA methods are more sensitive than the colorimetric method, however results cannot be compared between assays as commercial standards are not available and reactions conditions vary between kits or laboratories[129]. More recently, several fluorophores able to react with protein carbonyls have been described and validated to determine protein carbonyl content. Although these methods are usually more sensitive than the DNPH colorimetric assay, they also necessitate extensive washing to

remove unreacted fluorescent probes, similarly to the DNPH colorimetric assay, and are therefore labor intensive and time consuming[126,130,131]. Stocker *et al* have described the use of 4-hydrazino-7-nitro-2,1,3-benzoxadiazole hydrazine (NBDH) for PC content determination. Unlike other fluorescent probes, NBDH becomes fluorescent only after it has reacted with carbonyls and does not need to be removed prior to fluorescence measurement[132].

1.2.3.4 Antioxidant enzymes

Many assays are commercially available for evaluation of antioxidant enzyme activity such as catalase, SOD, etc., which are often widely used in clinical studies. However, these assays only determine the enzyme activity, which may be dramatically changed under oxidative stress. Enzyme expression is usually not assessed and the results seems particularly prone to over-interpretation [112 133].

1.2.3.5 Low molecular weight antioxidants

Along with antioxidant enzymes, low molecular weight antioxidants (LMWAO) play a major role in antioxidant defenses. Countless molecules have antioxidant capacity, such as albumin, other proteins, vitamins C, E, A, glutathione, bilirubin, ceruloplasmin, and others [134]. Assays exist for most of these substances. In studies, very limited panels of LMWAO are tested. While there is no consensus on the LMWAO panel that should be tested in research, the consensus is that this panel should take into consideration the biological system and the source of oxidation tested. Cutler suggests a panel including 13 LMWAO and 22 trace elements[134] which, as suggested by McMichael a few years later, is unrealistic [135], especially in laboratory animal or small domestic animals, when limited amounts of samples can be collected. In addition to a comprehensive and meaningful panel of LMWAO this panel should also depend on the system studied. For instance, for the red blood cell antioxidant capacity, there is no need to assess albumin since there is very

little to no albumin in red blood cells. When assessing plasma antioxidant properties, on the other hand, it would be important to determine the albumin concentration, since this is the most abundant protein in plasma. Evaluation of low molecular weight antioxidants such as albumin is often not done[135]

1.2.3.6 Total antioxidant capacity

Many tests have been developed to assess the total plasma/serum antioxidant capacity. These tests can provide valuable information about systemic changes in total antioxidant capacity since they take into account all the antioxidants present in plasma or serum. The total antioxidant capacity is designed to overcome the absence of information on each individual antioxidant component of plasma or serum and their interactions. Indirect methods, including the measurement of redox couples such as GSH/GSSG or $NADH/NAD^+$, are suggested by some authors [112]. These tests are based on the assumption that the redox couple that is assessed is acting as a redox buffer, which is able to reduce every other LMWAO. This seems to be an over-simplification of the interactions between LMWAO. In general, direct assays are based on determination of all antioxidant reducing properties, i.e., their ability to reduce an indicator substance, whereas indirect methods are based on the assessment of inhibition of oxidation of an indicator substance[136]. Examples of direct total antioxidant capacity assays include the total radical-trapping antioxidant parameter (TRAP), the total oxidant scavenging capacity (TOSC), the total antioxidant status (TAS) and the oxygen radical absorbance capacity (ORAC). Diphenylpicrylhydrazyl stable radical decolorization, ferric-reducing activity of plasma (FRAP), and cupric ion reducing antioxidant capacity (CUPRAC) are the most popular examples of indirect methods[112].

Both indirect and direct methods use a variety of reagents. The variation in pH and solution content or the species of ROS generated for these methods makes it difficult or impossible to

compare results obtained with different techniques. Additionally, most of the assays are performed in aqueous solution disregarding the contribution of the antioxidant lipophilic substances such as vitamin E. When performed on plasma, the most important contributors to the antioxidant capacity are albumin and uric acid (in people) and thus, the results from these assays are correlated with the concentrations in these compounds[137]. This prevents any interpretation on potential specialized LMWAO such as ascorbic acid or GSH which are found in lower concentration in blood. Total antioxidant capacity likely does not assess the interactions between LMWAO, such as that between ascorbic acid and vitamin E. Another concern is that in blood only the plasma components are used to determine total antioxidant capacity and the contribution of cells is disregarded[136]. Thus, despite the widespread use of total antioxidant capacity, its significance for drawing conclusions about oxidative stress in complex biological systems is uncertain.

1.3 MicroRNAs in erythroid cells

1.3.1 Biogenesis of microRNAs

MicroRNAs are small (~22nt) non-coding RNAs able to regulate gene expression by suppressing mRNA translation. They are thought to regulate somewhere between 30 and 60% of all protein expression. In humans, microRNA genes are located in intragenic or intergenic regions. In intragenic regions, most of the microRNA genes are in intronic regions of genes while fewer are found in exonic regions[138]. In the canonical biogenesis pathway, transcription of a microRNA gene is performed by an RNA Polymerase II[139,140]. The transcript, called a primary microRNA contains complementary sequences resulting in the formation of a hairpin structure[138]. Primary microRNAs are then processed in the nucleus by a nuclear RNase III, Drosha, and the cofactor DiGeorge syndrome chromosomal region 8 (DGCR8), forming together the microprocessor complex [141,142]. Drosha possesses two RNase domains which cleave the 3’ strand of the primary

microRNA, creating an overhang while the second RNase domain cuts the 5' end leaving a phosphorylated end. This cut occurs approximately 11bp away from the basal junction of the primary microRNA and approximately 22bp away from the loop, forming a precursor microRNA (pre-microRNA). Both basal and loop junctions of the strand are reference points for Drosha slicing and ultimately defines the 5' or 3' end of the mature microRNA and its specificity[143-145]. Pre-microRNAs are exported to the cytoplasm by a GTP-dependent transport complex, the Exportin 5 (EXP5). Following translocation to the cytoplasm through a nuclear pore, GTP is hydrolyzed and the pre-microRNA is released[146,147]. In the cytoplasm, pre-microRNAs bind to Dicer, a RNase III protein, through recognition of the terminal loop and the 3' overhang. The catalytic domain of Dicer then cuts approximately 22nt away from the 3' overhang and the 5' phosphorylated end creating a double stranded RNA structure with the usually inactive passenger strand corresponding to the 3' end of the pre-microRNA, and the mature microRNA, corresponding to the 5' end of the pre-microRNA[148]. In fewer microRNAs, the mature microRNA corresponds to the 3' end of pre-microRNA while the passenger strand is the 5' end. The 5' phosphorylated end of the guide strand containing the mature microRNA interacts with a binding pocket in Argonaute proteins (AGO) which guides the RNA duplex in position in AGO. The 3' also interact with a domain (PAZ domain) of AGO[149]. Opening of the AGO protein for the microRNA duplex to have access to binding sites is ATP-dependent and involves heat shock proteins (HSP70 and HSP90)[150]. Following binding of the duplex microRNA to AGO proteins, the passenger strand is removed to form the RISC complex. Selection of the guide strand is not strict and can vary between microRNAs. The strand with the most stable 5'-end is usually selected as the guide strand. The first nucleotide of the sequence also influences the choice of the guide strand, with AGO proteins favoring U in first positions[151,152].

A variety of non-canonical microRNA biogenesis pathways also have been described. The presence of a hairpin structure resembling pre-microRNAs is conserved in these alternative pathways. Sequences can originate from spliced-out introns, endogenous short hairpin RNAs or other non-coding RNAs like tRNAs, small nucleolar RNAs or small nuclear RNA-like viral RNAs. Although these precursor-like microRNAs bypass Drosha, they are all processed by Dicer. Another alternative pathway bypassing Dicer, but not Drosha, has been described. The prototypical microRNA following this path is miR-451. After primary microRNA synthesis, miR-451 is cleaved by Drosha to form a pre-microRNA; however, the stem of the hairpin formed is too short to be processed by Dicer, and after translocation into the cytoplasm, pre-miR-451 is directly loaded onto AGO2. AGO2 slices the 3' strand of the pre-microRNA, leaving a 30 nt long intermediate structure consisting of the loop and part of the 3' strand. Finally, a poly(A)-specific ribonuclease trims down the 3' end of the sequence to approximately 23 nt[153]. Similarly, to miR-451, miR-486 also necessitate slicing by AGO2, but only to remove the passenger strand as pre-miR-486 is processed by both Drosha and Dicer. Both these microRNAs are needed for adequate erythropoiesis. Interestingly, AGO2 is the most abundant AGO protein in erythropoietic cells, contrary to almost all other cell types, which makes erythropoiesis unique and could explain the maintenance of slicing amongst AGO proteins[154].

Once loaded onto AGO proteins, microRNAs base pair with mRNA, generally imperfectly. This base pairing is nucleated by the seed region, usually corresponding to nucleotides 2-8 in the 5'-end region of this microRNA[155]. Mechanisms for microRNA-mediated mRNA expression inhibition are multiple. AGO proteins can interfere with initiation step of the mRNA translation by repressing recruitment of ribosomal subunit 40S and 60S and by disrupting active polysomes. They are also responsible for destabilizing the mRNA by deadenylation[155]. Eventually,

translationally inactive mRNAs accumulate into discrete cytoplasmic granules called P-bodies or stress granules, which are temporary storage site for mRNAs. Translational repression of these mRNAs must be lifted or they are ultimately degraded[156]. At this stage, mRNA storage and degradation are not dependent on microRNAs.

1.3.2 Regulation of erythropoiesis by microRNAs (**Figure 1.2**)

During erythropoiesis, pluripotent stem cells capable of self-renewal, differentiate into common myeloid progenitor and thereafter into common erythroid-megakaryocytic progenitor cells. These progenitor cells, committed to the erythroid lineage, form burst forming units-erythroid (BFU-E) and colony-forming unit-erythroid (CFU-E) sequentially. BFU-E proliferation and differentiation necessitate stem cell factor (SCF) while CFU-E differentiation into pro-erythroblasts, basophilic erythroblasts, polychromatophilic erythroblasts and acidophilic erythroblasts depends only on erythropoietin (EPO)[157]. Acidophilic erythroblasts become reticulocytes after extrusion of their nucleus and mature into RBCs. Both reticulocytes and mature red blood cells can be found in circulation in most species. The main transcription factors involved in erythroid differentiation are GATA-1 and GATA-2[158]. As molecular switches, microRNAs play an essential role in directing hematopoietic stem cells development toward the erythroid lineage.

1.3.2.1 MicroRNAs in hematopoietic stem cells

In hematopoietic stem cells, several microRNAs, miR-221, miR-222, miR-150, miR-126, miR-24, miR-15a and miR-210 are responsible for proliferation and self-renewal. MiR-221 and 222 target c-kit, a receptor for SCF. Therefore, they inhibit the progression of BFU-E towards red blood cell formation[159,160]. Similarly, miR-150 and miR-126 modulate the expression of the transcription factor c-Myb, while miR-24 inhibits activin A receptor type 1B (ALK4) expression and erythroid differentiation[161], as both c-Myb and ALK4 are needed to drive the common

erythroid-megakaryocytic progenitor toward erythropoiesis[162-164]. Simultaneously, the expression of miR-15a is responsible for maintaining erythroid stem in an undifferentiated state[165]. MiR-210, upregulated under hypoxic conditions, inhibits globin production and erythroid progenitor cells maturation[166].

1.3.2.2 MicroRNAs in erythroid committed progenitors

In erythroid committed progenitors, the expression of miR-126, moR-15a, miR-221, miR-222, miR-223 and miR-24 is considerably decreased. This results in the increased expression of c-kit, c-Myb and ALK4. C-Myb upregulates the expression of GATA-1, c-kit, LMO2, and KLF1[167-169]. LMO2 (LIM-only protein 2) functions as a bridge molecule to assist in the formation of transcription factor complexes such as GATA-1 and its downregulation by miR-223 inhibits erythroid cell progression towards differentiation [170,171]. At this stage, activation of the EPO receptor by c-kit or by EPO mediates STAT5 and phosphatidylinositol 3-kinase phosphorylation and promotes cells proliferation and differentiation while inhibiting cell death. Simultaneously, c-Myb and GATA-1 induce the expression of miR-451, which in turn inhibits protein 14-3-3ζ translation and GATA-2 expression, a transcription factor involved in early erythropoiesis[172-174]. In the absence of miR-451, protein 14-3-3ζ accumulates in the cytoplasm of erythroid cells and sequester a transcription factor (FOXO3). By repressing protein 14-3-3ζ, miR-451 allow FOXO3 to translocate into the nucleus where it induces the expression of antioxidant factors such as SOD, GPx, Prx and Trx reductase 2 as well as Trx, increasing red blood cells resistance to oxidative stress[174-176]. GATA-1 also upregulates the expression of miR-144 which suppress nuclear factor-erythroid 2 (NRF2). NrF2 binds to antioxidant responsive elements and induces the expression of antioxidant enzymes such as SOD, catalase, and GPx. Thus, increased expression of miR-144 decreases resistance of red blood cells to oxidative stress, demonstrating an opposite role to

miR-451. The exact interaction of miR-451 and miR-144 for the regulation of the antioxidant response is not known[177]. C-Myb also induces the expression of miR-486 which participate in the commitment of progenitor cells to the erythroid lineage, while it also mediates erythroid survival through the transcription factor FOXO1[168,178-180]. In erythroid cells, activation of KLF1 and ALK4 expression results in adult β-hemoglobin synthesis and repression of the fetal γ-hemoglobin. MiR-15a, miR-16 and miR-96, miR-339, miR-486, miR-451, and let-7b, are responsible for the repression of the fetal γ-globin synthesis, while upregulating the expression of the adult α and β-globins; however, the mechanisms involved have not been elucidated[181-185]. Let-7d interacts with the DMT1 gene transcript and inhibits its expression. In erythroid cells, DMT1 participate in the transfer of iron into the cells, needed for effective hemoglobinization of the erythroblasts[186].

1.3.2.3 MicroRNAs in maturation of erythroid cells

During terminal maturation, erythroid cells do not respond to EPO stimulation as they lose their EPO receptor[187]. Downregulation of miR-191 is required for chromatin condensation and enucleation[188]. Interestingly, red blood cells maintain an important pool of mature microRNAs after their release into circulation, despite their lack of protein synthesis capability as confirmed by the absence of ribosomal RNA and the markedly decreased mRNA content in comparison to reticulocytes[189]. Even if individual mature erythrocytes contain only small amounts of microRNAs, considering total red cell mass, the red blood cell derived microRNAs represent an abundant pool of microRNAs, that has been somewhat neglected so far. These microRNAs are so abundant that caution must be taken in interpreting whole blood or plasma microRNA profiles. Plasma profile may be largely a reflection of "spill-over" from the RBC pool. Several studies have shown that the abundance of plasma microRNAs may be significantly influenced by hematocrit and hemolysis[190-192].

1.3.3 Mature erythrocyte miRNome

Few studies have looked at mature RBC miRNome and changes under different conditions. One study looked at reticulocyte and mature RBC microRNA content in sickle cell disease by microarray. In this study, the authors found 162 highly abundant microRNAs amongst which 83 were reticulocyte-specific. When microRNAs from sickle cell disease patients were compared to healthy individuals, four microRNAs were over-represented in healthy people, miR-320, let-7 family, miR-181 and miR-141, while four microRNAs were over-represented in the affected individuals, miR-29a, miR-144, miR-451, and miR-140. When they compared the expression of the 83 reticulocyte-specific microRNAs between sick and healthy individuals, sickle cells disease was associated with a mature red blood cells microRNA profile closer to reticulocytes than from healthy mature erythrocytes. MiR-320 targets and downregulate transferrin receptor and is responsible for cell survival and differentiation. The low miR-320 content of sickle cell erythrocytes was responsible for maturation inhibition and decrease cells survival while transferrin receptor expression was maintained during terminal differentiation[193].

In a later study, next generation sequencing was performed to compared mature RBC and reticulocytes miRNomes. In this study, reticulocytes contained approximately eight times more microRNAs than mature RBC, which is in adequation with the capacity of reticulocyte to synthesize proteins. One hundred and ninety-seven microRNAs were identified. MiR-451 was the most abundant microRNA sequenced, representing approximately 60% of the reads. MiR-451 and miR-144 form a single microRNA cluster (multiple microRNA genes closer than 1 Kb, transcribed together, from the same promoter), yet, in this study, the authors note that miR-144 was over 400 times less abundant than miR-451. This study also demonstrated that miR-451 is largely incorporated to AGO2, possibly mediating repression of protein 14-3-3 ζ expression in

reticulocytes[189]. A more recent miRNome study compared the microRNA content of individuals living at different altitudes by next generation sequencing. This study identified 516 microRNAs in erythrocytes and significant differences in the abundance of 40 microRNAs between people living at low and high altitudes. The author suggested a possible relation with hypoxia; however, the absence of reticulocytes was not assessed, and reticulocytes may partially have impacted these results[194].

The reason for the abundance of microRNAs in reticulocytes and mature erythrocytes is still not clear. Protein synthesis occurs in reticulocytes and microRNAs play a role in regulating this synthesis, likely insuring that reticulocytes mature adequately[195]. It is also possible that microRNAs in erythrocytes participate in the degradation of the mRNA during terminal differentiation. In mature red blood cells, microRNAs may also be a defense mechanism against intraerythrocytic parasite like *Plasmodium* sp. Patient with sickle cell disease are less susceptible to malaria infection than people with normal hemoglobin, it is speculated that the difference in microRNA content may play a role[193]. *In vitro* experiments have shown that malaria infected RBC release microparticles loaded with hundreds of human microRNAs, including miR-451, loaded on AGO2. These microparticles are transferred to other RBC and transferred miR-451 protected RBC from parasite infection[196]. They may also play a role in red blood cells survival; however, evidence for this function are lacking[195]. An additional role of mature red blood cells has been suggesting recently based on the release of microparticles containing AGO bound microRNAs in circulation. *In vitro* studies have shown that these particles can be transferred to endothelial cells and change gene expression in these cells, hence they appear to play a role in cell-to-cell communication [197-199]. Clearly more work is needed to unravel the possible role for microRNAs of mature RBCs in cellular communications.

The overall goal of this work was to identify a set of microRNAs in mature erythrocytes and evaluate changes in their expression under conditions of oxidative stress. It was postulated that individual microRNAs identified in this study, may serve to generate new study hypothesis about the role these molecular switches play in erythropoiesis, antioxidant defenses of RBC, as well as their potential role in cell-to-cell communication either to enhance antioxidant defenses in target cells or as triggers of diabetic complications.

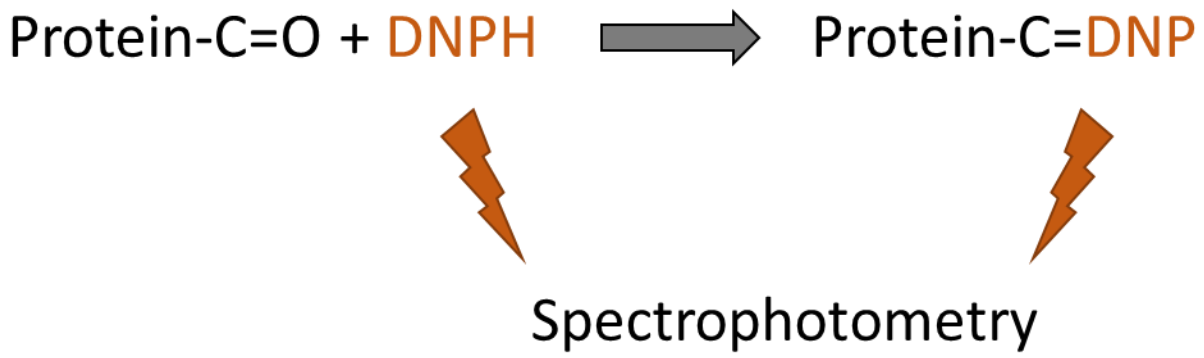

Figure 1.1: Colorimetric determination of protein carbonyl content with 2,4-dinitrophenylhydrazine (DNPH)
Protein carbonyls (C=O) react with DNPH to yield a protein dinitrophenylhydrazone. Both the hydrazine and hydrazone forms are detected spectrophotometrically.

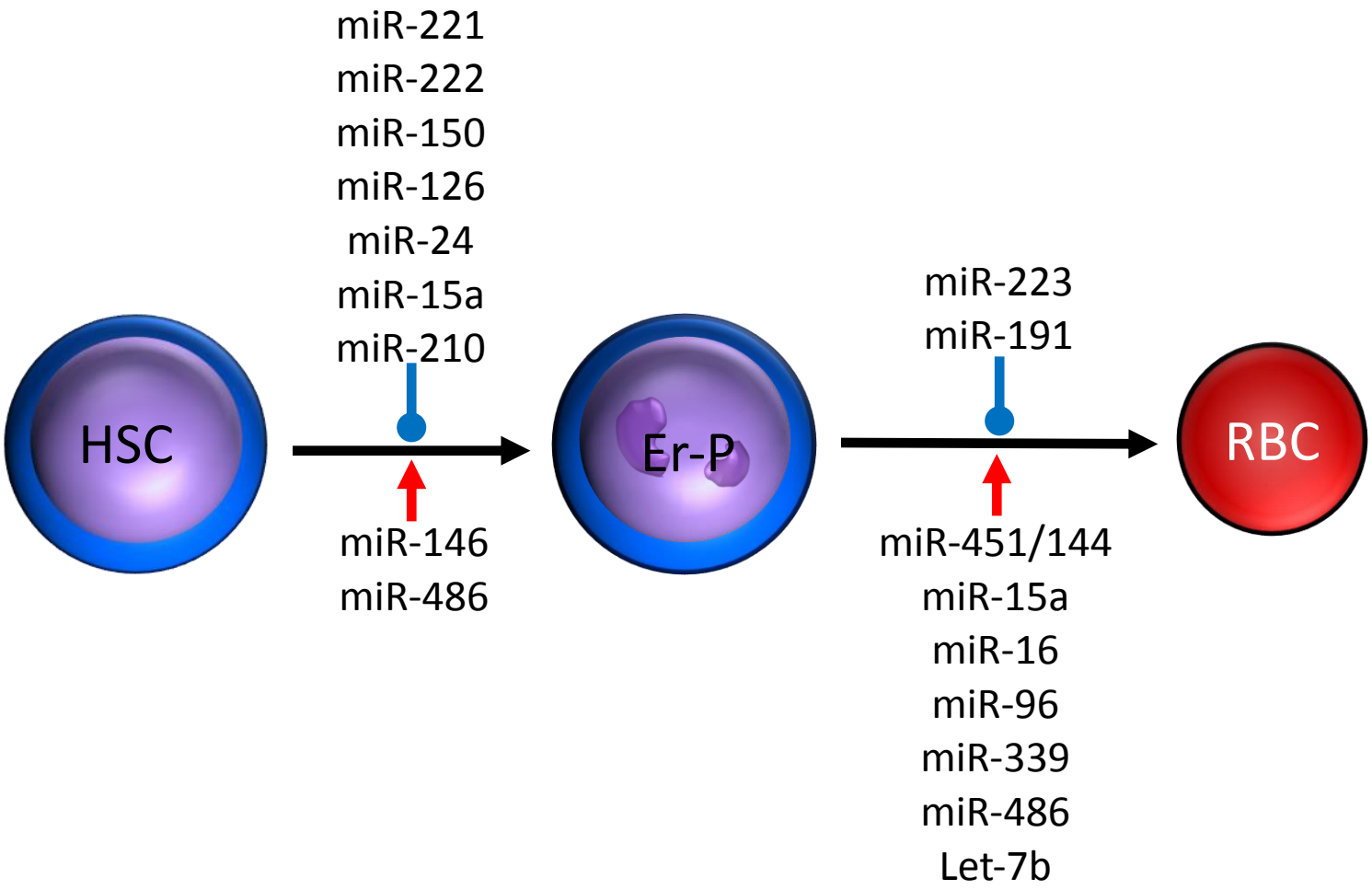

Figure 1.2: microRNAs controlling erythropoiesis
MicroRNAs can either drive (arrow) hematopoietic stem cells (HSC) or erythroid precursors (Er-P) differentiation and maturation into a mature erythrocyte (RBC) or repress (round arrowhead) differentiation and maturation.

CHAPTER 2. COLORIMETRIC DETERMINATION OF SERUM AND PLASMA PROTEIN CARBONYL CONTENT IN CATS

2.1 Abstract

Oxidative stress is the result of a disproportionate production of reactive oxygen species (ROS) in comparison to antioxidant defenses. Protein carbonyls (PC) result from the non-specific attack of ROS on protein side chains. In people and in laboratory animals, PC content is considered an early biomarker of protein oxidation. There is currently no validated method to assess ROS damages to proteins in cats. Therefore, the aim of this study was to describe and evaluate a colorimetric method, the 2,4-dinitrophenylhydrazine (DNPH) assay, for protein carbonyl (PC) content determination in feline serum and plasma samples. Specimens obtained from client, staff, student and faculty-owned cats were used to determine within- and between-run coefficients of variation, linearity, limits of quantification, ranges of values observed in the feline population, and interferences from hemolysis and lipemia. Additionally, diabetic cats were compared to healthy controls to document the potential usefulness of this assay.

The protocol for PC content determination in feline serum and plasma samples as described herein has adequate within-run variability (<10%), a low limit of quantification (0.25nmol/mg) and good linearity over a wide range of values (from 0.25nmol/mg to 10nmol/mg). Between-run variability was found to be 38% for serum and 69% for plasma. Additionally, hemoglobin had a major effect on PC content, in contrast to lipemia. Despite some limitations, this assay identified increased PC content in diabetic cats in comparison to healthy controls and should be a useful tool for understanding the role of protein oxidation in other feline diseases and evaluating antioxidant treatments.

2.2 Introduction

Reactive oxygen species are highly reactive chemical components, able to target non-specifically macromolecules such as proteins, lipids, and nucleic acids causing reversible or irreversible cellular damage and loss of function. However, oxidant damage may be prevented by various antioxidants mechanisms. Oxidative stress is defined by an imbalance between antioxidants and oxidants in favor of the latter, resulting in the accumulation of ROS-induced damages to cell components and loss of biological functions. In cats, a variety of diseases have been associated with oxidative stress, including diabetes [22,39,200], chronic kidney disease [201-203], feline immunodeficiency virus infection [204], hyperthyroidism [205], hypertrophic cardiomyopathy [206] and feline infectious peritonitis [207].

The introduction of carbonyl groups to amino acid side chains proline, arginine, lysine and threonine results from direct oxidation by ROS or by reaction with nucleophilic amino acids with aldehydes or carbonyl derivatives produced during lipid peroxidation. The latter results in the formation of advanced glycation/lipoxidation end-products [125]. Protein carbonyl (PC) content is currently the most commonly used indicator of protein oxidation, and accumulation of these products has been observed in several human diseases including diabetes mellitus, Alzheimer's disease, inflammatory bowel disease and arthritis[208]. However, PC has not been previously described in domestic animals.

Historically, the most commonly used assay for PC measurement is a colorimetric procedure. It is based on the derivatization of protein carbonyls by 2,4-dinitrophenylhydrazine (DNPH), yielding dinitrophenyl hydrazone [127] that can be detected spectrophotometrically. The DNPH technique is commercially available and has been adapted to a microplate format. However, these kits have not been validated for veterinary use and information regarding the performance of

the DNPH assay is sparse. Additionally, stability of PC using this colorimetric method has not been documented [209] and limited information is found regarding the possibility of interferences due to hemolysis. Hemoglobinemia is known to falsely increase PC content, however it is suggested that a sample blank may be used to correct for such interferences in this assay. The latter information has not been published.

The goal of this study is to describe and validate a microplate colorimetric technique for PC content determination in feline plasma and serum, and to document the stability of this analyte as well as the interferences caused by hemolysis and lipemia.

2.3 Materials and methods

2.3.1 Samples

Samples used in this project were collected with the approval of the Purdue University Animal Care and Use Committee (protocol # 1504001221 and 1610001489). Bother serum and plasma were obtained from healthy cats and cats with a variety of conditions as described below.

2.3.2 Reagents

All chemicals were of analytical grade, from Thermo Scientific except for the 2,4-dinitrophenylhydrazine, which was acquired from Tokyo Chemical Industry America.

2.3.3 Colorimetric determination of protein carbonyl content

This assay is based on the reaction of DNPH with carbonyls, yielding a dinitrophenyl hydrazone product detected spectrophotometrically. Total protein concentration of the specimens was determined by refractometry (Reichert VET 360, Reichter Technologies) and serum or plasma specimens were diluted to 5 g/L with double distilled water (ddH_2O). The method to quantify protein carbonyl content was adapted from the historical 2,4-dinitrophenylhydrazine (DNPH)

derivatization technique described by Levine et al[127]. For each specimen a blank and a test specimen were run in parallel. Briefly, 200 µL of diluted serum or plasma were pipetted into two, 2 mL microcentrifuge tubes. Eight hundred microliters of a 2.5 M hydrochloric acid aqueous solution were added to the blanks while 800 µL of DNPH working solution (10 mM DNPH in 2.5 M hydrochloric acid) were added to the test specimens. After mixing, preparations were incubated in the dark for 1 h with homogenization by vortexing every 15 min. At the end of the incubation, 900 µL of a 20% trichloroacetic acid (TCA) aqueous solution were added to both tubes. The preparations were placed on ice for 10 min and then centrifuged at 10000g for 15 min at 4 °C. Supernatants were discarded without disturbing the pellet and 1 mL of a 10% TCA aqueous solution was pipetted into the tubes. Preparations were homogenized with the FastPrep®-24 (MP Biomedicals), placed on ice for 10 min and centrifuged at 10000 g for 15 min at 4 °C. After the supernatant was discarded, pellets were washed three times with 1 mL of ethyl acetate/ethanol (1/1; v/v) to remove unreacted DNPH. Following the addition of ethyl acetate/ethanol, samples were mixed with the FastPrep®-24 and centrifuged at 10000 g for 15 min at 4 °C, except after the last wash when the preparations were centrifuge at 20000 g for 15 min at 4 °C. Supernatants were carefully aspirated and discarded after the last wash; the pellets were left to dry in a fume hood, in the dark for approximately 30-45 min. Pellets were resuspended in 500 µL of a 6 M guanidinium hydrochloride, 2 mM KH_2PO_4 solution at pH = 2.5. Two hundred and twenty microliters of the blank and test protein suspensions were placed in a transparent 96-well microplate (SpectraPlate-96 MB, PerkinElmer). All measurements were carried out in duplicates on the SpectraMax i3x microplate reader (Molecular Devices) with absorbance measured at 375 nm. Absorbance was averaged from the duplicates. The protein concentration of blank and test specimens was

determined with the Pierce™ BCA Assay kit (Thermo Fisher) following the manufacturer's instructions after the specimens were diluted 10 times in ddH_2O.

Two calculation methods were evaluated to determine the PC content. Method 1 involved correcting the absorbance of test specimens by subtracting the absorbance of the corresponding blank prior to protein carbonyl content determination, while using method 2, the PC content of both the blank and sample were calculated and then the PC content of the blank was subtracted from that of the corresponding test specimen. The Beer-Lambert law was used to calculate the PC content with a molar absorptivity coefficient of 22000 $M^{-1}.cm^{-1}$.

2.3.4 Preparation of oxidized and reduced BSA

BSA was oxidized by adding 49 µL of a 12% sodium hydrochloride solution to 100 mL of a 1 g/L BSA solution in ddH_2O and incubated in a water bath at 37 °C for 15 min. BSA was reduced by adding 100 mg of sodium borohydride to 100 mL of a 5 g/L BSA solution in ddH_2O. The preparation was incubated 30 min at room temperature and then neutralized with hydrochloric acid 1 M. Oxidized and reduced BSA solution were concentrated and desalted with Pierce Protein Concentrators, PES, 30K MWCO, 5-20 mL (Thermo Fisher) using PBS 1X pH = 7.4 for desalting. Protein concentration of both solutions was measured by refractometry (Reichert VET 360, Reichter Technologies) and aliquots of the solutions were kept at -80 °C until used. PC of reduced and oxidized BSA were determined by colorimetry as described previously.

2.3.5 Test performances

To evaluate the performances and range of this assay in feline specimens, 50 serum and 50 EDTA plasma samples were obtained from the Purdue University Clinical Pathology Laboratory. Samples were retrieved only after all analyses ordered by the clinicians had been completed.

To determine the range of PC content, 50 non-hemolyzed and non-lipemic serum and 50 non-hemolyzed and non-lipemic plasma samples from healthy and diseased cats were evaluated. Specimens were grouped into the following categories based on diagnosis indicated in the animal's medical record: healthy, lymphoma, diabetes, hyperthyroidism, renal disease, infectious disease, inflammatory disease with no evidence of infection, non-lymphoma cancer, others. Serum specimens originated from castrated males (33), spayed females (16) and one intact female, grouped into junior (5), prime (9), mature (5), senior (14) and geriatric (17) cats, following the American Association of Feline Practitioners and the American Animal Hospital Association classification of cats lifestage[210]. These cats were healthy cats (5), and cats with a variety of diseases, including kidney disease (16), lymphomas (7), inflammatory diseases without evidence of infection (5), cancer other than lymphoma (4), diabetes (3), hyperthyroidism (3), infectious diseases (2) and other diseases (5). Tested plasmas were collected from 23 castrated males, 25 spayed females, one intact male and one intact female, separate also into junior (5), prime (15), mature (10), senior (7), and geriatric cats (13). These cats were healthy (7) or diagnosed with kidney disease (11), non-lymphoma cancer (8), lymphoma (7), inflammatory disease with no evidence of infection (5), infection (2), hyperthyroidism (2), diabetes (1) and other diseases (7). Student *t*-tests were performed to compared PC content between groups.

Intra-run precision was determined by measuring the protein carbonyl content at 3 different levels: low (reduced BSA), medium (pooled serum and plasma) and high (oxidized BSA) levels, 20 times for each level. Between-run precision was determined by measuring the protein carbonyl content at a medium level (pooled plasma and serum) over 10 different runs on separate days. Precision was expressed as the coefficient of variation (CV). Linearity was evaluated by spiking pooled plasma and serum with reduced BSA or oxidized BSA to maintain an identical protein

concentration while varying the PC content. The limit of quantification was determined as recommended by the US-FDA [211]. Briefly, the lowest concentration of the standard curve which was at least five times the blank value and at which value, CV was less than 20% was considered the limit of quantification. Interference from hemoglobin and triglycerides was evaluated by spiking pooled plasma and serum with increasing amounts of a hemoglobin solution from hemolyzed red blood cells or Intralipid 20% (Fresenius Kabi USA) to a final concentration of 0, 0.25, 1, 2 and 8 g/L for hemoglobin and 0, 0.25, 0.5, 1 and 2 g/L for triglycerides. Samples were analyzed in duplicate during a single run. Interference was considered significant when PC content of spiked samples differed by ±20% from the serum and plasma PC content with no interferent.

To assess the stability of PC content, 10 serum and 10 EDTA plasma samples from client, student, staff, and faculty-owned cats were collected by jugular venipuncture. After a physical exam, a hemogram and a chemistry panel were performed to confirm the health status of the cats, remaining serum and plasma were aliquoted. One aliquot was used to measure PC immediately after blood collection while the other aliquots were stored at 4 °C, -20 °C or -80 °C to evaluate the stability of PC content over time, under different storage conditions. PC content was measured in all aliquots after 1 and 2 weeks, and for the frozen aliquots, also after 1 month and 3 months. Results were assessed graphically and compared using a Wilcoxon signed rank test.

Finally, serum and EDTA plasma were also collected from four diabetic cats with ketoacidosis and evidence of systemic oxidative stress, patients at the Purdue Veterinary Teaching Hospital. A physical examination, hemogram and chemistry panel were performed. Inclusion criteria included a history, physical examination, chemistry panel and urinalysis consistent with ketoacidotic diabetes mellitus and the presence of Heinz bodies on over 50% of the red blood cells confirmed the presence of oxidative stress. Four age and sex-matched, student, staff and faculty-

owned healthy controls, based on the absence of history of disease, a normal physical examination and unremarkable hemogram and biochemistry profiles were recruited. Serum and plasma from the diabetic cats and the age and sex matched healthy controls were stored at -80 °C until the assay was performed. A Student's *t*-test was performed to compare the PC content of diabetic cats and healthy controls serum and plasma. For this project, JMP®, version 13.2.0 (SAS Institute Inc.) was used for statistical analyses and a P value inferior to 0.05 was considered significant.

2.4 Results

Results of the imprecision study are shown in table 2.1 and 2.2. Within-run CV was approximately less than 10% for the pooled serum and plasma specimens as well as for the high protein carbonyl samples for method 1, while it was less than 20% for the same samples using the second calculation method. On the other hand, the CV for the low PC specimens (reduced BSA) was higher than for the other specimens, rising to about 20% when the first calculation method was used and to over 100% with the second calculation method.

Linearity studies revealed that the assay measured proportionally in the analytical range from approximately 0.25 to 10 nmol/mg (**Figure 2.1**). When the highest theorical PC content value was excluded based on the loss of linearity for such PC content value, the regression curve obtained by the least square method ($p<0.0001$) was associated with a Spearman's coefficient of $r = 0.99$. Thus, excellent correlation was obtained between theoretical and measured PC content values in the linear range of the assay.

The limit of detection for both serum and plasma were of 0.25 nmol/mg using the first calculation method. With the second calculation method, the limit of quantification was 0.82 and 0.91 nmol/mg for plasma and serum, respectively. A negative interference was detected at all

hemoglobin concentrations tested using both calculation methods in serum and plasma **(Figure 2.2)**. In contrast, no significant interference was observed with triglycerides at any of the concentration tested in serum or plasma **(Figure 2.3)**. Over the period of 3 months, there was no statistically significant changes in the PC content as evaluated by the Wilcoxon sign rank test, regardless of the storage condition. Visually, no significant variations could be observed **(Figure 2.4 and 2.5)**.

PC content ranged from 0.35 to 2.13 nmol/mg for serum and 0.35 to 2.27 nmol/mg for plasma **(Figure 2.6)**. There was no significant difference between the serum and plasma PC content of the different sex and age groups, nor was there a significant difference between healthy cats and cats from each diagnosis groups. Additionally, and no significant difference was found between healthy and sick felines in serum and in plasma.

The protein carbonyl content of serum and plasma of four clinically healthy and diabetic cats was determined. Diabetic cats had a higher PC content than healthy controls in both serum (P=0.03) and plasma (P=0.005) **(Figure 2.7)**.

2.5 Discussion

In this article, we report the performances of a colorimetric microplate assay for PC content determination in feline serum and plasma. This assay performs adequately within-run but has a great between-run variation. Linearity is observed over a large range of values and the PC content from feline serum and plasma samples were found within the limit of quantification and limit of linearity for the assay. This is the first description of a method for PC content measurement in cats and the first validated test to evaluate oxidative stress related damages to proteins in feline patients. This test adds to the list of oxidative stress assays available for domestic animals. Amongst these

tests, only few have been validated and proven to perform adequately [135,203,207,212,213]. No difference was seen in the PC content of serum and plasma of cats related to the health status of the patients. This could be due to the low number of individuals in each group and/or the variability between individuals and the absence of age and sex match controls. In this part of the study, the goal was to document the range of PC content in a variety of cats and the samples were randomly selected from the Purdue Clinical Pathology laboratory to have a large range of values. When carefully selected individuals with a high probability of systemic oxidative stress i.e. diabetic cats with ketoacidosis and Heinz bodies were compared to age and sex-matched healthy control cats, a significant difference was observed. The difference was significant despite the low number of individuals per groups, which suggests that this test shows promising results for future studies.

One of the advantages of this test is that it does not require the use of standards as the molar absorptivity coefficient is used to determine the PC content; however, the use of standards may improve the between-run variation and should be further assessed. We did not identify any significant variation in PC content over time nor under different storage conditions, however more extensive storage times and conditions should be evaluated. While it has been assumed that the PC content as determined by the DNPH-based assay is stable over time [209], to the best of our knowledge, this has not been previously documented. Similarly, it is assumed that hemoglobin falsely increases the PC content of samples, since its molar extinction coefficient peaks close to 375nm, the absorbance at which PC content is measured. The use of a sample blank is meant to correct the PC content for this interference [127,214]. We show herein that hemoglobin has the opposite effect on PC content, decreasing it drastically, even with minimal hemolysis. We speculate that hemoglobin may directly inhibit the reaction of DNPH with protein carbonyls. Thus, this information may be relevant not only to feline samples, but hemolyzed samples from any species.

No previous information could be found regarding the influence of lipemia on the measurement of PC content using the DNPH-based assay. Our study shows that lipemia had no effect on PC content as determined by this assay. It is likely that the extensive protein precipitation and washing steps removed the vast majority of lipids from samples before colorimetric measurements are obtained.

The best method to calculate the PC content from the absorbance and the protein concentration of the sample and sample blank is unclear. The two methods tested herein are well documented in the literature and in commercial kits, but have not been previously compared; interestingly, plasma protein carbonyl concentrations determined after subtracting the absorbance of the blank appears to be the most commonly used method[214]. In our study, method 1 performed better, in terms of tighter CVs, than method 2. Method 1 does not take into consideration the different protein loss between the sample and sample blank, whereas method 2 does. However, method 2 necessitates four measurements (PC of the sample and sample blank and protein concentration of the sample and sample blank). The addition of random error for these four measurements may have introduced greater variability into the calculations, accounting for the higher CVs seen in this study. During this project, we noticed that the protein loss was greatly influenced by the pellet resuspension method (manual vs homogenizer); our use of the FastPrep®-24 likely limited variations in the protein loss. In another laboratory setting, the first calculation method may not be the most robust.

Protein carbonyls are a valuable tool for detection of oxidative damage and our results suggest that the DNPH-based assay is promising for use with feline plasma and serum samples. However, this assay is labor-intensive and time-consuming with each run taking between 8 and 10 hours to complete. It is clear that to be clinically useful, a faster assay must be developed in the future and validated for use in felines.

2.6 Conclusion

This study describes a method for serum and plasma PC content measurement in feline serum and plasma samples. Although this technique has the advantage of being easy to perform, needing relatively basic lab equipment and inexpensive reagents, the limitations include the low number of samples that can be run at a time, time needed to perform this assay and poor between-run reproducibility. We have shown that protein carbonyls may serve as a biomarker of global oxidation in cats and in the future, its determination may prove useful in our understanding of the sequelae of oxidative stress in various diseases and how best to treat these conditions.

2.7 Conflict of interest statement

None of the authors have financial or personal relationships that could inappropriately influence or bias the content of the paper.

2.8 Acknowledgements

Funding for P. Deshuillers was made possible with support of Morris Animals Foundation (Grant #D15FE-902), and Purdue University through the Comparative Pathobiology department and the Andrew's fellowship.

Table 2.1: Results of the within-run imprecision study for PC content using 2 different calculation methods

	Method 1		Method 2	
	Mean PC content (nmol/mg)	Within-run CV (%)	Mean PC content (nmol/mg)	Within-run CV (%)
Reduced BSA	0.09	18.1	0.09	338.0
Pooled feline plasma	0.86	9.3	0.82	19.5
Pooled feline serum	0.98	8.5	0.91	18.9
Oxidized BSA	21.24	9.9	20.93	10.1

Table 2.2: Results of the between-run imprecision study for PC content using 2 different calculation methods

	Method 1		Method 2	
	Mean PC content (nmol/mg)	Between-run CV (%)	Mean PC content (nmol/mg)	Between-run CV (%)
Pooled feline plasma	0.72	69	0.09	80
Pooled feline serum	0.085	38	0.82	40

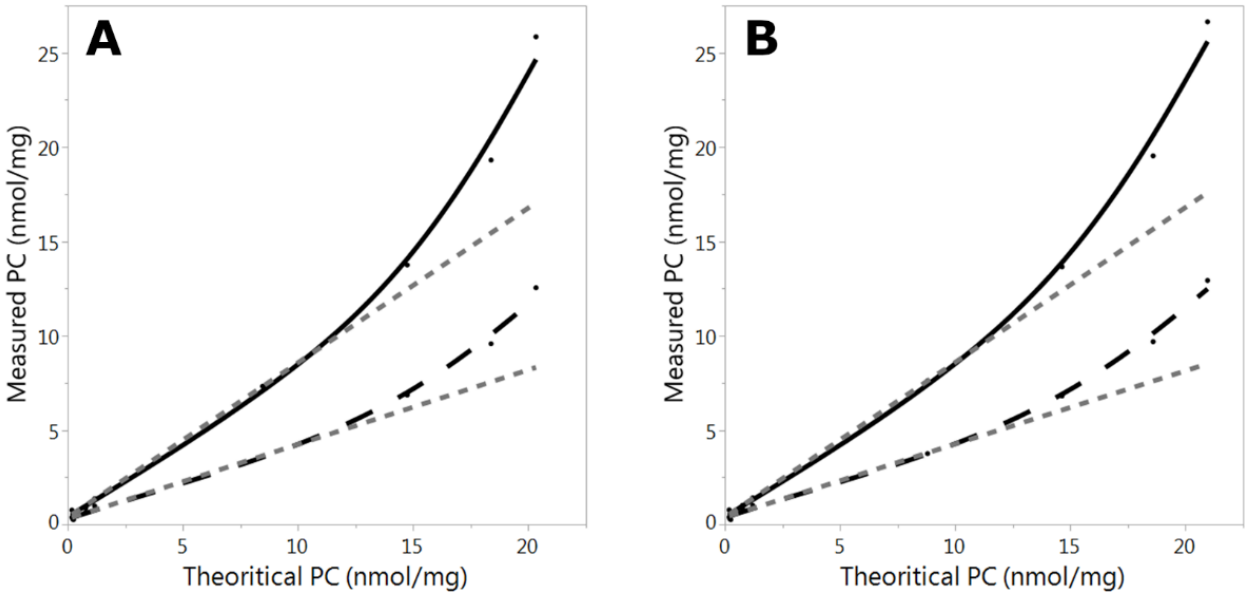

Figure 2.1: DNPH linearity study.
Serum (A) and plasma (B) samples were spiked with oxidized or reduced BSA to obtain a large range of PC content values. The measured PC content was calculated by two different methods and plotted against the calculated theoretical PC content of the spiked samples. The black solid and dashed lines represent the regression curves for the measured protein carbonyl content (method 1: solid line, method 2: dashed line) while the gray dashed lines illustrate linear relationship between the theoretical PC content and the measured PC content. Linearity is observed between 0.25 nmol/mg and 10 nmol/mg.

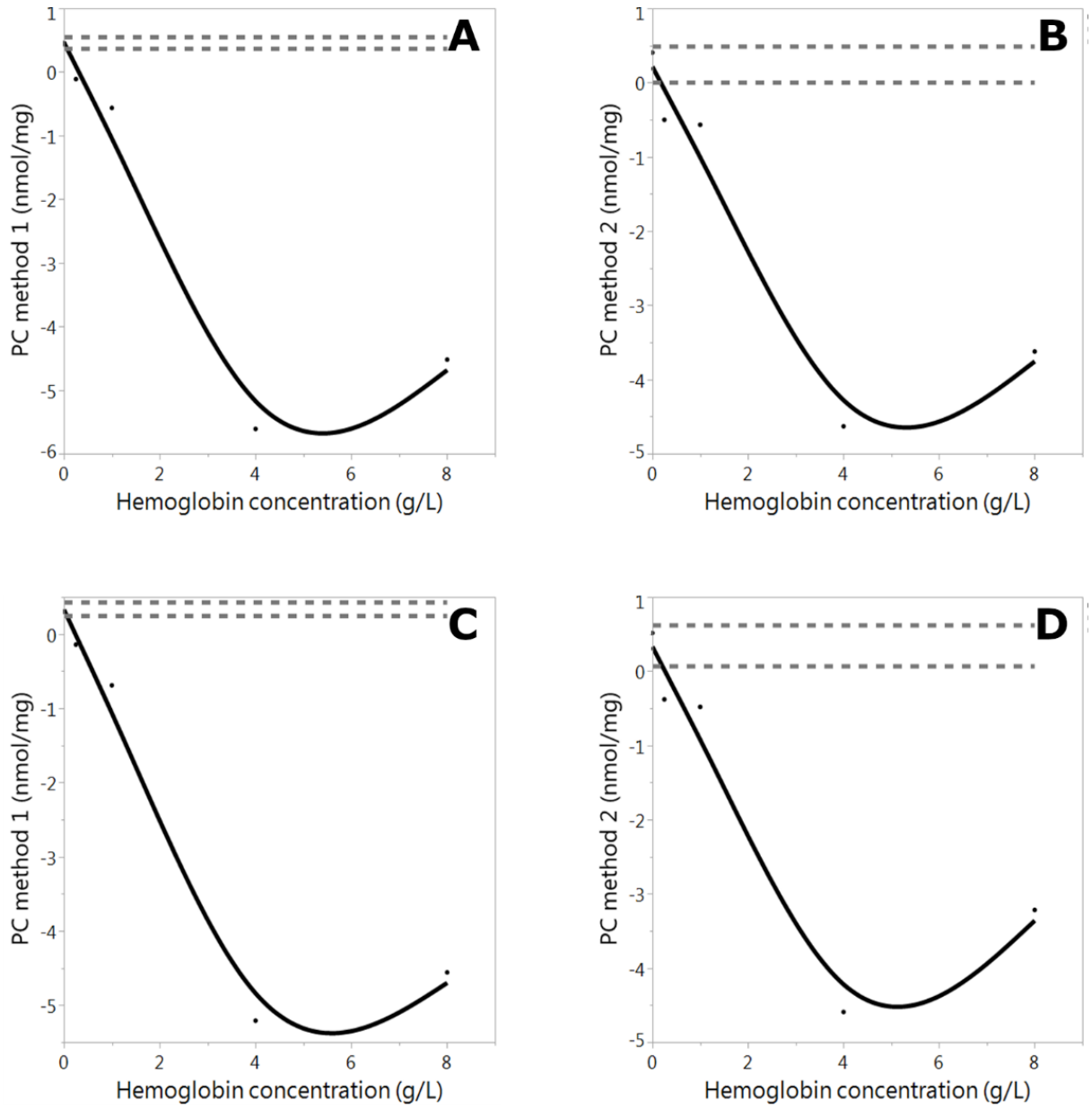

Figure 2.2: DNPH interference study
Pooled plasma (A and B) and serum (C and D) were spiked with hemoglobin over a wide range of hemoglobin concentrations. The measured PC content determined by the 2 calculation methods (method 1 depicted in figures A and C, method 2 is depicted in figures B and D) was plotted against the hemoglobin concentration. Black lines represent the regression curve determined by the least square method from the measured PC content while the dashed gray line represents the PC content of the sample without interferent ±20%. Marked negative interference was observed in all spiked samples regardless of the hemoglobin concentration.

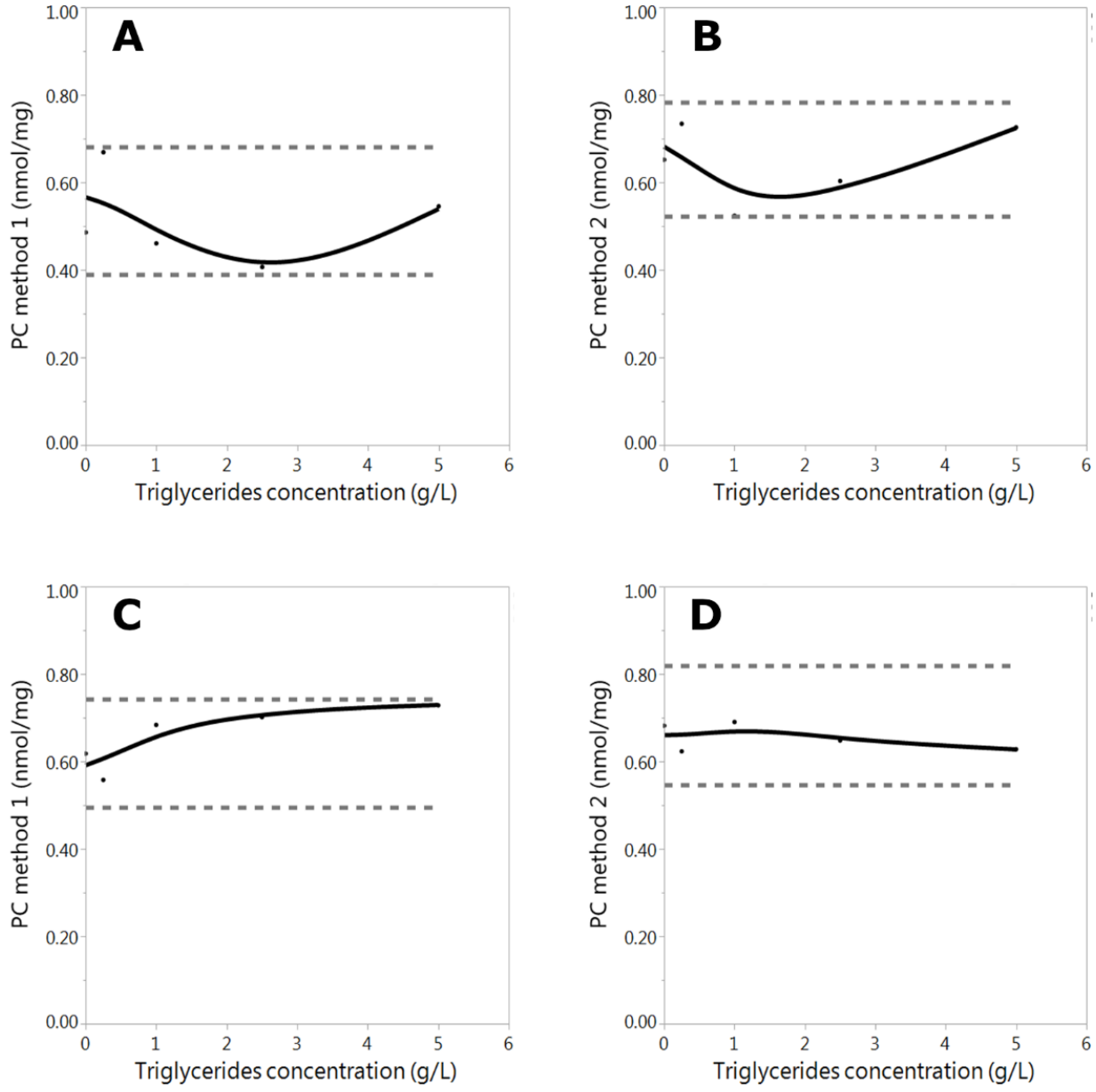

Figure 2.3: DNPH interference study

Pooled serum (A and B) and pooled plasma (C and D) were spiked with triglycerides over a wide range of triglyceride concentrations. The measured PC content was calculated with 2 different methods (method 1 is illustrated by figures A and C while method 2 is illustrated by figures B and D) plotted against the triglyceride concentration. The black lines represent the regression curves as determined by the least square method. The gray dashed lines represent the PC content of the sample without interferent ±20%. The PC content measurement remains within the acceptable limits (PC content measurement without interference ±20%) for both calculation methods. Indicating the absence of significant interference of triglycerides.

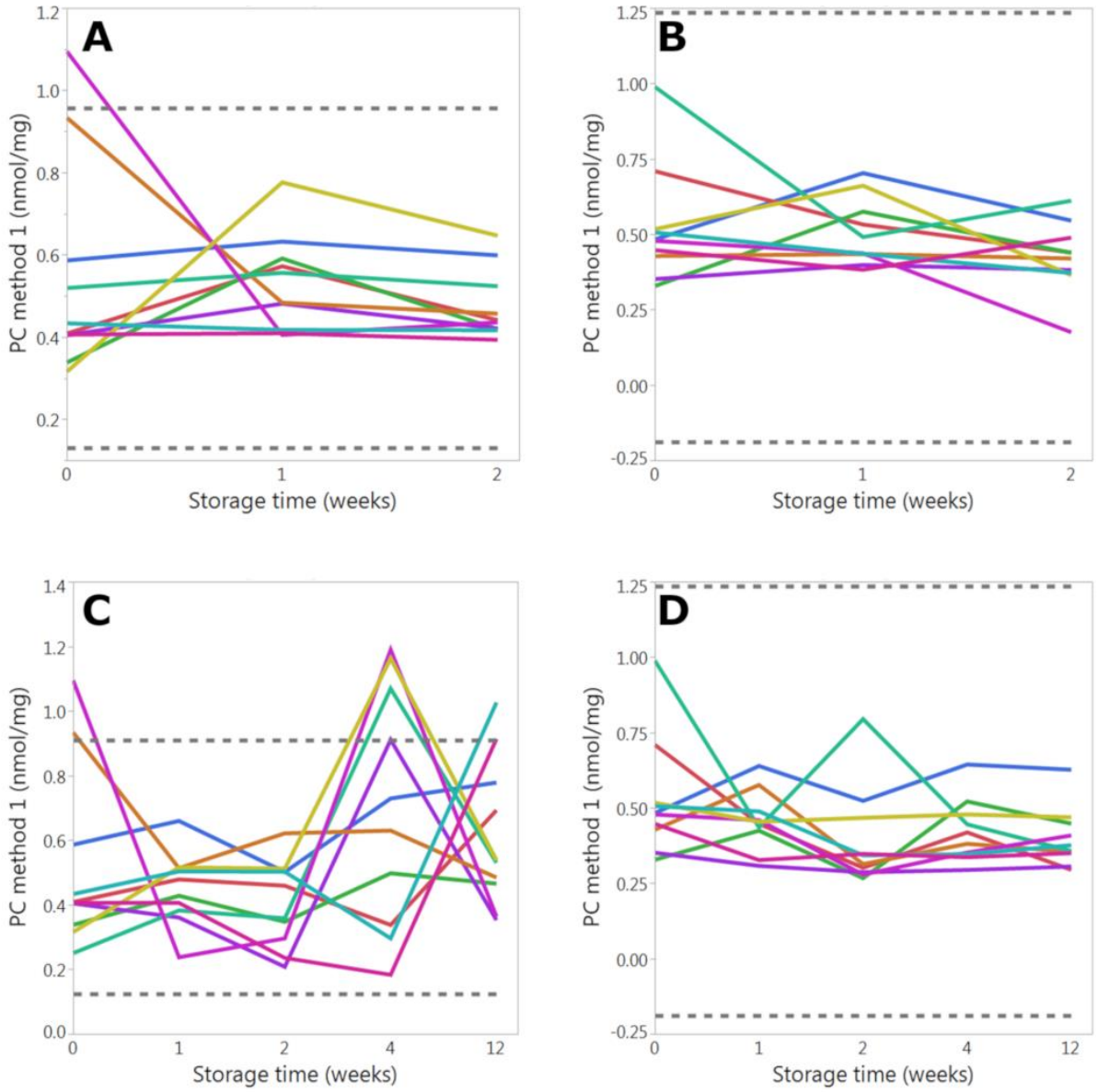

Figure 2.4: DNPH PC stability evaluation (calculation method 1)
Serum (figures A, C and E) and plasma (figures B, D and F) were stored at 4 °C (figures A and B), -20 °C (figures C and D) and -80 °C (figures E and F) for up to 2 weeks or up to 12 weeks. The PC content calculated with the method 1 was plotted against the storage time. The different color lines represent the 10 different specimens tested over time while the grey dashed line represent the average of the 10 specimens ±2 between-run CVs. Most of the measurement remain between the dashed lines and all samples remained between their initial values ±2 between-run CVs indicating that no significant change in the PC content could be detected over time.

Figure 2.4 continued

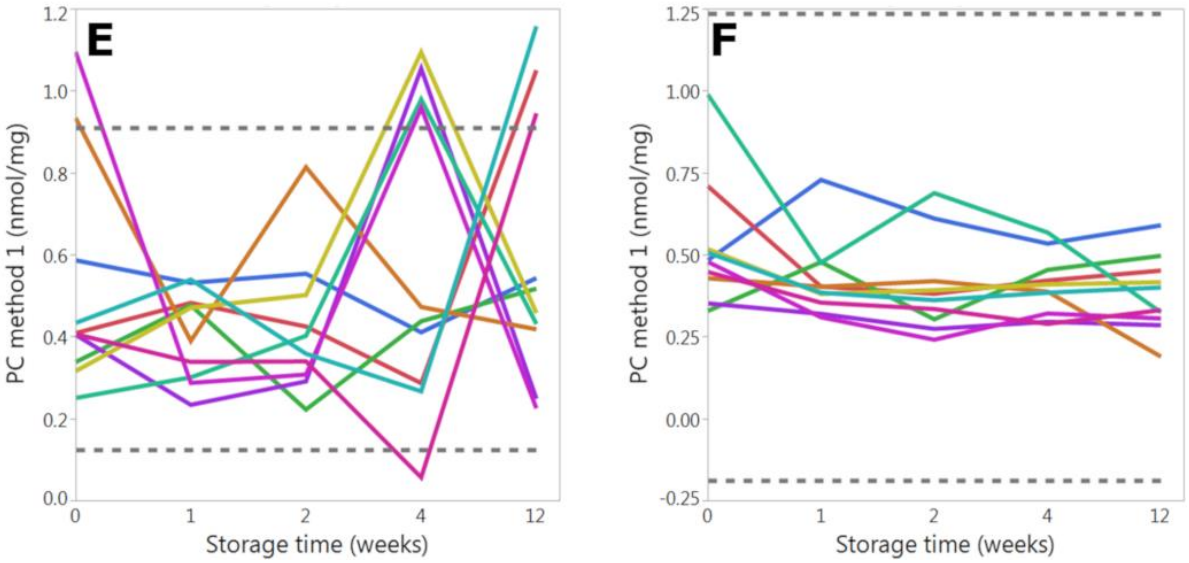

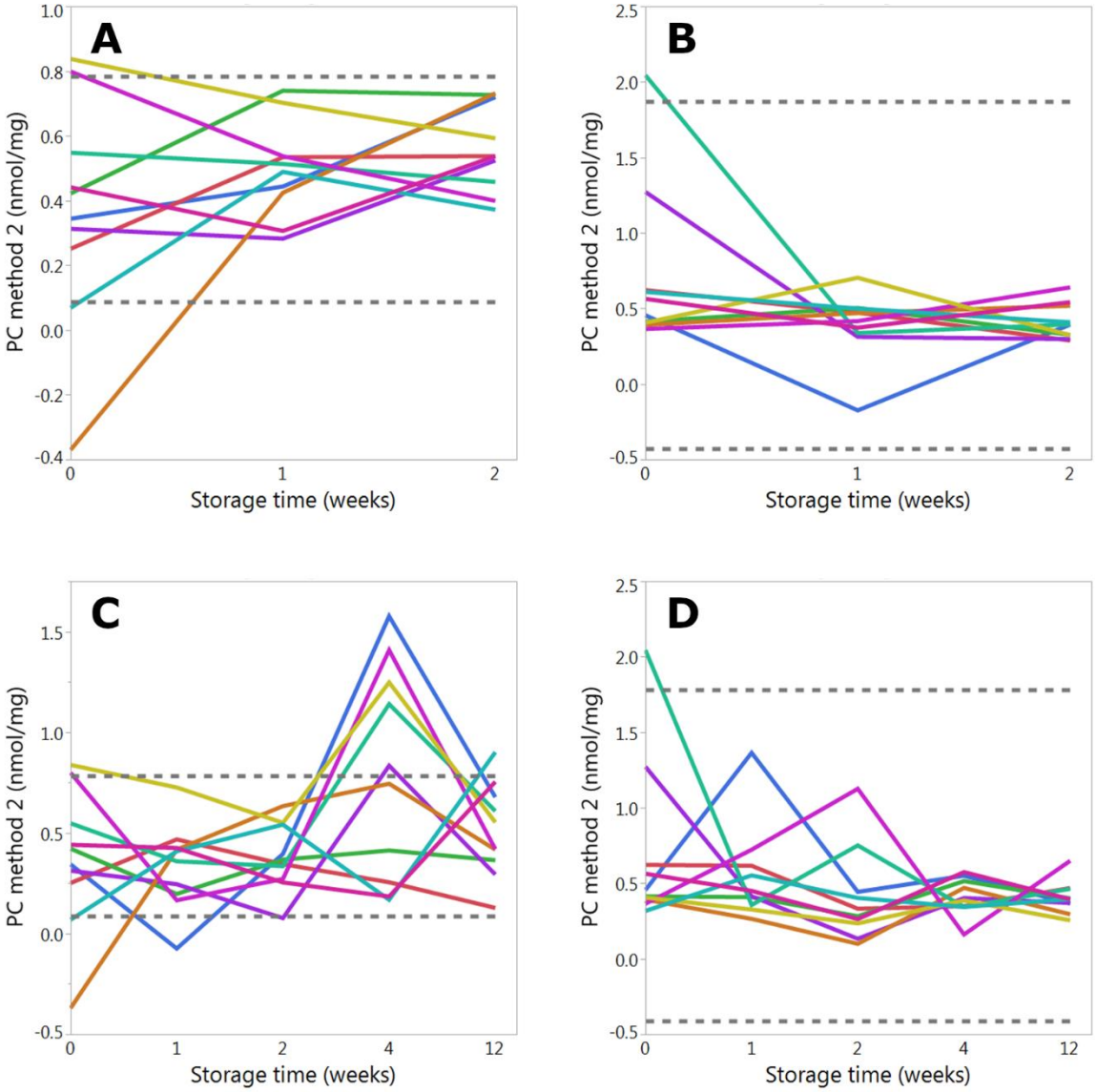

Figure 2.5: DNPH PC stability evaluation (calculation method 2)
Serum (figures A, C and E) and plasma (figures B, D and F) were stored at 4 °C (figures A and B), -20 °C (figures C and D) and -80 °C (figures E and F) for up to 2 weeks or up to 12 weeks. The PC content calculated with the method 2 was plotted against the storage time. The different color lines represent the 10 different specimens tested over time while the grey dashed line represent the average of the 10 specimens ±2 between-run CVs. Most of the measurement remain between the dashed lines and all samples remained between their initial values ±2 between-run CVs indicating that no significant change in the PC content could be detected over time.

Figure 2.5 continued

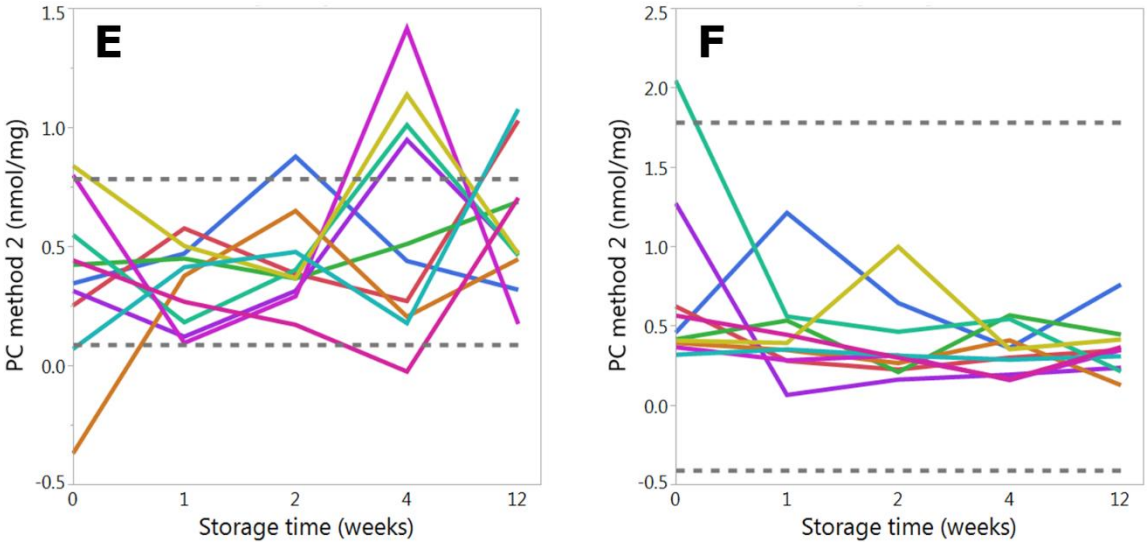

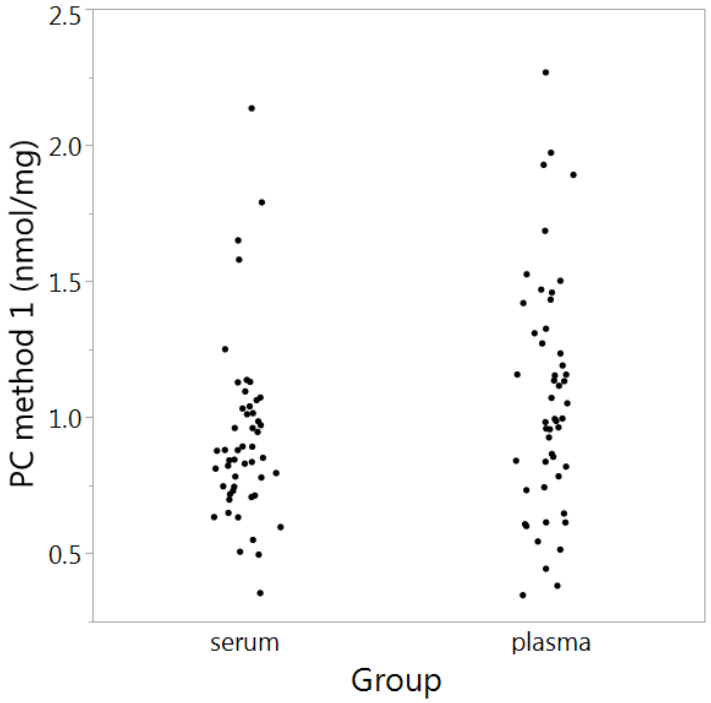

Figure 2.6: Range of PC content
In serum, values ranged from 0.35 to 2.14 nmol/mg while in plasma, PC content ranged from 0.34 to 2.27 nmol/mg.

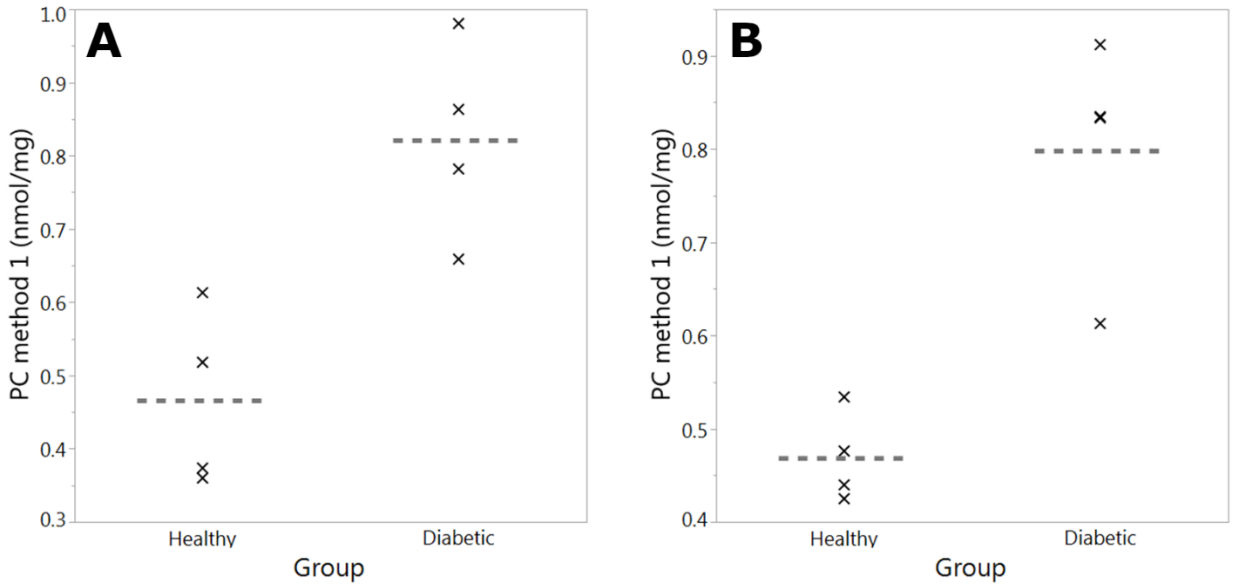

Figure 2.7: PC content comparison between healthy and diabetic cats
Diabetic cats had a significantly higher serum (A) and plasma (B) PC content than healthy cats ($P<0.01$). The gray dashed line represents the mean.

CHAPTER 3. DEVELOPMENT AND VALIDATION OF A RAPID, FLUORESCENT-BASED ASSAY, FOR PROTEIN CARBONYL CONTENT QUANTIFICATION, IN FELINE SERUM AND PLASMA

3.1 Abstract

Protein carbonyls (PC) result from the oxidation of amino acid side chains by reactive oxygen species during oxidative stress and increased PC carbonyl content has been described in humans and laboratory animals in association with a variety of diseases. We have previously described a colorimetric method to assess PC in feline serum and plasma samples; however, this technique is time-consuming, labor-intensive and prone to variation between-runs. The goal of this study was to describe and evaluate the performances of an alternative, fluorimetric technique using 4-hydrazino-7-nitro-2,1,3-benzoxadiazole hydrazine (NBDH). Serum and plasma specimens were obtained from client, staff, student and faculty owned cats to determine within and between-run variability, linearity, limit of detection, ranges of values found in feline samples, and the effect of hemolysis and lipemia on PC content. Comparison of the colorimetric assay and this new method was performed. Finally, the serum and plasma PC content of diabetic cats was evaluated to document the potential usefulness of this assay.

This new fluorimetric assay revealed low within and between-run variability (<20%). The limit of detection was low (0.09 nmol/mg) and linearity was maintained over a wide range of PC content (0.09 to 9nmol/mg). Both hemolysis and lipemia interfered significantly when over 2g/L. Cats involved in this study had serum and plasma PC content ranging from 0.45 to 2.98 nmol/mg and 0.17 to 3.61 nmol/mg respectively. When compared, the colorimetric and fluorimetric methods correlated strongly even if constant and proportional biases were identified. Finally, this assay detected a significant difference in the PC content of serum and plasma of diabetic cats when

compared to healthy controls, suggesting that it may be a good alternative to the colorimetric assay and may help better understand the role of oxidative stress in feline diseases.

3.2 Introduction

Protein carbonyls (PC) result from the direct oxidation of amino acid side chains by reactive oxygen species (ROS) or from oxidation by aldehyde intermediates produced during lipid peroxidation and from the glycoxidation of lysine moieties yielding advanced glycation end-products[208]. PC are considered early biomarkers of oxidative stress and their accumulation has been described in a variety of human diseases including diabetes mellitus, Alzheimer's disease, inflammatory bowel disease and arthritis[208]. In cats, oxidative stress has been documented in multiple diseases such as diabetes mellitus[22,39,200], chronic kidney disease[201-203], feline immunodeficiency virus infection[204], hyperthryroidism[39,205], lymphoma[39], hypertrophic cardiomyopathy[206] and feline infectious peritonitis[207]; yet, PC have not been investigated.

The historical, most commonly used method to determine PC content is a colorimetric technique using 2,4-dinitrophenylhydrazine (DNPH)[127]. The major advantage of this assay is that it does not require standards as the PC content can be determined directly from the absorbance and the extinction coefficient of DNPH. However, this assay is work-intensive and time-consuming and has a high between run variation. ELISA assays using anti-DNPH antibodies to detect DNPH-reacted proteins are often employed; yet, they are time consuming, expensive to run and results cannot be compared between laboratories[128,129]. Several fluorophores able to react with protein carbonyls have been described in the literature[130] and some of them have been validated in cell lysate[126] or plasma[126,131]; however, assays using these fluorophores need extensive washing or filtration to remove unreacted fluorescent probes except for 4-hydrazino-7-nitro-2,1,3-

benzoxadiazole hydrazine (NBDH) which is not fluorescent contrary to its protein-hydrazone[132]. NBDH was used for plasma and cell lysate protein carbonyl testing but the published protocol is unclear, and we were not able to repeat it.

So, the goal of this study was to develop and validate a new NBDH-based fluorimetric assay for protein carbonyl determination in feline serum and plasma samples.

3.3 Material and methods

3.3.1 Samples

Samples used for this project were collected with the approval of the Purdue University Animal Care and Use Committee (protocol # 1610001488). Both serum and plasma were obtained from healthy cats and cats with a variety of conditions as described below.

3.3.2 Reagents

All chemicals were of analytical grade, from Thermo Scientific (Waltham, WA, USA) except for the 2,4-dinitrophenylhydrazine and the 4-hydrazino-7-nitro-2,1,3-benzoxadiazole hydrazine (NBD-H) which were acquired from Tokyo Chemical Industry America (Portland, OR, USA).

3.3.3 Colorimetric determination of protein carbonyl content

This assay is based on the reaction of DNPH carbonyls, yielding to a dinitrophenyl hydrazone product detected spectrophotometrically. Total protein concentration of the specimens was determined by refractometry (Reichert VET 360, Reichter Technologies) and serum or plasma specimens were diluted to 5 g/L with double distilled water (ddH_2O). The method to quantify protein carbonyl content was adapted from the historical 2,4-dinitrophenylhydrazine (DNPH) derivatization technique described by Levine et al[127]. For each specimen a blank and a test

specimen were run in in parallel. Briefly, 200 µL of diluted specimen were pipetted into two, 2 mL microcentrifuge tubes. Eight hundred microliters of a 2.5M hydrochloric acid aqueous solution were added to blanks while 800 µL of DNPH working solution (10mM DNPH in 2.5M hydrochloric acid) were added to the test specimens. After mixing, preparations were incubated in the dark for 1h with homogenization every 15 min. At the end of the incubation, 900 µL of 20% trichloroacetic acid solution were added, preparations were placed on ice for 10 min and then centrifuge at 10000g for 15 min at 4 °C. Supernatants were discarded without disturbing the pellet and 1 mL of 10% TCA solution was pipetted into the tubes. Preparations were homogenized with the FastPrep®-24, placed on ice for 10 min and centrifuged at 10000g for 15 min at 4 °C. After the supernatant was discarded, pellets were washed three times with 1 mL of ethyl acetate/ ethanol (1/1; v/v) to remove unreacted DNPH. Following the addition of ethyl acetate/ethanol, samples were always mixed with the FastPrep®-24 and centrifuged at 10000g for 15 min at 4C except after the last wash when the preparations were centrifuge at 20000g for 15 min at 4C. Following the last wash, supernatants were carefully discarded, and pellets were left to dry in a fume hood, in the dark (for approximately 30-45 min). Pellets were resuspended in 500 µL of a 6M guanidinium hydrochloride, 2mM KH_2PO_4 solution at pH=2.5. Two hundred and twenty microliters of the blank and test protein suspensions were placed in a transparent 96-well microplate (SpectraPlate-96 MB, PerkinElmer). All measurements were carried out in duplicates on the SpectraMax i3x microplate reader (Molecular Devices) with absorbance measured at 375 nm. Absorbance was averaged from the duplicates and the molar coefficient of 22,000 $M^{-1}cm^{-1}$ was used to quantify the protein carbonyl content. Blanks and tests were diluted 10 times in ddH_2O prior to protein quantification by the Pierce™ BCA Assay kit (Thermo Fisher) following the manufacturer's instructions.

3.3.4 Fluorimetric determination of protein carbonyl content

This assay is based on the reaction of the non-fluorescent NBDH with protein carbonyl moieties yielding a highly fluorescent hydrazone. An aqueous 2 mg/mL NBDH stock solution was prepared, aliquoted and frozen at -20 °C until use. The working solution was prepared by diluting the stock solution 10 times in ddH_2O, just before use. Serum and EDTA plasma specimens were prepared similarly: total protein concentration was determined by refractometry (Reichert VET 360, Reichter Technologies) and, adjusted to 20 g/L with ddH_2O. One hundred microliters of diluted specimens were placed in a 2 mL microcentrifuge tube. Four hundred microliters of methanol and 100 µL of chloroform were added to the specimens and samples were homogenized. Following the addition of 300 µL of ddH2O, samples were vortexed and centrifuged for 10 minutes at 4 °C, 20000g. The upper aqueous phase was carefully removed and discarded before adding 400 µL of methanol. Samples were homogenized and centrifuged again for 10 min at 4° C, 20000g. Supernatant was discarded, and the protein pellets were dried in a fume hood. Pellets were then resuspended in 400 µL of a 6M guanidinium hydrochloride, 2mM KH_2PO_4 solution adjusted to pH=2.5. One hundred microliter of standard solutions and processed specimens were placed in a black opaque 96-well microplate (OptiPlate-96 Black, PerkinElmer). All measurements were carried out in triplicates on a SpectraMax i3x microplate reader (Molecular Devices, San Jose, CA) with excitation at 480nm and emission at 560 nm. Plates were read immediately after the addition of 100 µL of NBDH working solution, every three minutes, for one hour. The remainder of the processed samples was diluted 10 times in ddH_2O and protein concentration was measured by the Pierce™ BCA Assay kit (Thermo Fisher) following the manufacturer's instructions.

3.3.5 Preparation of oxidized (oxBSA) and reduced BSA (redBSA)

Bovine serum albumin (BSA) was oxidized by adding 49 uL of a 12% sodium hydrochloride solution to 100 mL of a 1 g/L BSA solution in ddH_2O and incubated in a water bath at 37 °C for 15 min. BSA was reduced by adding 100 mg of sodium borohydride to 100 mL of a 5 g/L BSA solution in ddH_2O. The preparation was incubated for 30 min at room temperature and then neutralized with 1M hydrochloric acid. OxBSA and redBSA were concentrated and washed in Pierce Protein Concentrators, PES, 30K MWCO, 5-20 mL (Thermo Fisher, Waltham, WA, USA) using 1X PBS pH=7.4 for cleaning. Protein concentrations of both solutions were measured by refractometry (Reichert VET 360, Reichter Technologies, Buffalo, NY, USA) and aliquots of the solutions were kept at -80 °C until use. Protein carbonyl content of redBSA and oxBSA were determined by colorimetry as described previously.

OxBSA and redBSA stock solutions were diluted to 5 g/L in a 6M guanidinium hydrochloride, 2mM KH_2PO_4 aqueous solution at pH=2.5, just before use. Different volumes of diluted oxBSA and redBSA solutions were mixed to create a standard curve while maintaining a constant total protein concentration. Six standards were used for the standard curve: 60, 40, 20, 10, 5, and 0% oxBSA and 40, 60, 80, 90, 95, and 100% redBSA respectively.

3.3.6 Specimens and test performances

Performances of the fluorimetric assay were evaluated using serum and plasma samples from the Purdue University Clinical Pathology Laboratory, remaining after all analyses prescribed by the clinicians had been performed and validated.

First, to determine the time needed for the NBDH to react with protein carbonyls, fluorescence was followed over time for feline serum, plasma and a mixture of oxBSA and redBSA every three minutes for one hour. For the remainder of the experiments, calculations were

performed at the 15 min timepoint. Then, intra-run variation was determined by measuring the PC content at three different levels: low (redBSA), medium (serum and plasma) and high (oxBSA), 20 times in the same run. Between run variation was established by measuring the PC content of serum and plasma samples in 10 consecutive runs over 10 days. Linearity was assessed by mixing different amounts of serum and plasma with oxBSA and redBSA to obtain a wide range of PC content while maintaining the protein concentration. In the linear range, a least-squares regression analysis was performed to assess correlation between fluorescence and theoretical PC content. The limit of quantification was determined as recommended by the US-FDA[211]. Interferences from hemolysis and lipemia were tested by spiking serum and plasma samples with increasing amounts of hemoglobin and triglycerides (Intralipid 20%, Fresenius Kabi USA). Hemoglobin was obtained from feline red blood cells lysed in ice-cold ddH_2O. Hemoglobin concentration was determined spectrophotometrically. Interference was considered significant when a difference of more than 20% was observed between the initial PC content and the PC content of the spiked samples. To document a range of PC content that can be found in feline serum and plasma, 50 non-hemolyzed, non-lipemic serum and 50 non-hemolyzed, non-lipemic plasma specimens were assayed. Specimens were grouped into the following diagnosis categories: healthy, lymphoma, diabetes, hyperthyroidism, renal disease, infectious disease, inflammatory disease with no evidence of infection, non-lymphoma cancer, and others. Serum specimens used to determine the range of values observed in cats were collected from 29 castrated males, 20 spayed females and a one intact male. These cats, separated into age groups following the American Association of Feline practitioners and the American Animal Hospital Association[210], consisted of seven junior, six prime, 16 mature, 10 senior and, 11 geriatric cats. They were healthy felines with no known disease (8), and patients with renal disease (12), lymphoma (7), inflammatory disease with no evidence of

infection (6), cancer other than lymphoma (5), hyperthyroidism (4), infectious disease (2), diabetes (1) and other diseases (5). Similarly, plasma was obtained from 14 castrated males, 33 spayed females and, 3 intact females, consisting in seven junior, six prime, eight mature, 12 senior and, 17 geriatric cats. These cats were healthy (7) or had a variety of diseases including, renal disease (14), lymphoma (9), cancer other than lymphoma (4), inflammatory disease with no evidence of infection (4), hyperthyroidism (3), diabetes (2), infectious disease (2) and other diseases (5). Normality was assessed by the Shapiro-Wilk test and Student *t*-tests or Kruskal-Wallis test were performed to compares PC content between groups.

A comparison of PC content between the colorimetric and this new fluorimetric method was performed as previously recommended[215-218]. To cover a wide range of PC content, five serum and plasma samples were utilized. Protein concentration was adjusted to 20 g/L and samples were mixed with increasing amounts of a 20 g/L oxBSA aqueous solution. Correlation and agreement between the two methods were determined by Passing-Bablok regression and Bland-Altman analyses. Normality of the distribution of differences between paired NBDH and DNPH PC contents was assessed by the Shapiro-Wilk test.

Finally, serum and plasma were collected from four diabetic cats with ketoacidosis and evidence of systemic oxidative stress as indicated by the presence of increased Heinz bodies on the surface of red blood cells. Samples were stored at -80 °C until the PC contents were determined by fluorimetry. A Student *t*-test was run to compare groups.

For this study, all statistical analyses were performed with JMP®, version 13.2.0 (SAS Institute Inc.) a P value <0.05 was considered significant. For the Passing-Bablok regression and the Bland-Altman analysis, an add-in to JMP® can be found at this address

(https://community.jmp.com/t5/JMP-Add-Ins/Method-Comparison/ta-p/21520) (accessed the last time on 09/01/2018).

3.4 Results

Fluorescence of oxBSA, redBSA, serum and plasma samples increased over time to reach a plateau at 15 min and remained stable thereafter for the 60-minute time span of fluorescence measurement. **(Figure 3.1)**. All the calculations for subsequent studies were obtained using fluorescence values at 15 min. Results of the imprecision study are shown in **Table 3.1**. Within run CV was less than 10% in pooled serum and plasma samples as well as in oxBSA. CV for redBSA was less than 20%. Fluorescence was plotted against the theoretical PC content of the samples to determine linearity **(Figure 3.2)**. A linear relationship was observed between the theoretical PC content of specimens and fluorescence from 0.09 to 9 nmol/mg for both serum and plasma. When samples with a PC content above 9 nmol/mg were excluded, regression analysis by the least-squares method showed an excellent correlation between the PC content and fluorescence ($P<0.0001$, coefficient of determination $r^2 = 0.99$ for serum and 0.98 for plasma). For both serum and plasma, the lower limit of quantification was 0.09 nmol/mg. When serum and plasma samples were spiked with hemoglobin or triglycerides, a significant negative interference was identified when interferent concentration reached 2g/L **(Figure 3.3)**.

In serum and plasma samples, no significant difference between sex and age groups was observed. No significant difference was identified in serum or plasma between healthy felines and cats from each diagnosis groups. Additionally, no significant difference was found between healthy and sick cats. PC content ranged from 0.45 to 2.98 nmol/mg and 0.17 to 3.61 nmol/mg with averages at 1.26 nmol/mg and 0.93 nmol/mg for serum and plasma, respectively **(Figure 3.4)**.

Results of the correlation and agreement study are summarized in **Table 3.2**. An excellent correlation was observed between the fluorimetric and colorimetric method to determine PC content in serum and plasma ($P<0.001$ and Spearman's correlation $r = 0.93$ for serum and 0.98 for plasma) **(Figures 3.5)**. Regression analysis showed a constant bias (0.82, 95% CI: 0.57; 1.37) and non-significant proportional bias (0.91, 95% CI: 0.79; 1.03) in serum. In plasma, a constant (0.83, 95% CI: 0.47; 1.07) and proportional bias (0.86, 95% CI: 0.78; 0.95) were present. For both serum and plasma, the distribution of the difference between the PC content determined by the fluorimetric and colorimetric method was considered normal. In serum, a positive constant bias (1.08; 95% CI: 0.4; 1.76) and a proportional negative bias (-0.15; 95% CI: -0.27; -0.02) were identified **(Figure 3.5)**. Similarly, in plasma a positive constant (0.92; 95% CI: 0.35; 1.48) and a negative proportional bias -0.16; 95% CI: -0.27; -0.05) were observed **(Figures 3.5)**.

Mean serum and plasma protein content in diabetic cats were respectively 1.66 and 1.48 nmol/mg while 1.18 and 1.02nmol/mg in age and sex-matched healthy controls. In both serum and plasma, differences were significant ($P=0.008$ in serum and 0.002 in plasma). **(Figure 3.6)**.

3.5 Discussion

A new method for PC content assessment in feline serum and plasma samples is described herein. This assay showed adequate performances over a large range of PC content. In comparison to other PC assays [126-129,131], this technique is significantly less time-consuming and work-intensive as removal of unreacted NBDH is unnecessary. Additionally, this assay requires easily available reagents, a centrifuge and a plate reader, equipment that are often available in research laboratories. A low between-run variation allows for a larger number of samples to be tested over multiple runs. Hence, this assay is a good alternative to the historical DNPH (colorimetric), ELISA and other

fluorimetric tests. In domestic animals, the number of validated assays for oxidative stress assessment is limited [135,203,207,212,213] and so far, only one has been validated for PC content (see chapter 2). In contrast to the colorimetric DNPH assay, this method requires a standard curve that is obtained by mixing oxBSA and redBSA in different proportions. The PC content of oxBSA and redBSA must still be determined by colorimetry. However, large amounts can be prepared and kept frozen for extended periods of time, since PC are considered stable when frozen [209].

Interestingly, both hemoglobin and triglyceride concentrations above 2g/L showed significance interference with the PC content. Visually, this corresponds to moderate-to-marked hemolysis and lipemia (**Figure 3.7**). To the best of our knowledge, the influence of hemolysis or lipemia on values obtained by fluorescence for PC content has not been previously studied. We recently determined, in a companion study, that the results obtained with the colorimetric assays were greatly influenced by the presence of hemoglobin, regardless of the hemoglobin concentration. On the contrary the colorimetric assays results were not altered by the presence of triglycerides (see chapter 2). This may be due to the different protein precipitation procedure and the number of washes required in the colorimetric assay. Nevertheless, hemolyzed and lipemic samples for PC content, whether determined by a fluorometric or colorimetric method, should be interpreted with caution.

When 50 random samples were collected to determine a range of PC content observed in feline serum and plasma no difference was identified between health status / diagnosis. Overall, the PC content observed were similar or close to those found for humans or laboratory animals [132,214,219,220]. The absence of significant difference between groups is likely due to the low number of individuals in each group and the variation within the groups. This variation likely results from the absence of control over the intensity or stage of the diseases as well as other factors such as

dietary pro-oxidant or antioxidant intake as they can modify the plasma PC content [221-223]. The goal of the section was to document PC content in cats and not to identify difference between health status groups. This would require much larger numbers of individuals per group.

In humans and laboratory animals, diabetes, especially when uncontrolled, is associated with increased oxidative stress. We are currently studying oxidative stress as part of broader study of systemic oxidant damage in cats with diabetes. Heinz bodies, inclusions within red blood cells of the cat, are considered evidence of oxidative stress related-damage to the hemoglobin molecule and are commonly observed in keto-acidotic diabetic patients [39]. However, these structures are insensitive indicators of oxidant damage; thus, blood and plasma protein carbonyls are also being determined as a quantitative measure of overall oxidative status in these patients. For this study, we selected diabetes as an oxidative stressor and when diabetic patient with ketoacidosis were compared to age and sex matched healthy cats, there was a significant difference in the serum and plasma PC content. Despite the low number of individuals, it appears an increase in systemic oxidative stress can be detected in such individual. This new assay will be useful for studying other diseases where there is evidence that induction of oxidative stress is a key process in the onset of disease complications.

3.6 Conclusion

In conclusion, this study described a new fluorimetric method for PC content determination in serum and plasma of cats. This technique is easy to perform and rapid requiring relatively cheap and easily available reagents and equipment. This assay is a new tool for the evaluation of oxidative stress-related damages to proteins and may prove useful in understanding the role of oxidative stress in diseases and to evaluate the effects of treatments.

3.7 Conflict of interest statement

None of the authors have financial or personal relationships that could inappropriately influence or bias the content of the paper.

3.8 Acknowledgments

Funding for P. Deshuillers was made possible with support of Morris Animals Foundation (Grant #D15FE-902), and Purdue University through the Comparative Pathobiology Department and the Andrew's fellowship.

Table 3.1: Results of the within-run imprecision study for PC content

	Mean PC content (nmol/mg)	Within-run CV (%)
Reduced BSA	0.09	18.1
Pooled feline serum	1.01	9.3
Pooled feline plasma	1.13	8.3
Oxidized BSA	9.9	8.4

Table 3.2: Results of the correlation and agreement study between the colorimetric DNPH method and the fluorimetric NBDH method for PC quantification in serum and plasma, 95% confidence intervals are presented in parentheses.

		Serum	Plasma
Passing-Bablok regression analysis	Significance	< 0.001	< 0.001
	Spearman's coefficient r	0.93	0.94
	Slope	0.91 (0.79; 1.03)	0.86 (0.78; 0.95)
	Intercept	0.82 (0.57; 1.37)	0.83 (0.47; 1.07)
Bland-Altman analysis	Shapiro-Wilk test	P = 0.15	P = 0.67
	Mean difference	0.40 (0.03; 0.77)	0.18 (-0.15; 0.50)
	Mean difference +2SD	1.99 (1.34; 2.64)	1.56 (1; 2.12)
	Mean difference -2SD	-1.19 (-0.54; -1.84)	-1.21 (-0.65; -1.77)
	Constant bias	Yes	Yes
	Proportional bias	Yes	Yes
	Slope	-0.15 (-0.27; -0.02)	-0.16 (-0.27; -0.05)
	Intercept	1.08 (0.4; 1.76)	0.92 (0.35; 1.48)

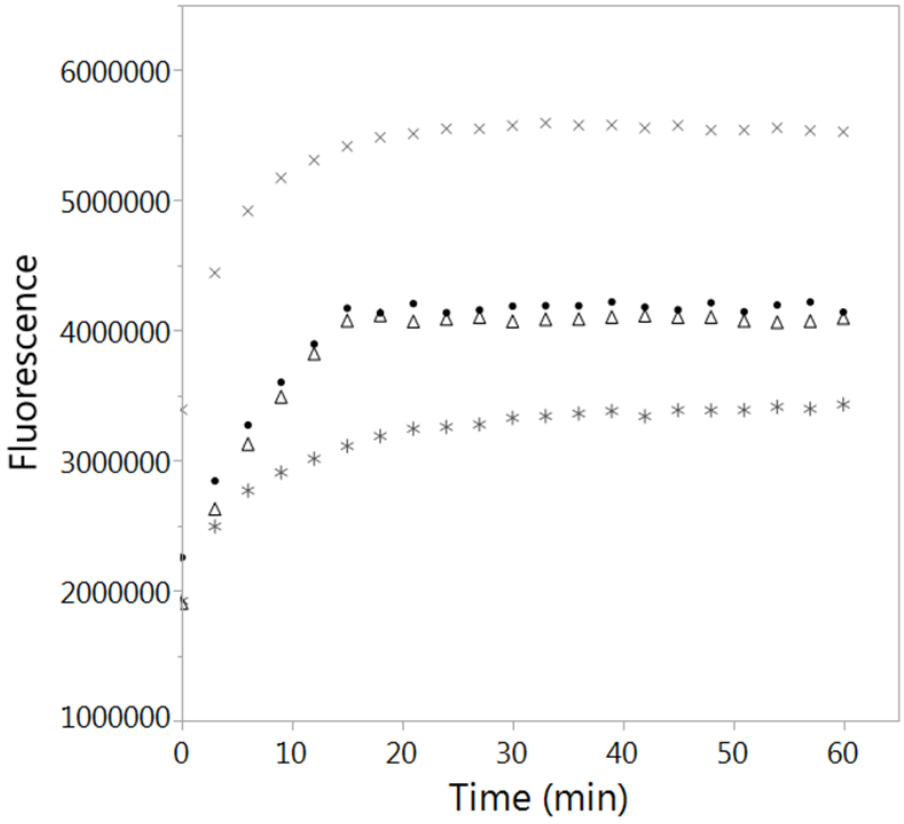

Figure 3.1: NBDH kinetic study
Fluorescence from oxidized and reduced BSA mixture (gray * and x, respectively), feline plasma (•) and serum (Δ) mixed with NBDH work solution was measured every three minutes for an hour. Fluorescence reached a plateau at 15 min, where all the following measurements where performed.

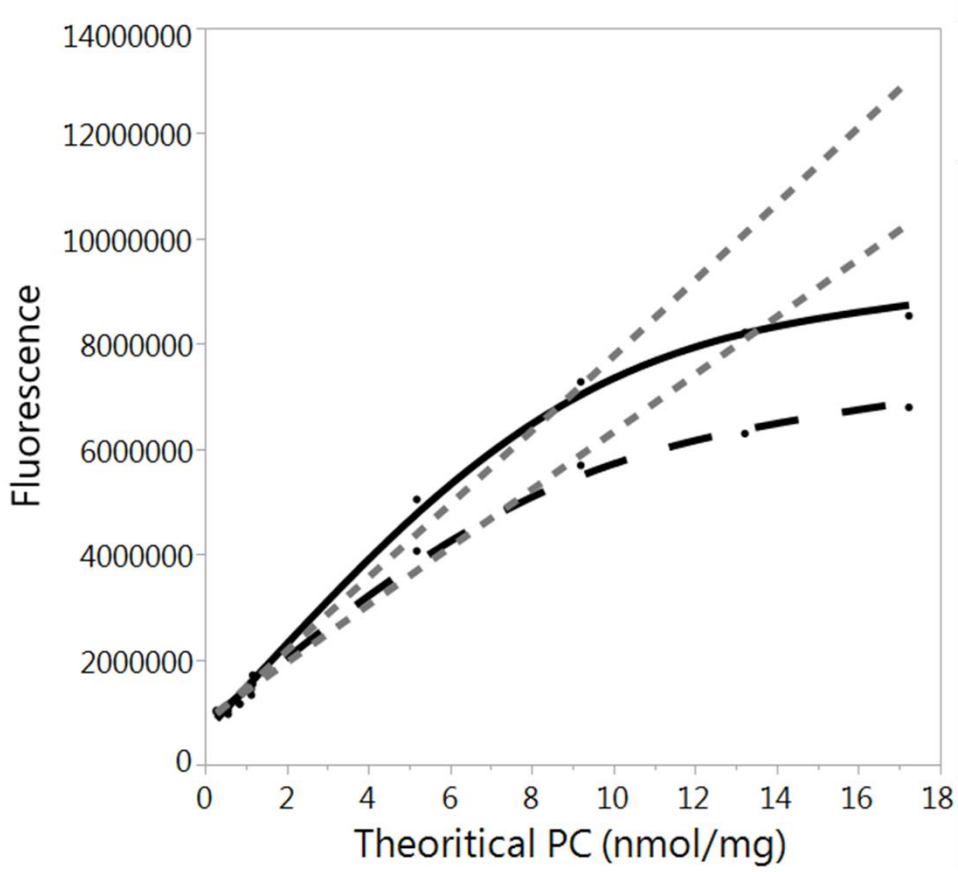

Figure 3.2: NBDH linearity study
Feline serum (black line) and plasma (dashed black line) samples were spiked with oxidized or reduced BSA while maintaining the same protein concentration. Dashed gray lines represent linearity which was observed between 0.09 nmol/mg and 9 nmol/mg.

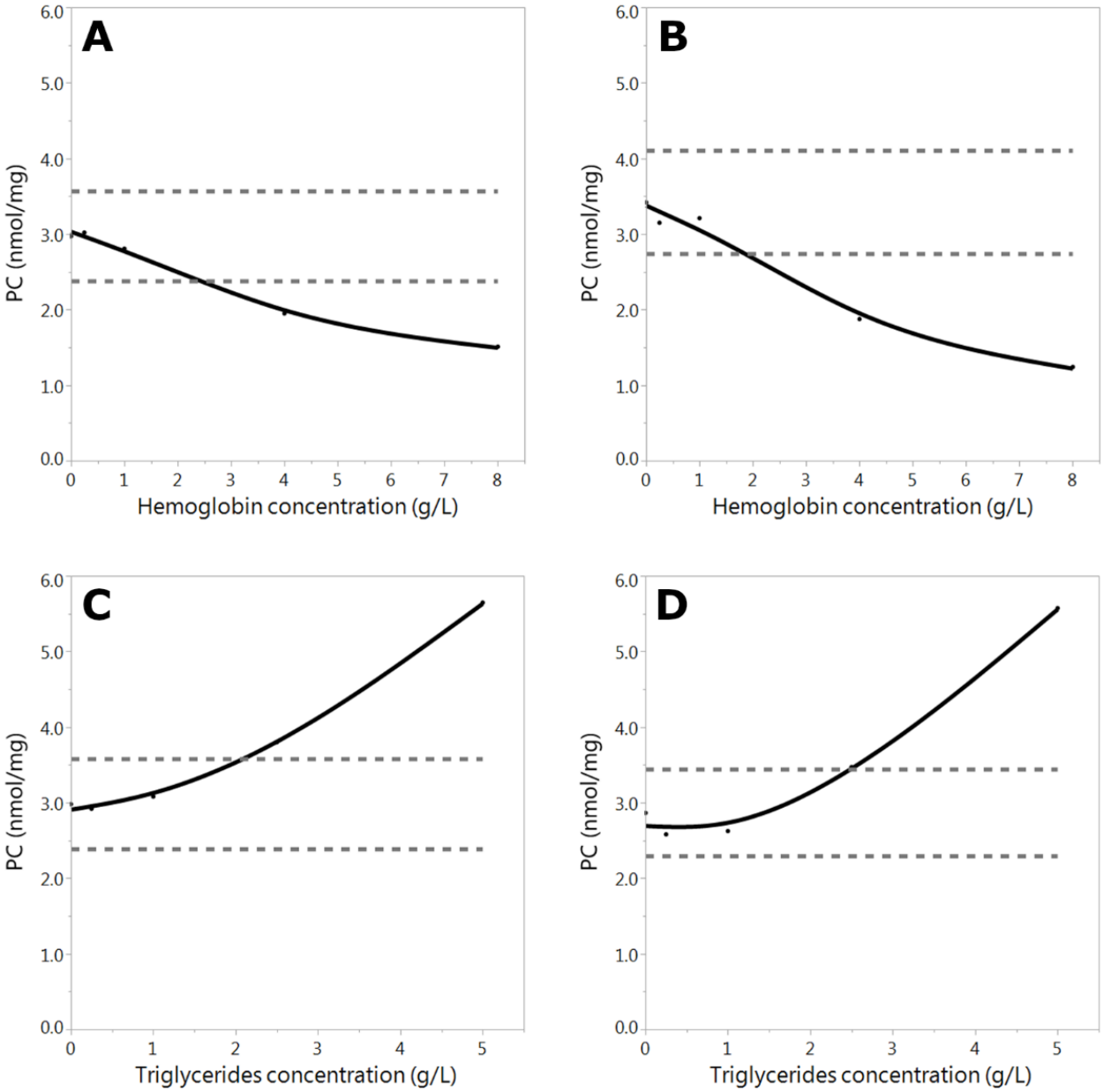

Figure 3.3: NBDH interference study
Feline serum was spiked with variable amounts of hemoglobin (A) and triglycerides (C). Similarly, feline plasma was spiked with hemoglobin (B) and triglycerides (D). Black lines represent the regression curves as determined by the least square method while the gray dashed lines represent the PC content of the specimens without interferent ±20%. Hemoglobin and triglycerides interference were considered significant above 2g/L.

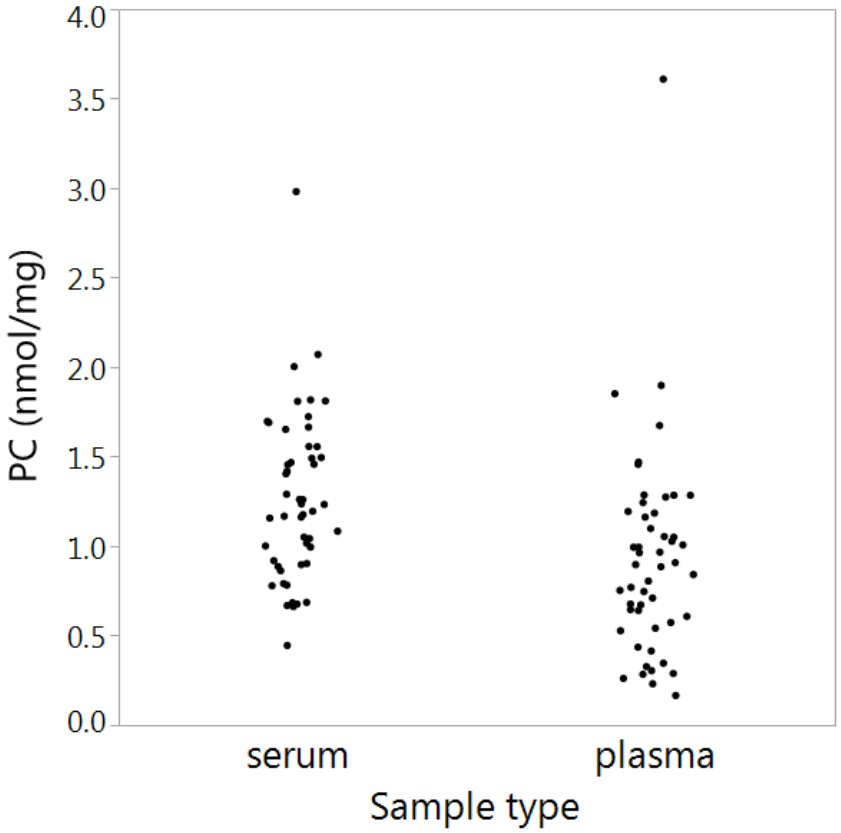

Figure 3.4: Range of PC content
In these cats, PC content ranged from 0.45 to 2.98 nmol/mg in serum and from 0.17 to 3.61 nmol/mg in plasma.

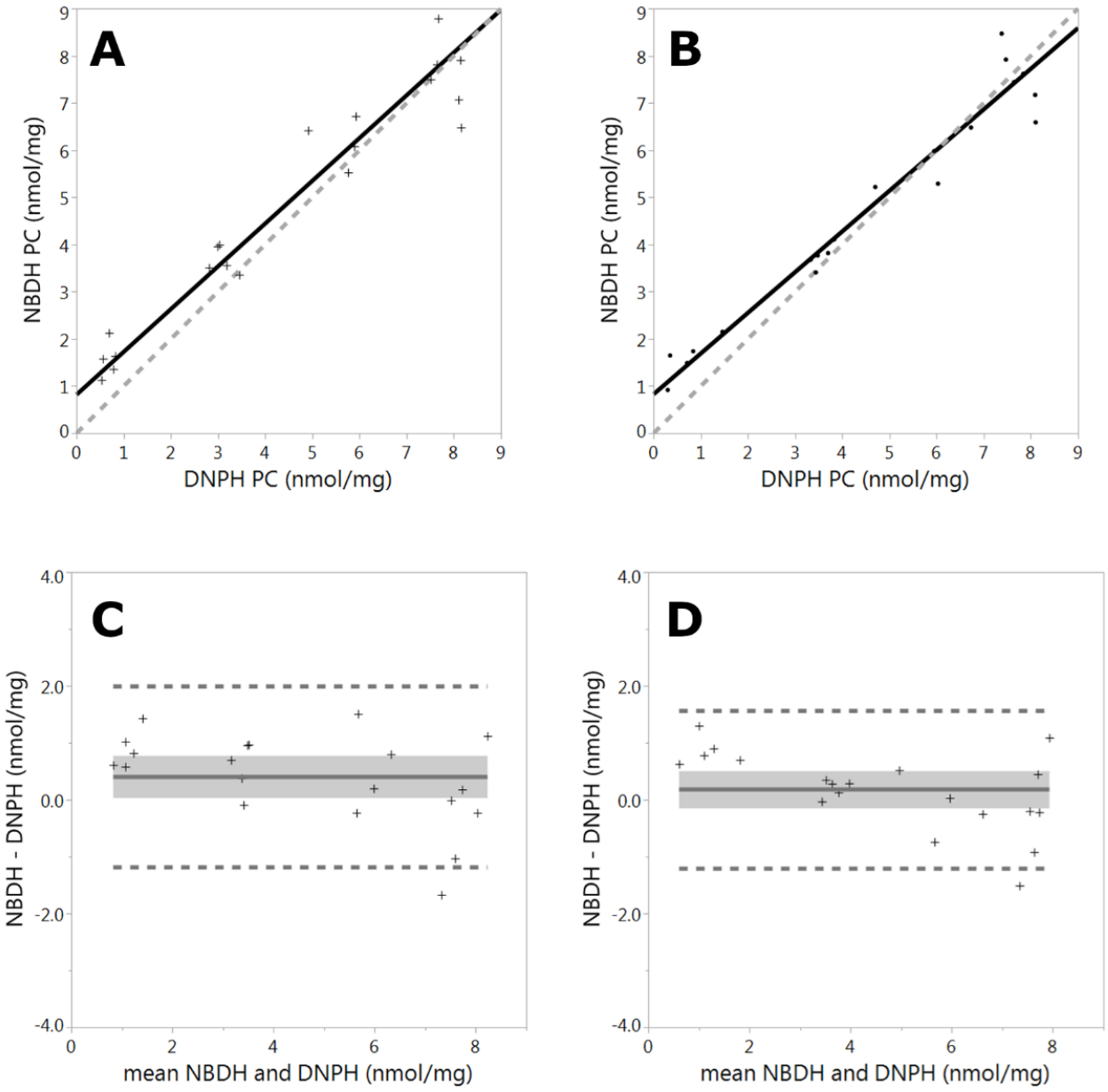

Figure 3.5: Comparison of PC content determined by the fluorimetric NBDH and the DNPH colorimetric assay

The fluorimetric PC content of serum (A) and plasma (B) specimens spiked with oxidized BSA was plotted against the colorimetric PC content. The black line represents the regression curve determined by Passing-Bablok regression analysis while the gray dashed line represents identity (y = x). A good correlation between the two techniques was observed. Serum (C) and plasma (D) Bland-Altman plots revealed a constant bias for serum and proportional biases for both specimen types. The gray line represents the overall mean of PC differences between the two methods while the solid gray area represents its 95% CI. The dashed lines illustrate the mean ±2 SD.

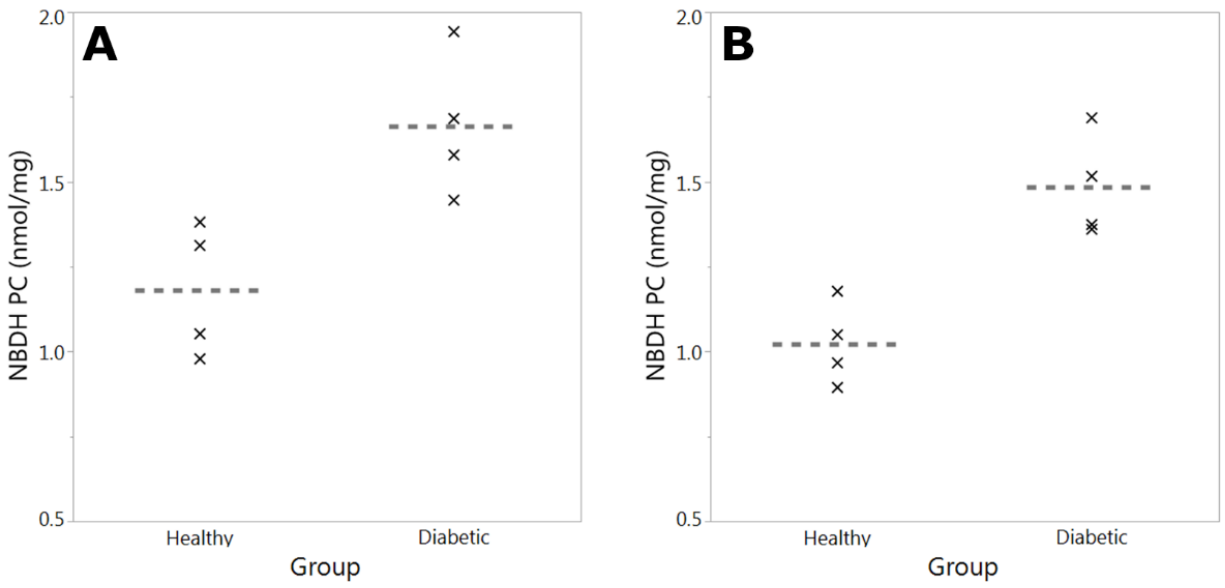

Figure 3.6: Comparison of serum and plasma PC content between healthy and diabetic cats Serum (A) and plasma samples(B) from diabetic cats had a significantly higher PC content than healthy controls ($P<0.01$).

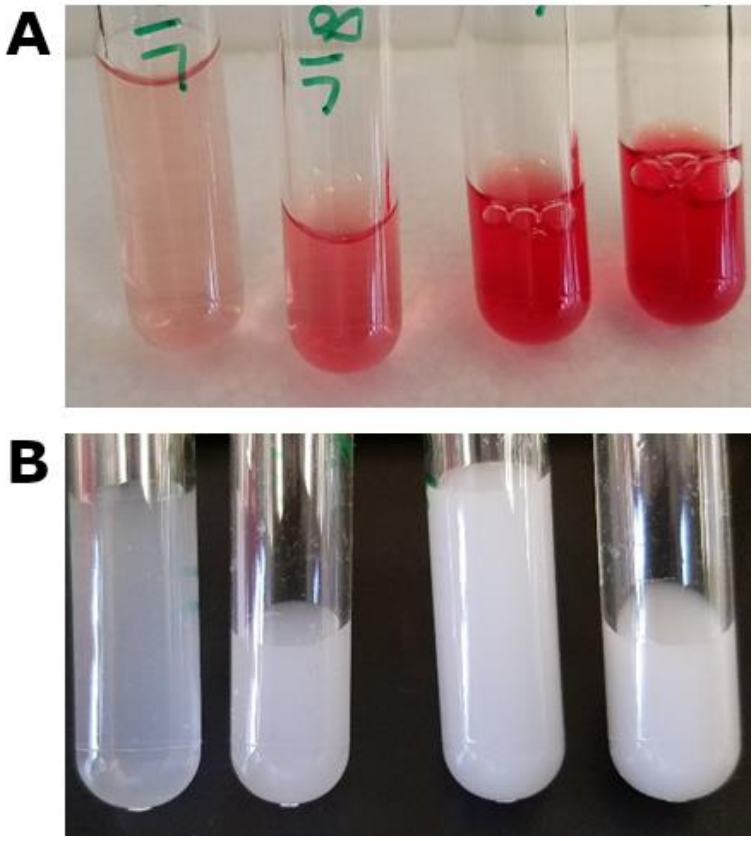

Figure 3.7: Visual aspect of serum and plasma samples spiked with hemoglobin or triglycerides
Serum and plasma were spiked with increasing amounts of hemoglobin (A) to obtain increasing degrees of hemolysis corresponding to increasing hemoglobin concentrations. From left to right hemolysis was mild (0.25 g/L), moderate (1 g/L) and marked (4 and 8 g/L). Similarly, serum and plasma samples were spiked with triglycerides (B) to obtain increasing degrees or lipemia corresponding to increasing triglyceride concentration. From left to right, lipemia was mild (0.25 g/L), moderate (1 g/L) and marked (2.5 and 5 g/L).

CHAPTER 4. SERUM TOTAL ANTIOXIDANT CAPACITY, EDTA-PLASMA F_2-ISOPROSTANES, AND ERYTHROCYTES GLUTATHIONE CONCENTRATION IN DIABETIC AND HEALTHY CONTROL CATS

4.1 Abstract

Oxidative stress results from the generation of reactive oxygen species (ROS) able to react non-specifically with biological components such as membrane lipids, proteins and nucleic acids. The level of ROS is normally kept under control by various antioxidants mechanisms. Diabetes mellitus has been associated with increased oxidative stress in people and animals. The goals of this study were to document oxidative stress and the potential usefulness of biomarkers not yet investigated in diabetic cats. Four diabetic and four age and sex-matched healthy controls cats were enrolled. Serum total antioxidant capacity, plasma F_2-isoprostanes concentration and erythrocyte glutathione concentrations were measured and compared between groups. Diabetic cats showed increased plasma F_2-isoprotanes and erythrocyte total glutathione in comparison to healthy controls. Despite a trend towards an increased oxidized glutathione concentration and increased total-to-oxidized glutathione ratio, differences were not significant. In our hands, the total antioxidant capacity assay did not work. As predicted, these results suggest oxidative stress related damage to cell membranes and an imbalance of the redox status of red blood cells towards oxidation. Our data provides support for further investigations into the use of isoprostanes and glutathione as biomarkers of oxidative stress in cats.

4.2 Introduction

Oxidative stress results from the increased generation of reactive oxygen species (ROS) and / or decreased antioxidant defenses. When ROS are not neutralized by antioxidant mechanisms,

they can attack non-specifically any biological components, including proteins, lipids, sugars, as well as nucleic acids. The effects of ROS on cell membrane polyunsaturated fatty acids are often dramatic as they can start a chain reaction of lipid peroxidation resulting in extensive membrane damage. During these reactions, isoprostanes are produced and released into the extracellular fluids where they can be measured[119-121]. F2-isprostanes are currently considered sensitive and specific markers of oxidative stress-related damages to cell membranes with increased plasma concentrations reported in a variety of human diseases[121]. ELISA method for isoprostane assessment have been developed; yet, when tested on feline samples, they were considered unreliable, and the gold standard gas chromatography coupled with mass spectrometry is prefered[122,123]. Isoprostanes can be measured in plasma or in urine, since they are filtered by the kidneys[119]. Despite increased isoprostanes being reported in a variety of human diseases[121], only one study performed in feline patients with kidney disease, has been published[121]. Surprisingly, cats with late stage, chronic renal disease in this study had lower urinary F2-isoprostane concentrations than healthy cats or cats with early kidney disease[122]. No information is available in diabetic cats.

To counteract the effect of ROS on biological components, there is an abundance of antioxidant mechanisms. In the cells, glutathione, as a universal electron donor, is at the cross-roads of antioxidant defenses. Glutathione is a tripeptide (γ-glutamyl-L-cysteinyl-L-glycine) synthesized by hepatocytes and released in plasma where it can be internalized by other cells. Additionally, all cells, included red blood cells can synthesize it *de novo*[72-74]. In people, decreased glutathione has been described in inherited deficiencies of the GSH-synthetizing enzymes, infectious, liver, pulmonary, cardiovascular and metabolic disease such as diabetes, as well as in cancer[80-82,224,225]. A previous study described a correlation between the presence of Heinz bodies

in red blood cells, the presence of plasma β-hydroxybutyrate (a ketone body) and decreased erythrocyte glutathione concentration in diabetic cats[41]. However, this study only assessed total glutathione and did not assess its oxidized form, which could provide further information about the redox status of the cell.

In addition to glutathione, plasma contains many components with antioxidant abilities such as albumin, bilirubin, uric acid, vitamins C and E as well as polyaromatic compounds originating from food. Antioxidant activity testing provides information on the total antioxidant potency of the medium tested, regardless of the contribution of each antioxidant components[226]. In feline, previous studies reported a decreased serum antioxidant capacity in chronic kidney disease, feline infectious peritonitis and pyometra[201,207,227,228]; however, information is lacking in diabetes.

The goal of this study was to investigate the potential utility of three biomarkers of oxidative stress in diabetic cats. We hypothesized a decreased serum antioxidant capacity, increased plasma F2-isoprostanes concentration and decreased erythrocyte total glutathione and an increased oxidized glutathione concentration.

4.3 Material and methods

4.3.1 Study population and obtention of samples

Four diabetic and four age and sex-match healthy control cats were included in this study (please see chapter 5 for more details). The goal was to document the presence of oxidative stress as a potential cause for erythrocyte microRNA changes. This study was approved by the Purdue University Animal Care and Use Committee (protocol # 1504001221) and blood was collected once consent was given by the owner. Serum remaining from the biochemistry analysis was

aliquoted and stored at -80°C until use while red blood cells were obtained from pelleted red blood cells remaining after gentle centrifugation of EDTA-blood and collection of the lower portion of the red blood cell pellet by gravity flow in the next chapter (see chapter 5).

4.3.2 Serum total antioxidant capacity

Serum total antioxidant capacity was measured spectrophotometrically on the SpectraMax i3x microplate reader (Molecular Devices) with the Antioxidant Assay kit (Cayman Chemical) per the manufacturer's instructions. Briefly, this colorimetric assay relies on the capacity of the serum to inhibit the oxidation of 2,2'-azino-di-3-ethylbenzthiazoline sulphonate (ABTS®) after the addition of metmyoglobin to the samples. The antioxidant capacity of the samples is compared to a tocopherol analogue standard. Serum samples were diluted 20 times and 40 times prior to testing. Measurements were carried out in duplicates.

4.3.3 EDTA-plasma F_2-isoprostanes concentration

Serum total isoprostanes concentration was carried at the Eicosanoid Core Laboratory (Vanderbuilt University Medical Center) where after gas chromatography, F_2-isoprostanes concentration was determined by mass spectrometry. This protocol has been described in detail elswhere[123].

4.3.4 Total and oxidized erythrocyte glutathione concentrations

Total and oxidized glutathione concentrations were determined as indicated in the Glutathione Assay Kit (Cayman Chemical). Following centrifugation at 1,000g for 10 min at 4°C, pelleted red blood cells were collected by gravity flow in 2 mL microcentrifuge tubes and lysed in four volumes of ice cold double distilled water. After a 5 min incubation, samples were centrifuged at 10000g for 15 min at 4°C. One milliliter of supernatants was collected and placed in new 2 ml

microcentrifuge tubes. Deproteination was carried out by adding one milliliter of an, 100g/L aqueous solution of metaphosphoric acid (Sigma-Aldrich), prepared just before use, to the RBC lysates. Following a 5 min incubation at room temperature samples were centrifuged at 2000g for 10 min at 4°C. Supernatants were collected, aliquoted and stored until use at -80°C. Before glutathione determination, samples were thawed and a 4M triethanolamine solution (Sigma-Aldrich) was used to normalized samples pH, as per the manufacturer's instructions. In this assay, total glutathione can be measured directly; however, additional sample processing is needed for oxidized glutathione. To measure oxidized glutathione, reduced glutathione is derivatized with a 1M solution of 2-vinylpyridine (Sigma-Aldrich) in molecular biology grade ethanol (ThermoFisher Scientific). Two sets of standards were used: one for total glutathione and one for oxidized glutathione. All measurements were carried out in duplicates on the SpectraMax i3x microplate reader (Molecular Devices).

4.3.5 Statistical analyses

A Student's *t*-test was performed to compare total antioxidant capacity, F2-isoprostanes concentration and erythrocyte glutathione concentrations between diabetic and healthy cats. For this project, JMP®, version 13.2.0 (SAS Institute Inc.) was used for statistical analyses with a P value less than 0.05 considered significant. Results are expressed as means.

4.4 Results

Although all standards for the total antioxidant capacity gave expected results, we failed to obtain meaningful results for test samples in our setting as both healthy and diabetic cats had the same order of antioxidant capacity, which varied dramatically with dilution of the samples, possibly suggesting an interfering substance in the serum of cats, interfering with this assay. On

the other hand, diabetic cats showed a trend toward a higher ($p = 0.078$) EDTA-plasma F_2-isoprostanes (0.374 ng/mL) than healthy control cats (0.136 ng/mL) **(Figure 4.1)**. RBC total glutathione concentration was also significantly higher ($p = 0.0085$) in diabetic cats (332.9 µM) when compared to healthy controls (228.9 µM). Interestingly, despite not being significant ($p = 0.058$), there was a trend towards a higher oxidized glutathione concentration in diabetic cats (68.5 µM) in comparison to healthy controls (35.9 µM). The total glutathione over oxidized glutathione ratio was calculated; although the difference was not significant ($p=0.153$), diabetic cats tended to have lower glutathione ratios (5.3) than healthy controls (6.9) **(Figure 4.2)**.

4.5 Discussion

We attempted to document the serum total antioxidant capacity of diabetic cats, using the Antioxidant Assay from Cayman Chemical. This assay has not been previously validated for use in feline serum and as such may not be appropriate for use in cats. This could explain the aberrant results observed herein. If this test is to be used in feline serum, it should be thoroughly evaluated.

We detected a trend towards an increased EDTA-plasma concentration of F_2-isoprostanes in diabetic cats when compared to age and sex-matched healthy controls. F_2-isoprostanes result from the peroxidation of polyunsaturated fatty acids, especially in cell membranes, by reactive oxygen species. Therefore, it is likely that the various diseases in which oxidative stress has been previously described may be associated with increased concentrations of plasma F_2-isoprostanes. They are filtered in the kidney and can be measured in urine[119]. In humans, so far, increased F_2-isoprostanes have been reported in systemic inflammatory diseases, cardiovascular diseases, diabetes, pulmonary diseases, neurological diseases and cancer[119,121]. In cats, a single study looked at the changes in urine F_2-isoprostanes in association with kidney disease progression. Isoprostanes

were measured by ELISA and showed a decreased urine concentration with progression of kidney disease. Our study lends support to further investigation of isoprostanes as markers of oxidative stress-induced damages to cell membranes in cats.

The diabetic cats involved in this study were all ketoacidotic and revealed the presence of Heinz bodies in red blood cells, upon evaluation of peripheral blood smears. Heinz bodies result from the precipitation of oxidized hemoglobin or oxidized lipids and/or proteins in the inner membrane leaflet of red blood cells[73]. Diabetes, especially when accompanied by ketoacidosis, is a well-known condition associated with the formation of Heinz bodies in feline patients[39,41]. Therefore, oxidation of cell membranes, was suspected and a trend towards increased isoprostanes support our suspicions of its presence in the study cats.

Glutathione is a tripeptide thiol, essential for protection against oxidative stress[73]. In our study we found that total glutathione was significantly increased in red blood cells of diabetic cats in comparison to healthy controls. There was also a trend toward an increased concentration of oxidized glutathione which could indicate increased oxidation in the erythrocytes as suspected by the presence of Heinz bodies. The overall effect, even if diabetic cats were not significantly different from healthy control cats, was a trend towards a decreased total-to-oxidized glutathione ratio. This suggests that despite an attempt to respond to oxidative stress by increasing the amount of intracellular glutathione, oxidation of biological molecules was still happening. Little is known about changes in erythrocyte glutathione concentration in disease in cats. One study compared the erythrocytic reduced glutathione concentration between healthy and sick cats; however, no significant difference was noted[229]. Another study reported a decreased total glutathione content in cats with diabetes ketoacidotic[41], which is similar to findings in diabetic rat models and in humans[80-82,225]. Additional studies are warranted to further investigate these discrepancies.

The conclusions that can be drawn from our study are somewhat limited by the low number of individuals in the healthy and diabetic groups. Nonetheless, the results obtained for F_2-isoprostanes and glutathione should prompt validation studies as well as investigation of these tests as potential biomarkers of oxidative stress. These tests may be valuable new tools to further our understanding of the role that oxidative stress plays in diseases of the cat.

4.6 Conclusion

This study investigated the serum antioxidant capacity, plasma F_2-isoprotanes concentration and erythrocytic glutathione content of diabetic and healthy cats. Diabetic cats had higher plasma F_2-isoprotanes concentrations and erythrocytic total glutathione content in comparison to healthy control cats, indicating increased oxidative damage to cell membranes and possibly an attempt of the red blood cells to counteract increased oxidative stress. No significant difference was observed for the serum total antioxidant capacity, erythrocytic oxidized glutathione and total to oxidized glutathione ratio. In conclusion, the results herein suggest that isoprostane and glutathione may be valuable new tools for understanding the role of oxidative stress in feline diseases.

4.7 Conflict of interest statement

None of the authors have financial or personal relationships that could inappropriately influence or bias the content of the paper.

4.8 Acknowledgements

Funding for P. Deshuillers was made possible with support of Morris Animals Foundation (Grant #D15FE-902), and Purdue University through the Comparative Pathobiology department and the Andrew's fellowship.

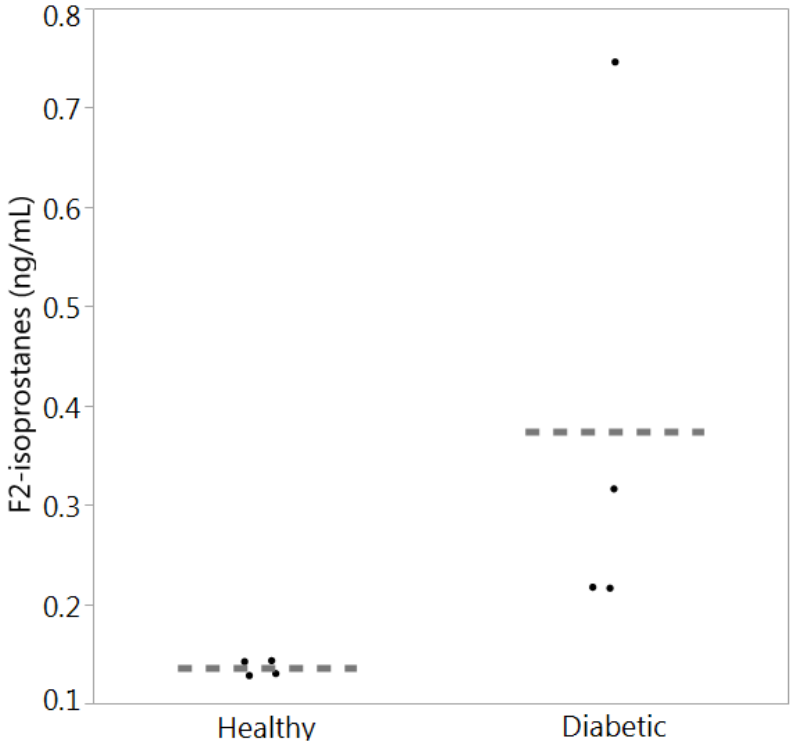

Figure 4.1: Comparison of EDTA-plasma F2-isoprostanes concentrations between diabetic and healthy control cats

Diabetic cats show a trend toward a higher EDTA-plasma F2-isoprostanes concentration than healthy control cats; however, this difference did not reach significance (P = 0.78). The dashed grey line depicts the mean for each group.

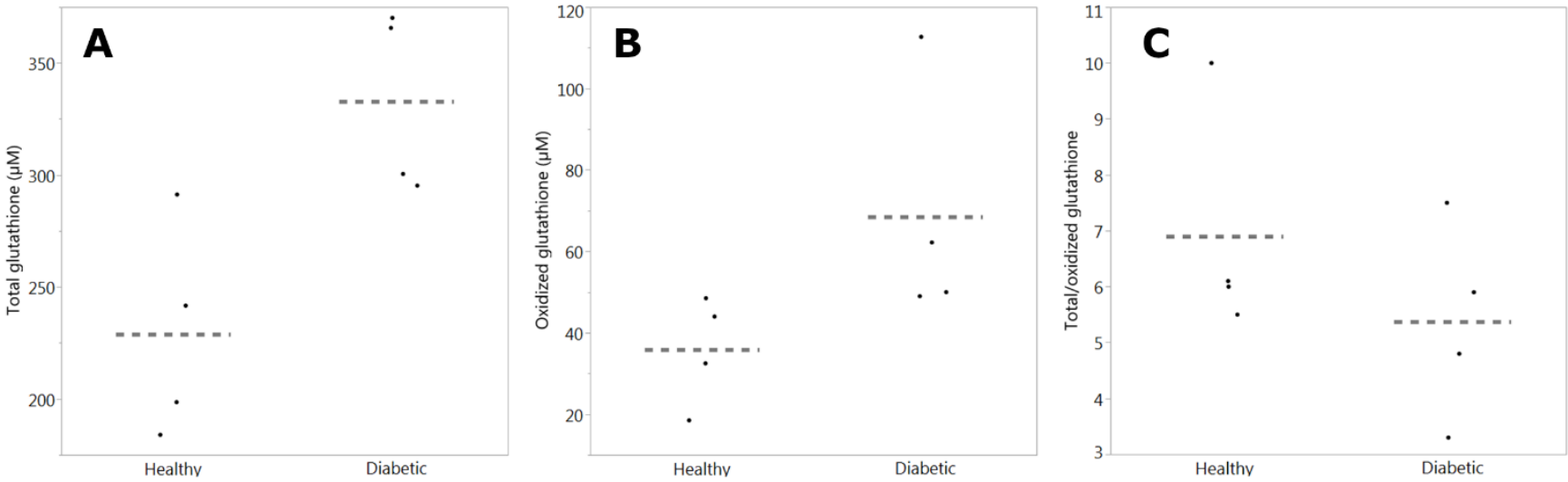

Figure 4.2: Comparison of the erythrocyte total, oxidized glutathione concentrations and total/oxidized glutathione ratio
Diabetic cats had a significantly higher total erythrocyte glutathione concentration (P = 0.0085). Despite a trend towards a higher oxidized glutathione concentration in diabetic cats and lower total/oxidized glutathione ratios, significance was not reached (P = 0.058 and P = 0.153 respectively). The dashed grey line depicts the mean for each group.

CHAPTER 5. CIRCULATING MATURE ERYTHROCYTE MICRORNA EXPRESSION IN HEALTHY AND DIABETIC CATS

5.1 Abstract

Domestic cats can serve as natural models for a variety of human and animal diseases. Although the feline genome was published in 2005 and updated in 2011, little is known about feline microRNA expression profiles (miRNome). MicroRNAs are small non-coding RNAs that serve as regulators of gene transcription. Variable erythrocyte microRNA profiles have been identified in certain disease states and may be objective biomarkers for diagnosis and treatment response. This study was undertaken to investigate the presence of microRNAs in mature erythrocytes, populate the microRNA database with feline sequences, and document changes in the mature erythrocyte microRNA content in diabetic cats, which may serve to inform hypothesis driven research. High throughput sequencing of microRNAs was performed in eight healthy cats to populate a local microRNA database, later used to compare changes in erythrocyte microRNA abundance between four diabetic and four age and sex-matched healthy cats. We identified 899 microRNA sequences including 356 microRNAs similar to human or canine sequences, and 543 feline specific sequences. Bioinformatic analysis of RNA-Seq results identified 12 differentially abundant microRNAs between diabetic and healthy control cats, while RT-qPCR confirmed six. Five microRNAs were present in increased numbers in diabetic cats (let-7b, miR-1692, miR-339, miR-486 and a feline specific microRNA) and one was found in lower amounts (miR-451). This is the first study to report differences in erythrocyte microRNAs in feline diabetes. While the role of microRNAs in erythrocytes remains to be elucidated, the possibility of exploiting these microRNAs as biomarkers for diabetes should be further investigated.

5.2 Introduction

MicroRNAs are small non-coding RNAs regulating gene expression post transcriptionally. When mature, they are incorporated into the RNA-induced silencing complex (RISC) and inhibit mRNA translation or degrade the target mRNA[153,230]. The specificity of mature microRNAs for their target results from the complementarity of the seed region (2-8 first nucleotides at the 5' end) to the mRNA; the central region of the microRNA plays only a minor contribution[231,232]. MicroRNAs are involved in many cellular processes from cell development, proliferation, and maturation to survival, adaptation to stress, and apoptosis. Dysregulation of their expression has been documented in a variety of diseases, including cardiovascular[233,234], liver[235,236], kidney[237-239], and metabolic diseases such as diabetes[240-242] as well as cancer[243]. They have been considered potential biomarkers of disease but also possible therapeutic targets.

The function of microRNAs as molecular switches for cellular processes makes them essential to hematopoiesis where hematopoietic stem cells go through proliferation, differentiation and maturation before they can be released into circulation[244-246]. Their role in erythropoiesis is starting to be unraveled. For instance, miR-150 and miR-486 control the commitment of the common erythroid-megakaryocytic precursor cell toward the erythroid lineage while miR-15, miR-16, miR-144,miR-191, miR-221, miR-222, miR-339, miR-451 and miR-486 control the progression of the erythroid precursor towards maturation and hemoglobinization[247-249]. Dysregulation of these microRNAs has been associated with myeloid neoplasms including myelodysplastic syndrome, acute myeloid leukemia, and polycythemia vera[249-253]. Besides insuring progression of erythroid precursors towards maturation, microRNAs also fine tune the cells response to oxidative stress, helping to maintain erythrocyte homeostasis[174,254]. Interestingly,

anucleate mammal mature red blood cells maintain an abundant and diverse pool of microRNAs despite their lack of nuclei and protein synthesis[193,255]; however, their significance is still elusive.

Domestic cats can serve as a natural model for a variety of human diseases such as cardiac diseases[256], neurologic disorders such as Alzheimer disease[257], hereditary diseases[258], HIV and AIDS[259], bladder disease[260], as well as obesity and type 2 diabetes[212]. As in humans, feline diabetes is characterized by hyperglycemia, a relative or absolute lack of insulin action, and peripheral insulin resistance[261]. Systemic oxidative stress-related tissue damage is known to play an important role in the pathophysiology of diabetes and diabetic complications. In cats, hemoglobin is exquisitely sensitive to oxidant damage, resulting in this protein being denatured and presence of inclusions known as Heinz bodies within red cells[73]. Heinz body formation is commonly reported in association with ketoacidosis in diabetic cats, but is a relatively insensitive indicator of oxidative stress and other biomarkers are needed[41].

The cat genome was first published in 2005 and updated in 2011[258,262] meanwhile, information related to the feline microRNomes have just started to emerge[263-265]. It is well recognized that a dysregulation of normal physiologic microRNAs can lead to and the development of various diseases. The first goal of this study was to develop a method for red blood cell isolation from small volumes of feline whole blood and then extract enough microRNA for sequencing. The second goal was to generate the feline erythrocytes miRNome to populate the microRNA database with feline sequences. Finally, this study aimed at documenting changes in the abundance of erythrocyte microRNAs in association with disease as starting point to generate future research hypotheses. Diabetes was elected as type 2 diabetes resembles human type 2 diabetes and information obtained from cats may be translated to human research.

5.3 Material and Methods

5.3.1 Specimen Collection, mature erythrocyte isolation and RNA isolation

Specimens used in this project were collected from client, student, staff and faculty-owned cats, over 2 years of age and weighing at least six pounds. This project was approved by the Purdue University Animal Care and Use Committee (protocol # 1504001221) and the owner's consent was obtained prior to sample collection. First eight healthy cats were recruited to develop the mature red blood cells isolation method, confirm the presence of microRNAs in mature red blood cells of cats and to identify these microRNAs by RNA-Seq. Thereafter, four diabetic and four age and sex-matched diabetic cats were recruited to investigate change in the microRNA population in mature red blood cells of diabetic cats. Healthy cats involved in this study had no history or clinical signs of disease, unremarkable hemograms (Procyte Dx, Idexx Laboratories) and serum biochemistry profiles (Vitros® 350 Chemistry System, Ortho Clinical Diagnostics) as determined by a veterinary clinical pathologist. Biochemistry profiles included glucose, BUN, creatinine, phosphorus, calcium, sodium, chloride, TCO_2, anion gap, total proteins, albumin, globulins, total bilirubin, cholesterol, ALT, ALP, GGT, amylase and lipase activities. Additionally, they had not received a treatment in the last 6 months. Diabetic cats were recruited based on the presence of history, clinical signs, and biochemistry profiles indicating diabetes. Other more specific tests were performed when deemed necessary to rule in, or rule out other conditions such as kidney disease, pancreatitis, ketoacidosis. These tests included a urinalysis, repeat serum chemistry panel, pancreatic specific lipase, bilirubin fractions etc.

Approximately two milliliters of blood were collected in a red top tube and four milliliters were collected in an EDTA tube. Serum was used for the biochemistry profiles. A hemogram was performed with 200µL of EDTA blood. Additionally, blood films stained with Modified Wright's

(Hematek 3000 Slide Stainer; Siemens Healthcare Diagnostics) and with New Methylene Blue (New Methylene Blue N, Ricca Chemical, ThermoFisher Scientific) were prepared and examined to confirm the hemogram results, evaluate blood cells morphology and examined to detect the presence of Heinz bodies, frequently seen in cats with diabetes ketoacidotic. The remainder of the EDTA-blood was processed to isolate mature red blood cells.

5.3.2 Mature RBC isolation

Anticoagulated EDTA blood was processed to isolate mature by removing white blood cells (WBCs), platelets and reticulocytes. First blood was placed into a 5 ml syringe barrel closed at the bottom (Omniflix, B Braun) and centrifuged at 200g, 4 °C for 20 min. Following centrifugation, the WBCs and platelets are in the uppermost portion of the pelleted cells. Approximately one third to one half of the red blood cell pellet was removed by gravity flow into a clean glass tube and the same volume of cold 1X PBS pH=7.4 was mixed into the pelleted RBC. Additional leukoreduction was performed by filtration (Acrodisc® WBC Syringe Filter, Pall Corporation) following the manufacturer recommendations. The filter was rinsed with 1 volume of cold PBS. The filtrate was then centrifuged 5 minutes at 800g, at 4°C and approximately half of the supernatant was removed to obtain a fluidity like whole blood after homogenization by inversion. Any remaining leukocytes, platelets and reticulocytes were removed by immunocapture by biotinylated (EZ-link™ Sulfo-NHS-LC-Biotinylation kit, ThermoFisher Scientific) anti-CD18 (clone CA1.4E9, Bio-Rad), anti-CD61 (clone Y2/51, Bio-Rad) and anti-CD71 (G-8, Santa Cruz Biotechnology) monoclonal antibodies and Macs Miltenyi Biotec cell separation system (MS Columns and Anti-Biotin Microbeads, Macs Miltenyi Biotec) as per manufacturer's instructions. Anti-CD18 and anti-CD61 have been previously validated for use in cats. Immunoreactivity of the anti-CD71 antibody to feline transferrin receptor was evaluated by immunocytochemistry on feline

blood smears with a marked reticulocytosis following a protocol described elsewhere[266]. After this step, red blood cells were centrifuged one last time and supernatant was removed so that there would be as much supernatant as pelleted red blood cells. Once resuspended, 400µL of the RBC suspension were placed in a 2 mL microcentrifuge tube containing 1200µL of cold TRIzol Reagent (ThermoFisher Scientific). The preparations were vigorously homogenized, left at room temperature for 5 min and frozen at -80 °C until use.

5.3.3 Total RNA extraction

Samples of RBC in TRIzol were thawed just before total RNA was extracted. First, the specimens were centrifuged for 10min at 12000g, 4 °C to pellet cell debris. The supernant was placed in a clean 2 mL microcentrifuge tube and 240µL of chloroform (Ultrapure™ Phenol:Chloroform:Isoamyl Alcohol (25:24:1, v:v), ThermoFisher Scientific) were mixed with the supernatant and allowed to sit at room temperature for 5 min. The samples were centrifuged for 15 min at 10000g at 4 °C. The top aqueous phase was removed by aspiration, its volume measured, and transferred in a new 2 mL microcentrifuge tube. After this step, RNA isolation with the miRNeasy mini kit (Qiagen, Valencia, CA, USA) was conducted per manufacturer's instructions. Two elutions were performed with 30 and 50µL of RNase-free water. Samples were aliquoted and stored at -80 °C until use.

Control of the quality and quantity of RNA obtained was performed at the Purdue Genomic Core Facility on the first elute. Briefly, control of the size quality of extracted RNAs were performed on the Agilent Bioanalyzer 2100 (Agilent) using Agilent RNA 6000 Nano Kit (Agilent), whereas quantification of total RNA was done by fluorimetry (Qubit 4 fluorometer, Invitrogen). For the first eight cats, libraries were prepared from 1ng of total RNA with the TruSeq Small RNA Library Preparation Kit (Illumina). Library for diabetic and healthy control cats were constructed

with the NEXTFLEX®® Small RNA-Seq Kit v3 (Bioo Scientific) and then with the TruSeq Small RNA Library Preparation Kit (Illumina) to compare libraries from both library construction methods, since dramatic differences were observed. During library construction, each cat was attributed a barcode. The three libraries were sequenced on the HiSeq 2500 platform (Illumina, San Diego, CA, USA) in three different runs, on a TruSeq Rapid Run Flow Cell (Illumina) set up for single-end, 50bp reads pyrosequencing.

Data analysis for the first eight healthy cats was performed at the Purdue Bioinformatic Core Facility. Adapter trimming and clipping of four bases from both ends of the reads and quality trimming were performed through cutadapt software v1.13[267]. Quality trimmed reads were processed using miRDeep2 software v2.0.0.8[268] for microRNA analysis. The preprocessing of reads was achieved through the mapper.pl script from miRDeep2. Reads shorter than 15bp were excluded. Preprocessed reads were mapped against the cat reference genome[262]. The quantifier.pl script from miRDeep2 performed quantification and expression profiling of known microRNAs using a list of human and dog microRNAs downloaded from miRBase. The quantifier script from miRDeep2 generated the read count for the known microRNAs from each sample. Combined count matrices for known microRNAs of human and dog were generated using custom scripts. Prediction of novel microRNAs was performed using the miRDeep2 software. Quality trimmed reads from all samples were combined into single reads file followed by mapping to the cat genome using mapper.pl. Human and dog microRNAs from miRBase were used as related species to predict novel microRNAs using miRDeep2.pl script.

Data analysis for the diabetic and healthy control cats was performed similarly; except for the use of the feline microRNA sequences determined from the previous analysis as known microRNAs. To compare the abundance of microRNAs between diabetic cats and healthy controls,

read counts/abundance values for known and novel microRNA from each sample were used to create a count matrix. Differential abundance of known and novel microRNAs between diabetic and control group was calculated using the DESeq2 package v1.16.1[269] from R v3.4.2. A false discovery rate of 0.1 was considered significant.

5.3.4 Selection of a reference microRNA for RT-qPCR

Since mature red blood cells of cats are anucleate, we could not use small nucleolar RNA as reference microRNAs. Additionally, to the best of our knowledge, there is no accepted normalizer microRNA for mature red blood cells. To determine which microRNA could be used as a reference, 30 microRNAs with abundance fold change between healthy control and diabetic cats closest to one were selected. Amongst these microRNAs, miR-103 was chosen based on the relative abundance of reads closest to the abundance of microRNAs that were tested by qPCR.

5.3.5 RT-qPCR

Retrotranscription was performed on a MJ Research PTC-200 thermal cycler (MJ Research) with the miScript II RT kit from the miScript PCR system (Qiagen) using 1000 ng of total RNA as starting material. Following retrotranscription, 200 µL of RNase free water was added to cDNA. Sample were aliquoted and frozen at -20 °C until use. Quantitative PCR was performed on the Quantstudio™ 3 real time PCR system (ThermoFisher Scientific) and Quantstudio™ Design and Analysis Software (ThermoFisher Scientific) with the miScript SYBR® Green PCR kit (Qiagen) following the manufacturer's instructions. Except for miR-103, which sequence was identical to the canine sequence (Cf_miR-103_1 miScript Primer Assay, Qiagen), custom primers (Custom miScript Primer Assay, Qiagen) were designed based on the microRNA sequences determined RNA-Seq as shown in **Table 5.1**. For all qPCR, two microliters of diluted cDNA were used as template. Amplification efficiency was tested on five-time serial dilutions as recommended by the

RT-qPCR manufacturer. miR-103 was used as reference microRNA. Melting curve analysis was conducted to verify single amplicon. RT-qPCR results were analyzed by the $2^{-\Delta\Delta Ct}$ method as described previously[270]. A Student's *t*-test was performed to compare changes in microRNA abundance between diabetic and healthy control cats. All statistical analyses were performed with JMP®, version 13.2.0 (SAS Institute Inc.). A P value inferior to 0.1 was considered significant.

5.4 Results

5.4.1 Study population

The first eight healthy cats consisted of 5 castrated male and 3 spayed females, ranging in age from 2 to 6 years old (median 4 years). Clinical examination, hemograms and biochemistry profiles were within established reference intervals. Additionally, none of the cats had received vaccination or any medical treatment within the last 6 months.

The second set of cats consisted of four diabetic cats and four healthy cats. Details can be found in **Table 5.2**. Briefly, In the diabetic and healthy control group, age ranged from 10 to 17-year-old. Each group consisted of a single spayed female along with three castrated males. Upon examination of diabetic cats' blood smears, Heinz bodies were frequently found, while no Heinz bodies were seen in healthy cats. While Heinz bodies in diabetes cats are often associated with ketoacidosis, this condition was confirmed by the presence of hyperglycemia, glucosuria, metabolic acidosis, and ketosis in all diabetic patients. In the diabetic group, all cats had a calculated osmolarity over 310 mosm/kg, indicating hyperglycemic hyperosmolar syndrome. One cat was also diagnosed with pancreatitis and cholestasis (diabetic cat 2). Healthy controls had unremarkable biochemistry findings.

5.4.2 Mature RBC isolation

Immunocytochemistry using the antibodies for immunocapture of leukocytes (anti-CD18), platelets (anti-CD61) and reticulocytes (anti-CD71) was tested on feline blood smears. All leukocytes showed marked surface immunoreactivity with the CA1.4E9 anti-CD18 **(Figure 5.1)**. Similarly, platelets and platelet clumps showed marked surface immunoreactivity with the Y2/51 anti-CD61 antibody **(Figure 5.1)** and marked diffuse to clustered surface immunoreactivity was observed on reticulocytes with the anti-CD71 G-8 antibody **(Figure 5.1)**. Mature red blood cells were successfully isolated from feline whole blood as illustrated in **Figure 5.2.** The mature red blood cell isolation and depletion of WBC and leukocytes was followed using an automated hematology instrument (Procyte Dx) at all steps of the process. After centrifugation and leukoreduction, few platelets could still be detected by flow cytometry on the red blood cell / platelet channel **(Figure 5.2)**. The immunodepletion step removed the remaining platelets and reticulocytes in whole blood **(Figure 5.2)**. Likewise, most leukocytes were removed by gentle centrifugation and collection of the pelleted red blood cells by gravity flow **(Figure 5.2)**. The remaining white blood cells were filtered out in the leukoreduction step **(Figure 5.2)**. No leukocytes could be detected after immunodepletion. Blood smears prepared and evaluated, in conjunction to the cell counts, confirmed the instrument findings.

5.4.3 MicroRNA sequencing and bioinformatic analysis

Immediately after total RNA extraction, RNA concentrations were determined and were found to vary from 6.3 to 35.8ng/µL for the first eight healthy cats and from 39.6 to 139.2 ng/µL for the diabetic and healthy control cats **(Table 5.3)**. RNAs consisted mostly of small RNA between the 25 and 200 nt marks on the RNA Nano Chip electrophoretogram **(Figure 5.3)**, indicating an adequate extraction. In the absence of ribosomal RNA in mature red blood cells and

of significant 18S and 28S rRNA peaks, the ribosomal integrity number (RIN) was systematically low, ranging from 1 to 7.5 **(Table 5.3)**.

Sequencing and bioinformatic analysis of the microRNAs from the first eight healthy cats revealed the presence of 499 individual microRNAs sequences corresponding to 101 feline specific microRNAs when compared to human and canine microRNA databases. Three hundred and ninety-eight sequences corresponded to a human or canine microRNA. Among these 398 sequences, variable numbers of isomiRs were identified corresponding to 232 microRNAs **(Table 5.4)**. The number of isomiRs varied from 1 to 9 with let-7b having 9 different sequences. MiR-148a and miR-15b had the second and third highest number of isomiRs (8 and 7 respectively). The list of all microRNA sequences is found in **Appendix 1** and has been submitted to the microRNA database (miRBase). The 15 most abundant reads were the same across the samples **(Table 5.5 and Figure 5.4)** with miR-486 being by far the most abundant microRNA. miR-486 represented 78.2 to 90.6% of all reads. Interestingly, miR-451 represented between 0.7 and 1.7% of all reads.

Sequencing and bioinformatic analysis of the microRNAs from diabetic and healthy control cats identified, 899 individual microRNA sequences. Five hundred and forty-three microRNAs were specific to felines when compared to human and canine microRNA databases while 356 sequences matched human or canine microRNAs. Among these 356 sequences, variable numbers of isomiRs were identified equivalent to 169 microRNAs **(Table 5.6)**. The number of isomiRs varied from 1 to 20. Let-7b, miR-30d and miR-423a had the highest number of sequences with 20, 10 and 8 isomiRs respectively. All microRNA sequences from diabetic and healthy control cats are found in **Appendix 2**. The 15 most abundant reads and their microRNA identity are showed in **Table 5.7** and depicted in **Figure 5.5**. In contrast to the first RNA-Seq performed on healthy cats, by far, the most abundant microRNA was miR-451, accounting for 68 to 82.2%

of all reads while miR-486 represented only 0.7 to 2.7% of the reads. To determine if such changes in abundance of miR-451 and miR-486 were due to the samples or related to the sequencing process, new libraries for the first eight healthy cats were prepared with the same kit as the one used for the diabetic and healthy control cats (NEXTFLEX® small RNA library preparations kit). These results were consistent with the second sequencing (diabetic and healthy cats): miR-451 was the most abundant microRNA and represented 60.5 to 70.9% of all reads, while miR-486 was the second most abundant microRNA accounting for 3.2 to 7% of all reads **table 5.8** and **figure 5.6**.

Differential expression analysis between diabetic and healthy control cats revealed variable numbers of differentially abundant microRNAs depending on the reference database used. For a false discovery rate of 0.1, 4 microRNAs were differentially abundant when known canine microRNAs were used as reference. When microRNAs from the previous feline microRNA sequencing were used as reference, 12 microRNAs were differentially abundant. When novel microRNAs were used as reference, nine and eight microRNAs were found to be in significantly different amounts between diabetic and healthy cats, based on the canine database and on the previous feline microRNA sequencing, respectively. Overall, this corresponded to 21 differentially abundant expressed sequences; however, multiple isomiRs were included in this group of microRNAs: five for miR-339 and two for miR-374b **(Table 5.9)**. Furthermore, multiple sequences had no match in the canine database and by searching manually in miRBase, let-7b, miR-92a and miR-1692 were identified. The microRNAs identified as let-7b and miR-92a aligned perfectly with their human and murine counterparts amongst many other animal species. In contrast, miR-1692 showed three mismatches at the 3’ end with the only miR-1692 sequence of the database (*Gallus gallus*). Five additional sequences failed to match any known microRNAs in the miRBase; these microRNAs are denoted as “unknown”. Most microRNAs showed an

increased abundance in diabetic cats in comparison to healthy cats (let-7b, miR-128, miR-1692, miR-339-1, miR-339-2, miR-339-3, miR-339-4, miR-339-5, miR-365, miR-374b-1, miR-374b-2, unknown1 to 5). Only miR-210 and miR-92a were significantly decreased in diabetic patients.

5.4.4 Reference microRNA selection

Prior to RT-qPCR, we identified a reference microRNA from differential expression analysis files. Common reference small RNAs could not be used, since mature RBC do not have nuclei or ribosomal RNAs. Further, changes in abundance of microRNAs have not been previously studied. MiR-103 was chosen as reference microRNA based on a fold change close to 1 (fold change = 1.004), a non-significant false discovery rate of 0.98 and an overall number of reads similar to the microRNAs to be assessed by RT-qPCR.

5.4.5 Validation by RT-qPCR

For RT-qPCR, the custom designed microRNA primers were tested to determine the amplification efficiency of the PCR reactions. Efficiencies varied between 75 and 88%, which was considered adequate to use the $2^{-\Delta\Delta Ct}$ method to determine fold change. Quantitative RT-PCR was performed for all identified microRNAs, disregarding isomiRs, and for one unknown microRNAs (unknown 5). Additionally, RT-qPCR was also performed for miR-451, miR-486 as well as miR-144 as they may be involved in acquisition of antioxidant defenses of RBC during erythropoiesis. Results are showed in **Figure 5.7**. Five microRNAs, let-7b ($P < 0.1$), miR-1692 ($P < 0.1$), miR-339 ($P < 0.1$), miR-486 ($P < 0.05$) and unknown 5 ($P < 0.1$) were significantly more abundant in mature RBCs of diabetic cats in comparison to healthy cats while miR-451 was significantly less abundant in diabetic patients ($P < 0.1$). When diabetic and healthy control RT-qPCR results were examined individually **(Figure 5.8)**, some variations were noted between individuals in the same group; however, let-7b, miR-1692, miR-339, miR-486 and unknown 5 were also more abundant

in all diabetic cats individually. Two diabetic cats had increased amounts of miR-210 and in a single diabetic cat, miR-144, miR-365 and miR-92a were more abundant. One healthy cat stood out from the other healthy cats with a relative increased abundance of let-7b, miR-1692, miR-210, miR-339, miR-365, miR-451, miR-486, miR-92a and unknown 5 in comparison to other healthy cats.

5.5 Discussion

This is the first study to provide evidence for the presence of diverse microRNAs in mature feline erythrocytes. We also report for the first time a set of differentially expressed microRNAs that are present in the erythrocytes of cats with diabetes and not in healthy cats. The microRNA sequences reported in this study will populate the microRNA database, currently lacking feline sequences. This will provide essential information for future microRNA studies in cats.

One healthy cat stood out from the other healthy cats when microRNA abundance was documented in individual cats. No reason for such difference could be identified; however, this cat was the oldest healthy cat included in this study and it is possible that an underlying disease was not detected at the time of his recruitment, despite a physical examination, and hematologic and biochemistry analyses.

Of the differentially expressed microRNAs identified in this study either by RNA-Seq or RT-qPCR, several have been reported to play important roles in erythropoiesis. Let-7b, miR-210, miR-486 and miR-92a are involved in erythroid cell proliferation and survival ultimately resulting in increased erythropoiesis[185,271]. By far, miR-486 is the most studied microRNA in erythropoiesis. The MYB-miR-486-MAF axis increases erythroid proliferation and differentiation. The transcription factor MYB controls the expression of miR-486, which in turn regulates the

expression of MAF and drives the common erythroid/megakaryocytic progenitor cell toward the erythroid lineage[178]. In a chronic myeloid leukemia cell line, miR-486 was also shown to be involved in erythroid cells survival and proliferation through the transcription factor FOXO1 signaling[180]. MiR-210 expression is induced by hypoxia and inhibits globin production as well as erythroid progenitor cell maturation, increasing the proliferation of erythroid cell precursors while delaying their maturation[272].

Let-7b, miR-339, miR-451, and miR-486 are also involved in differentiation of erythroid cells. Let-7b has been shown to represses the synthesis of fetal hemoglobin in erythroid precursors [183], while miR-339 is necessary for erythropoiesis, but the mechanism is uncertain. It has been suggested that MiR-339 may target the erythropoietin receptor or the transcription factor STAT-5, involved in erythroid cell proliferation and differentiation[273,274]. Likewise, miR-451 drives erythroid cell maturation and hemoglobinization, but the exact mechanisms are unknown[175,184]. The roles of miR-1692 and miR-unknown 5 in erythropoiesis are unknown and need further investigation.

The microRNAs, miR-144 and miR-451, play a major role in the development of antioxidant defenses in erythroid precursor. Expression of the miR-144/451 cluster is regulated during erythroid differentiation by the transcription factor GATA1. Both microRNAs participate in the down regulation of GATA2 and provide a positive feedback loop to GATA1. MiR-451 also targets *Ywhaz* mRNA and decreases the expression of 14-3-3ζ protein resulting in the translocation of FOXO3 transcription factor to the nucleus of the erythroid precursor. A particularity of FOXOs transcription factors are specialized in antioxidant defenses as they induce the expression of antioxidant enzymes such as the manganese and copper superoxide dismutase, glutathione peroxidase 1, peroxiredoxins 3 and 5 and thioredoxin reductase 2 as well as the antioxidant

thioredoxin[175,176]. Further, cells lacking miR-451 show an increased susceptibility to oxidative stress in mice[254]. The precise role of the other differentially abundant microRNAs in mature erythrocytes identified in this study has not been described yet.

The function of microRNAs in mature red blood cell are largely unknown. During maturation, red blood cells of mammals lose their nucleus and in mature erythrocytes, the mRNAs, targets of the microRNAs also have been lost. What then is the role, if any, for microRNAs in mature erythrocytes? It is possible that microRNAs could be remnants of erythropoiesis and serve no function in these terminally differentiated cells. Perhaps the difference in abundance of certain microRNAs reflects the fine-tuning of cellular processes to external stimuli, such as hyperglycemia or oxidative stress. As such, the importance of microRNAs as biomarkers for events affecting erythropoiesis, should be further investigated in the future. It is also possible, as previously suggested, that microRNAs may have additional functional roles in mature red cells by a mechanism that is independent of mRNA targeting[193].

More recently, microRNAs have been recognized as messengers for local as well as distant cell-to-cell communications, especially between nucleated cells[199]. It is plausible that red blood cells merely serve as a vehicle for delivery of microRNAs to distant sites. Under oxidative stress conditions or senescence, RBC have been shown to shed microvesicles, potentially packed with microRNAs that could serve to communicate with or change the gene expression of target cells[275,276]. There is growing evidence that circulating red blood cells, particularly when infected with malaria, release microparticles containing microRNAs, especially miR-451 bound to AGO2. When endothelial cells internalize these microparticles, miR-451 resumes its function and alters gene expression in the new host cell. Gene studies have shown changes in genes responsible for cell adhesion and permeability, possibly pointing to a new mechanism of endothelial cell damage

and vascular dysfunction[196,198]. Whether such a comparable mechanism might contribute to cardiovascular or other complications seen in diseases, such as diabetes, is unknown.

Using different library construction protocols, the amount of miR-451 and miR-486 varied dramatically. In a previous human study looking at mature red blood cell microRNAs and employing a different sequencing method, the most abundant microRNA reads were from miR-451, representing approximately 60% of the reads[189]. This level of abundance for miR-451 was similar to that obtained in this study when using the NEXTFLEX® small RNA library construction kit. The majority of the other most abundant microRNAs described in this study were also the most abundant microRNAs present in our samples[189]. Therefore, we can suspect that the NEXTFLEX® small RNA library preparation kit was more accurate than the TruSeq small RNA library preparation kit. Ligation of adapters at both ends of small RNAs is recognized as the most critical step in deep sequencing and its bias can greatly affect sequencing results. Ligation bias is multifactorial as it depends on the small RNA sequences and secondary structure as well as on the adapter sequences, and the ligase employed. Here, miR-451 and miR-486 have inherently, different sequences which could contribute to ligation bias[277]. The NEXTFLEX® small RNA library construction kit has been conceived to circumvent such bias by adding degenerate nucleotides at the ends of the small RNAs prior to adapter ligation and an overnight incubation is required, in contrast to the TruSeq small RNA library preparation kit. This strategy could explain dramatically different results between the two library construction kits[277] with sequencing results from the NEXTFLEX® small RNA library construction kit being more accurate and consistent with other studies[189].

A limitation to this study is the small number of cats included. All cats involved in this study were either patients or student, staff or faculty owned cats, and therefore it was not possible

to control all variables possibly affecting microRNAs as closely as with laboratory animals. In this study, it is possible that some changes in microRNA expression may have been masked by the interindividual cat variability. Nonetheless, our study provides a starting point for further investigations about red blood cell microRNA content changes in sick individuals and exploring their significance.

5.6 Conclusion

This study describes a method for the isolation of mature erythrocytes from small volumes of feline blood. Such method could be easily transposed to other species for mature red blood cells studies. An abundant and diverse population of microRNAs were identified, and changes in the microRNA content of the erythrocytes was observed in disease, raising questions regarding their significance. This project paves the way for future studies regarding the role of erythrocyte microRNAs in disease, but also as potential messengers between circulating mature RBC and their surroundings.

5.7 Conflict of interest statement

None of the authors have financial or personal relationships that could inappropriately influence or bias the content of the paper.

5.8 Acknowledgment

Funding for P. Deshuillers was made possible with support of Morris Animals Foundation (Grant #D15FE-902), and Purdue University through the Comparative Pathobiology department and the Andrew's fellowship.

Table 5.1: List of microRNAs tested by RT-qPCR and their sequences
These sequences were used to design stem-loop primers for the RT-qPCR.

MicroRNA	**Sequence**
let-7b	AGGCAGUAGGUUGUAUAG
miR-128	UCACAGUGAACCGGUCUC
miR-144	GGAUAUCAUCAUAUACUGUAAG
miR-1692	GGCUAGCUCAGUCGGUAG
miR-210	ACUGUGCGUGUGACAGCGGCUGA
miR-339	UCCCUGUCCUCCAGGAACUG
miR-365	UAAUGCCCCUAAAAAUCC
miR-374	AUAUAAUACAACCUGCUAAG
miR-450	UUUUGCGAUGUGUUCCUAAUA
miR-451	AAACCGUUACCAUUACUGAG
miR-486	UCCUGUACUGAGCUGCCC
miR-92a	UAUUGCACUUGUCCCGGCCUG
unknown 5	AUCUUCGUGGGUCACUGCCU

Table 5.2: Hematology and biochemistry profile of four diabetic and four age and sex-matched healthy controls. Values outside of the reference intervals are bolded.

	Diabetic				Healthy				Reference interval	
	1	**2**	**3**	**4**	**1**	**2**	**3**	**4**		
Age	17	10	12	10	12	10	10	17		
Sex	FS	CM	CM	CM	CM	CM	SF	CM		
Hemogram										
RBC	8.01	9.27	10.5	8.06	10.1	9.8	7	7.7	6.8-10.5	M/µL
Hematocrit	37.7	33.5	41.2	33.8	45	43.6	35	33.9	33.6-47.4	%
Hemoglobin	12.9	11.9	14.6	11.8	14	13.7	12	11.2	10.5-14.6	g/dL
MCV	47	36.2	39.2	41.9	44.7	44.3	41.5	43.1	35.9-53.1	fl
MCHC	34.2	35.4	35.4	34.9	31.1	31.5	35.1	33.6	29-37.5	g/dL
Reticulocytes	53.8	11.5	10.9	16.1	39.2	22.6	9.1	6.9	<60	K/µL
WBC	14.5	6.6	8.4	12.49	10.1	9.2	7.1	8.4	5-15	K/µL
Segmented Neutrophils	11.5	5.8	7.3	9.73	6.3	6.7	3.9	5.9	3-12	K/µL
Lymphocytes	**0.7**	**0.4**	**0.8**	1.96	2.8	1.9	2.6	1.8	1.5-7	K/µL
Monocytes	0.44	0.33	0.73	0.4	0.2	0.37	0.43	0.17	0.05-0.85	K/µL
Eosinophils	**1.89**	0.07	0.22	0.36	0.81	0.09	0.21	0.59	0.1-1.5	K/µL
Basophils	0	0	0	0.0	0	0.09	0	0		K/µL
Platelets	351	-	423	294	-	257	-	334	250-600	K/µL
Heinz bodies	**many**	**few**	**few**	**few**	-	-	-	--		
Platelet comments	-	Clumps	-	-	Clumps	-	Clumps	-		
Biochemistry										
Glucose	**426**	**384**	**716**	**1185**	100	121	92	84	75-134	mg/dL
BUN	**45**	31	**73**	**50**	20	20	**48**	**43**	15-35	mg/dL
Creatinine	**2.7**	1.8	**3.3**	**3.4**	1.2	1.4	2.1	2.1	0.9-2.3	mg/dL
Phosphorus	5.8	3.4	3.7	6.9	4	3.8	3.9	3.9	2.6-8.8	mg/dL
Calcium	10	**8.7**	9.3	9.8	10.2	9.2	10	9.3	9-11.7	mg/dL
Sodium	156	**139**	**143**	**135**	153	152	154	152	148-157	mmol/L
Potassium	3.7	**2.7**	**2.8**	4	4.1	4	5.1	4.4	3.5-5.1	mmol/L

Table 5.2 continued

Chloride	**113**	**97**	**98**	**95**	119	121	116	118	115-128	mmol/L
Carbon dioxide	17	25	**9**	17	17	19	22	22	16-25	mmol/L
Anion Gap	**29.7**	19.7	**38.8**	**28**	21.1	16	21.1	16.4	10-23	mmol/L
Total Protein	**7.6**	5.7	**7.6**	**7.9**	**7.6**	6.7	6.7	7	5.5-7.1	g/dL
Albumin	3.5	**2.4**	4	3.5	3.5	3	3.2	2.8	2.7-3.9	g/dL
Globulins	**4.1**	3.3	3.6	**4.4**	**4.1**	3.7	3.5	**4.2**	2.3-3.8	g/dL
ALT	33	**305**	**314**	58	47	44	71	76	20-108	IU/L
ALP	66	**223**	88	71	34	32	32	25	23-107	IU/L
GGT	10	**13**	10	10	10	10	10	10	0-10	IU/L
Total bilirubin	<0.1	**7.3**	1	**0.6**	0.2	0.4	0.2	0.2	0.1-0.4	mg/dL
Conjugated bilirubin	-	**4**	-	0	-	-	-		0-0.2	mg/dL
Unconjugated bilirubin	-	**0.5**	-	0	-	-	-		0	mg/dL
Delta bilirubin	-	**2.8**	-	**0.6**	-	-	-		0-0.4	mg/dL
Cholesterol	259	231	**490**	214	238	225	103	128	45-274	mg/dL
Amylase	529	761	1168	929	899	891	962	775	440-1264	IU/L
Lipase	**3433**	782	**2139**	851	523	294	381	383	148-1746	IU/L
Ammonia	-	<8.7	-	-	-	-	-	-	0-39	µmol/L
Specific feline pancreatic lipase	-	**11.7**	-	-	-	-	-	-	0-3.5	µg/L
Ketones	-	**Pos**	**Pos**	**Pos**	-	-	-	-		Neg
Urinalysis										
Collection	Cysto.									
USG	1.029								1.010-1.030	
pH	6.5								5-8	
Proteins	**Trace**								Neg	
Glucose	**3+**								Neg	
Ketones	**Pos**								Neg	
Bilirubin	Neg								Neg	
Blood	Neg								Neg	

Table 5.3: Total RNA concentration determined by fluorimetry and RIN determined by electrophoresis.

	Specimens	**Total RNA concentration (ng/uL)**	**RIN**
First 8 healthy cats	Healthy 1	11.4	1.4
	Healthy 2	18.4	2
	Healthy 3	6.3	1
	Healthy 4	15.2	2.2
	Healthy 5	35.8	2.9
	Healthy 6	9.5	7.5
	Healthy 7	9.0	1.3
	Healthy 8	9.5	1.2
Diabetic and healthy controls	Diabetic 1	97.6	2.7
	Diabetic 2	139.2	2.7
	Diabetic 3	39.6	2.6
	Diabetic 4	72	2.6
	Healthy 1	101.2	2.7
	Healthy 2	80.8	2.8
	Healthy 3	134.6	2.6
	Healthy 4	113	2.6

Table 5.4: Number of isomiRs identified in feline mature RBCs after library construction with the TruSeq small RNA preparation kit.

Number of isomiRs	Number of microRNAs	List of microRNAs
1	142	let-7g-3p; miR-664a-3p; miR-519b-3p; miR-4659a-5p; miR-450b; miR-329b; miR-3150b-3p; miR-27a; miR-200c; miR-193a; miR-18b; miR-151a-3p; miR-8891; miR-8864; miR-8823; miR-8804; miR-8067; miR-8057; miR-8052; miR-7977; miR-7850-5p; miR-7703; miR-7111-3p; miR-6867-5p; miR-6854-5p; miR-6852-3p; miR-6850-3p; miR-6844; miR-6823-3p; miR-6812-5p; miR-6805-3p; miR-6794-3p; miR-6782-5p; miR-6777-3p; miR-6770-3p; miR-6765-3p; miR-6738-5p; miR-6736-3p; miR-6734-5p; miR-6512-3p; miR-6510-3p; miR-5708; miR-5695; miR-5682; miR-5590-3p; miR-5188; miR-5093; miR-5008-5p; miR-5002-3p; miR-4790-3p; miR-4778-5p; miR-4775; miR-4757-5p; miR-4747-5p; miR-4741; miR-4733-5p; miR-4732-3p; miR-4718; miR-4653-5p; miR-4648; miR-4536-5p; miR-4515; miR-4505; miR-4497; miR-4460; miR-4459; miR-4442; miR-4425; miR-4326; miR-4325; miR-4303; miR-4298; miR-3925-5p; miR-3922-3p; miR-3918; miR-3915; miR-3914; miR-3674; miR-3654; miR-3613-3p; miR-3200-3p; miR-3192-5p; miR-3191-5p; miR-3175; miR-3156-3p; miR-3133; miR-3064-5p; miR-2278; miR-1915-3p; miR-1908-5p; miR-1343; miR-1296; miR-1288-5p; miR-1278; miR-1276; miR-1271; miR-1203; miR-1199-3p; miR-889-5p; miR-874-5p; miR-767-3p; miR-744-5p; miR-660; miR-630; miR-590; miR-572; miR-532; miR-505-3p; miR-504-3p; miR-502; miR-500; miR-499; miR-498; miR-485; miR-425; miR-378; miR-375; miR-365; miR-362; miR-361; miR-345; miR-339; miR-335; miR-326; miR-320; miR-197; miR-194; miR-191; miR-188; miR-186; miR-155; miR-144-5p; miR-143; miR-142; miR-141-3p; miR-139-5p; miR-132; miR-129; miR-128; miR-107; miR-101; miR-28
2	54	miR-4433b-3p; miR-4419a; miR-378g; miR-374b; miR-33a-3p; miR-26a; miR-23b; miR-219a-1-3p; miR-19b; miR-18a-3p; miR-138b; miR-10a; miR-8903; miR-8853; miR-7106-5p; miR-6834-5p; miR-6832-5p; miR-6749-3p; miR-6727-5p; miR-6165; miR-4802-5p; miR-4688; miR-4520-2-3p; miR-4512; miR-4479; miR-4308; miR-3690; miR-3688-5p; miR-3117-3p; miR-1306; miR-1270; miR-1249; miR-1208; miR-1204; miR-1180-3p; miR-943; miR-939-3p; miR-877-5p; miR-766-3p; miR-628; miR-615; miR-580-3p; miR-574; miR-451; miR-328; miR-210; miR-199; miR-182; miR-153-5p; miR-140; miR-126; miR-22; miR-21; miR-9

Table 5.4 continued

3	19	miR-196b; miR-190b; miR-146b; miR-135b; miR-106a; miR-8886; miR-6835-3p; miR-4529-3p; miR-3661; miR-3074-5p; miR-1842; miR-1292-3p; miR-542; miR-448; miR-222; miR-192; miR-151; miR-150; miR-7-1-3p
4	5	miR-193b-3p; miR-8868; miR-671; miR-185; miR-24
5	7	miR-92b; miR-30d; miR-181a; miR-130b; miR-106b; miR-421; miR-324-3p
6	2	miR-29b; miR-486
7	1	miR-15b
8	1	miR-148a
9	1	Let-7b

Table 5.5: List of the most abundant microRNAs from eight healthy cats, after library construction with the TruSeq small RNA preparation kit.

	Specimen							
microRNA	**1**	**2**	**3**	**4**	**5**	**6**	**7**	**8**
miR-486	83.8	87.3	86.8	90.6	84.4	88.3	82.4	78.2
let-7f	4.9	2.6	3.4	2.4	3.0	2.7	4.2	6.2
miR-25	2.6	2.5	2.1	1.6	3.6	2.4	3.1	3.8
miR-92a	1.8	1.8	1.6	1.4	1.9	1.6	2.1	2.7
miR-451	1.3	1.1	1.2	0.7	1.7	1.0	1.7	1.6
let-7i	1.0	0.8	0.8	0.7	1.1	0.7	1.0	1.5
miR-16	0.8	0.8	0.6	0.4	0.8	0.6	1.0	1.0
miR-191	0.5	0.3	0.3	0.3	0.3	0.3	0.5	0.6
miR-423	0.5	0.3	0.4	0.3	0.4	0.3	0.5	0.4
let-7a	0.4	0.4	0.5	0.2	0.4	0.3	0.5	0.8
miR-93	0.3	0.2	0.2	0.1	0.3	0.2	0.3	0.3
miR-103a	0.2	0.2	0.3	0.1	0.4	0.2	0.4	0.3
miR-186	0.2	0.2	0.1	0.2	0.1	0.1	0.2	0.2
miR-107	0.2	0.2	0.3	0.1	0.4	0.2	0.3	0.3
miR-181a	0.2	0.1	0.1	0.1	0.1	0.1	0.2	0.3
others	1.4	1.1	1.4	0.8	1.3	1.0	1.5	1.9

Table 5.6: Number of isomiRs identified in feline mature RBCs after library construction with the NEXTFLEX® small RNA preparation kit.

Number of isomiRs	Number of microRNAs	List of microRNAs
1	84	miR-21; miR-24; miR-28; miR-95; miR-122; miR-126; miR-132; miR-143; miR-144-5p; miR-149; miR-182; miR-183; miR-184; miR-197; miR-212; miR-219-5p; miR-328; miR-345; miR-346; miR-350; miR-375; miR-383; miR-421; miR-448; miR-489; miR-490; miR-504; miR-505; miR-542; miR-580-3p; miR-615; miR-631; miR-708; miR-761; miR-1199-3p; miR-1208; miR-1288-5p; miR-1292-3p; miR-1301; miR-3133; miR-3613-3p; miR-3922-3p; miR-3925-5p; miR-4298; miR-4308; miR-4505; miR-4512; miR-4529-3p; miR-4733-5p; miR-4741; miR-5682; miR-6516; miR-6770-3p; miR-6777-3p; miR-6832-5p; miR-6834-5p; miR-6835-3p; miR-6844; miR-7850-5p; miR-7977; miR-8801; miR-8804; miR-8807; miR-8836; miR-8846; miR-8851; miR-8874; miR-8876; miR-8884; miR-8891; miR-106a; miR-133c; miR-138b; miR-151a-3p; miR-18a-3p; miR-216b; miR-219a-1-3p; miR-3150b-3p; miR-33a-3p; miR-34c; miR-508a; miR-519b-3p; miR-664a-3p; miR-8834a
2	48	miR-1; miR-9; miR-101; miR-128; miR-129; miR-140; miR-142; miR-145; miR-150; miR-153; miR-188; miR-191; miR-194; miR-211; miR-324-3p; miR-326; miR-335; miR-361; miR-362; miR-365; miR-425; miR-491; miR-502; miR-532; miR-574; miR-590; miR-660; miR-766-3p; miR-1249; miR-1343; miR-4802-5p; miR-7106-5p; miR-8789; miR-8827; miR-8853; miR-8886; miR-8903; miR-125b; miR-133b; miR-18b; miR-190b; miR-193a; miR-193b-3p; miR-200c; miR-23b; miR-450b
3	15	miR-7; miR-151; miR-185; miR-186; miR-192; miR-320; miR-378; miR-451; miR-499; miR-671; miR-1296; miR-1842; miR-135b; miR-26a; miR-374b
4	10	miR-22; miR-107; miR-222; miR-486; miR-1271; miR-8868; miR-10a; miR-148a; miR-19b; miR-27a
5	4	miR-339; miR-146b; miR-196b; miR-29b; miR-15b; miR-181a; miR-
6	2	miR-15b; miR-181a
7	3	miR-106b; miR-130b; miR-92b
8	1	miR-423a
10	1	miR-30d
20	1	Let-7b

Table 5.7: List of the most abundant microRNAs from four diabetic and four healthy control cats, after library construction with the NEXTFLEX® small RNA preparation kit.

	Diabetic				**Healthy control**			
microRNA	**1**	**2**	**3**	**4**	**1**	**2**	**3**	**4**
miR-451	82.2	75.5	74.0	68.0	76.5	71.9	70.2	76.2
miR-16	4.5	6.4	5.6	7.0	4.9	6.7	7.2	5.9
others	4.2	5.2	6.3	6.8	5.5	6.0	6.1	4.8
miR-92a	1.8	2.8	2.8	3.5	3.4	3.8	4.8	4.0
let-7f	1.0	1.3	1.2	1.5	1.3	1.1	1.7	0.7
miR-486	1.0	1.7	0.7	2.7	1.4	2.3	1.6	1.7
miR-191	0.8	1.1	1.7	2.4	1.4	1.8	1.6	1.4
let-7g	0.8	0.8	0.8	1.0	0.9	0.8	0.9	-
miR-15b	0.7	0.7	0.6	0.8	0.5	0.5	0.8	0.4
let-7a	0.6	0.7	1.5	1.7	0.8	0.9	1.0	0.5
miR-21	0.5	0.6	0.5	-	-	-	0.6	0.5
let-7i	0.5	0.7	0.7	0.7	0.7	0.7	0.8	0.5
miR-26a	0.4	0.6	0.8	0.9	0.5	0.6	0.7	0.7
miR-26b	0.4	0.5	1.0	0.9	0.5	0.7	0.7	0.7
miR-30e	0.4	1.0	-	0.6	0.5	0.6	-	0.6
miR-93	0.3	0.5	0.9	0.9	0.7	0.9	0.6	0.7
miR-25	-	-	0.8	0.6	0.5	0.7	0.7	0.7

Table 5.8: List of the most abundant microRNAs from eight healthy cats, after library construction with the NEXTFLEX® small RNA preparation kit.

	Specimen							
microRNA	**1**	**2**	**3**	**4**	**5**	**6**	**7**	**8**
miR-451a	68.1	63.2	68.0	66.4	68.4	70.4	70.9	60.5
miR-486	6.5	4.5	6.4	2.9	3.2	3.3	3.4	7.0
miR-16	4.4	5.1	4.2	5.2	4.6	4.7	4.6	5.2
miR-92a	3.5	4.1	3.4	3.8	3.8	4.2	3.3	6.2
miR-191	3.0	3.6	2.9	3.6	3.0	2.7	2.7	4.0
let-7a	1.8	2.8	1.6	2.2	1.9	1.8	1.8	2.1
let-7f	1.3	2.0	1.6	2.5	2.0	1.6	1.8	1.6
miR-25	0.8	0.9	0.9	0.8	0.7	0.7	0.6	1.1
miR-15	0.8	1.2	0.8	1.1	1.2	0.8	0.9	1.0
let-7b	0.8	0.8	0.4	-	0.5	0.5	0.4	0.8
miR-93	0.7	1.3	0.8	1.0	1.0	0.9	0.9	1.0
let-7g	0.7	1.2	0.9	1.3	1.1	0.8	1.0	0.7
miR-26b	0.5	0.7	0.5	0.5	0.6	0.5	0.4	0.6
let-7i	0.4	0.5	0.5	0.6	0.6	0.5	0.5	0.5
miR-423-5p	0.3	-	-	-	-	-	-	-
miR-107	-	0.5	-	0.5	-	0.4	-	0.5
miR-26a	-	-	0.6	-	0.6	-	0.4	-
miR-30e	-	-	-	0.6	-	-	-	-
others	6.2	7.7	6.2	7.2	6.7	6.3	6.4	7.3

Table 5.9: Differentially abundant feline mature erythrocyte microRNAs determined by RNA-Seq and miRDeep2 analysis.

mature microRNA	Fold change	P value category	mature microRNA sequence
let-7b	2.31	<0.05	AGGCAGUAGGUUGUAUAG
miR-128	1.85	<0.1	UCACAGUGAACCGGUCUC
miR-1692	12.98	<0.05	GGCUAGCUCAGUCGGUAG
miR-210	0.48	<0.1	ACUGUGCGUGUGACAGCGGCUGA
miR-339-1	3.29	<0.05	UCCCUGUCCUCCAGGAGCUC
miR-339-2	3.38	<0.05	UCCCUGUCCUCCAGGAGCU
miR-339-3	4.14	<0.05	UCCCUGUCCUCCAGGAACUG
miR-339-4	3.47	<0.05	UCCCUGUCCUCCAGGAGC
miR-339-5	3.33	<0.1	UCCCUGUCCUCCAGGAGCUCA
miR-365	1.97	<0.1	UAAUGCCCCUAAAAAUCC
miR-374b-1	1.81	<0.05	AUAUAAUACAACCUGCUAAG
miR-374b-2	1.84	<0.1	AUAUAAUACAACCUGCUAAGU
miR-92a	0.50	<0.05	UAUUGCACUUGUCCCGGCCUG
unknown 5	37.48	<0.05	AUCUUCGUGGGUCACUGCCU
unknown 1	3.17	<0.05	AUCUUUGUGGGUCACUGAC
unknown 3	3.18	<0.1	AUCUUUGUGGGUCACUGACU
unknown 4	2.01	<0.1	AAGGCAGUAGGUUGUAUAGU
unknown 5	35.40	<0.05	AUCUUCGUGGGUCACUGCCU
unknown 6	3.32	<0.1	UUUUGCGAUGUGUUCCUAAUA
unknown 8	5.18	<0.05	CAGUCGGUAGAGCAUGGG
unknown 2	2.21	<0.1	AUUCAGACUACUCUCCCCCGUCC

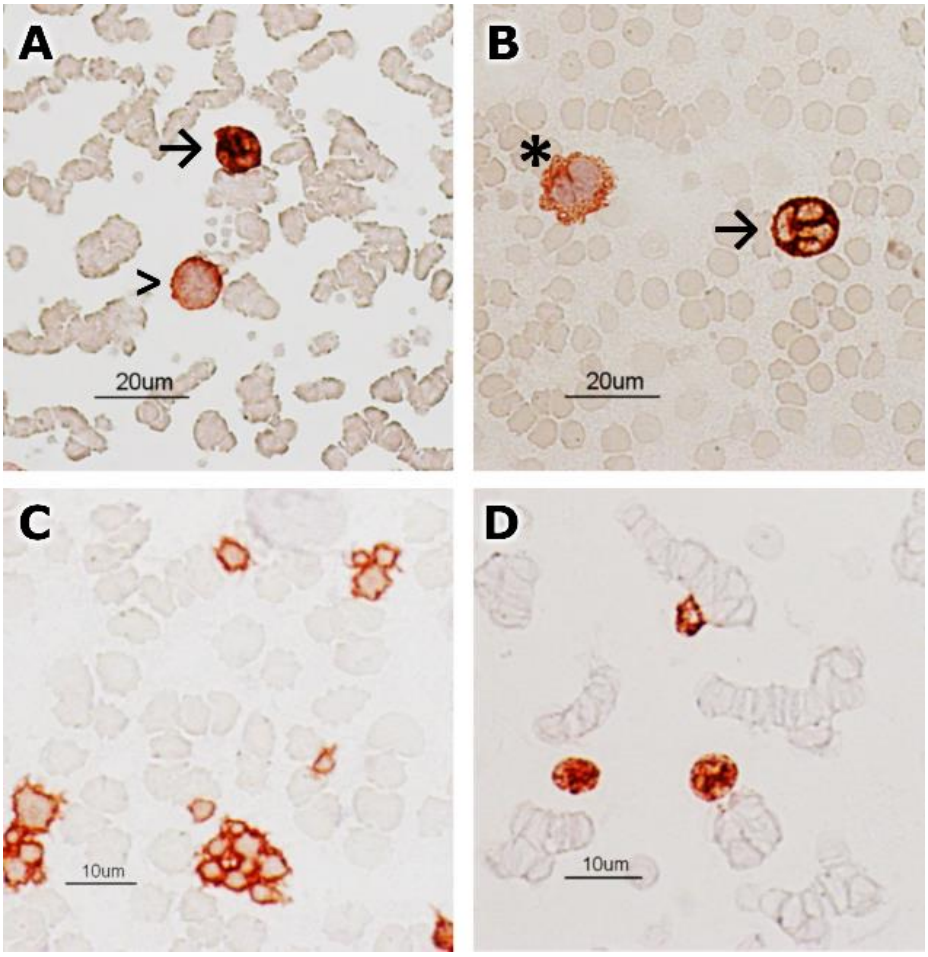

Figure 5.1: Immunocytochemistry performed on feline blood smears.
Marked surface diffuse immunoreactivity was observed on granulocytes (arrows), lymphocytes (arrow head) and monocytes (star) when the CA1.4E9 anti-CD18 was used as primary antibody (A and B). Figure C illustrates the diffuse surface immunoreactivity of platelet and platelet clumps when an anti-CD61 antibody was used as the primary antibody. Figure D demonstrates diffuse to clustered immunoreactivity on the surface of reticulocytes when anti-CD71 antibody was used. Negative controls did not show immunoreactivity.

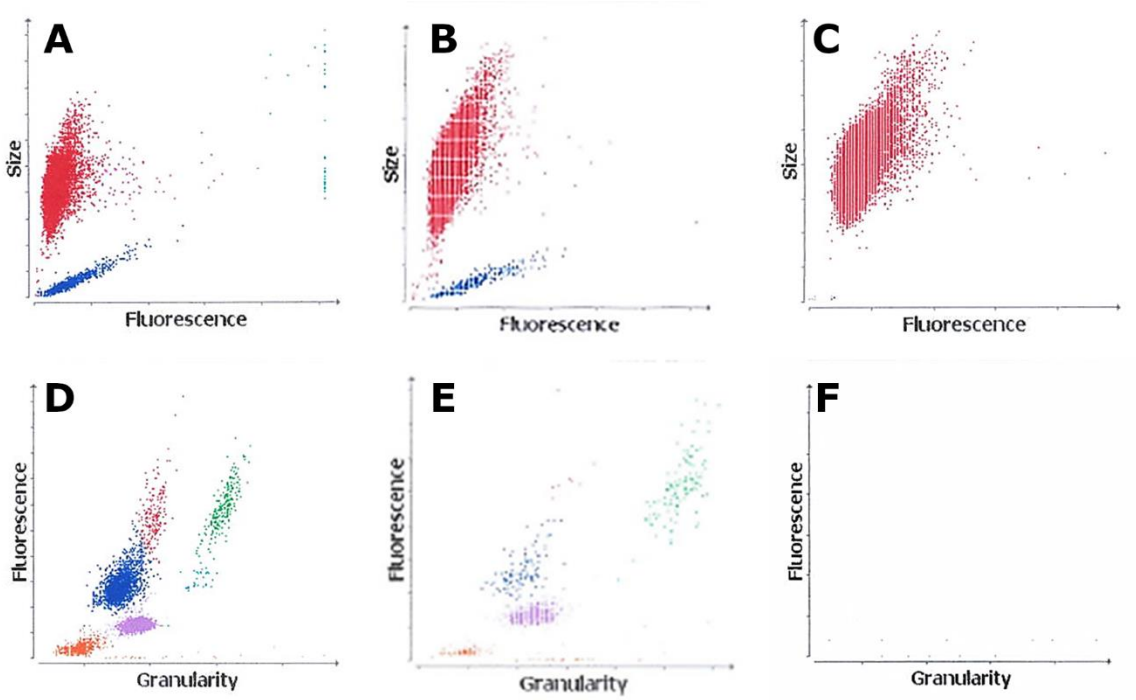

Figure 5.2: Mature erythrocyte isolation followed up with hematology analyzer scatterplots
Figure 5.2A represents the red blood cells / platelet channel. The red blood cell population appears as a red cloud while platelets are identified by the blue cloud. Rare event possibly representing few reticulocytes can be seen on the right of the red blood cell dot plot. After centrifugation and collection of the pelleted red blood cells by gravity flow and leukoreduction, platelets are still detected (B). These platelets were removed by immunodepletion (C). After immunocapture, no events were seen in the location of the reticulocytes. A variety of leukocytes and cell debris are detected in whole blood in the white blood cell channel (D). Most of the leukocytes were removed from the pelleted RBCs collected by gravity flow. The remainder were eliminated by leukoreduction and immunocapture (F).

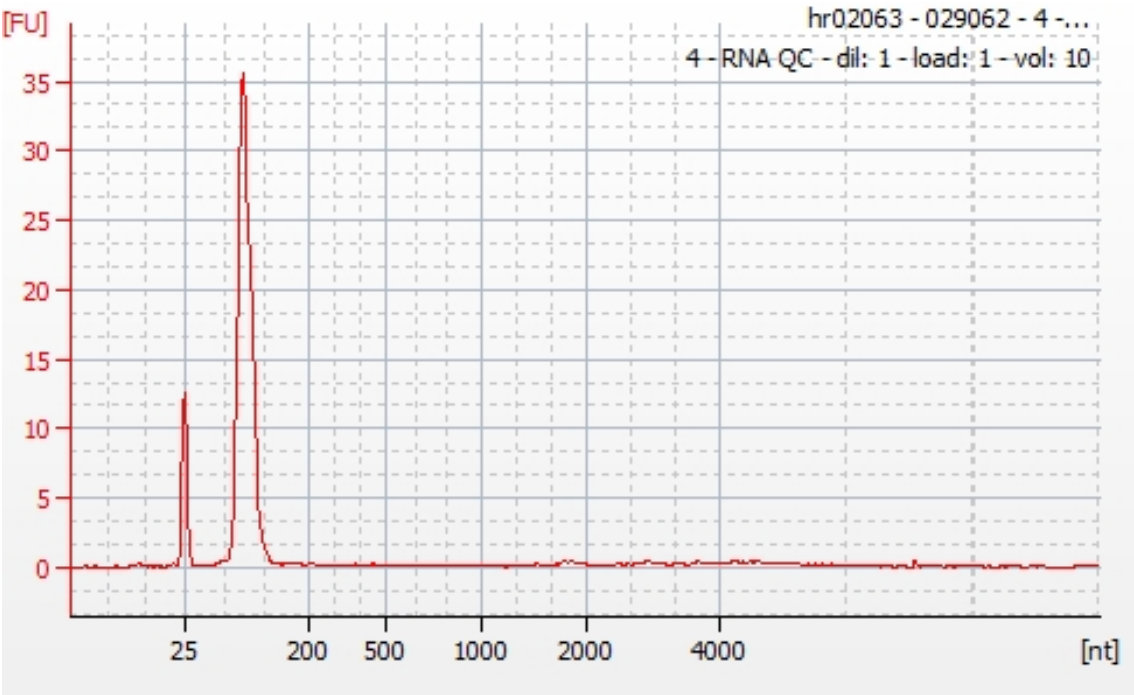

Figure 5.3: RNA electrophoretogram.
Note the absence of significant peaks representing the 18S and 28S rRNAs in the region between 2000 and 4000 nt. A single peak in the areas of small RNAs (between 25 and 200 nt) was seen, indicating an adequate extraction. The peak at the 25 nt mark is a marker added to the specimens.

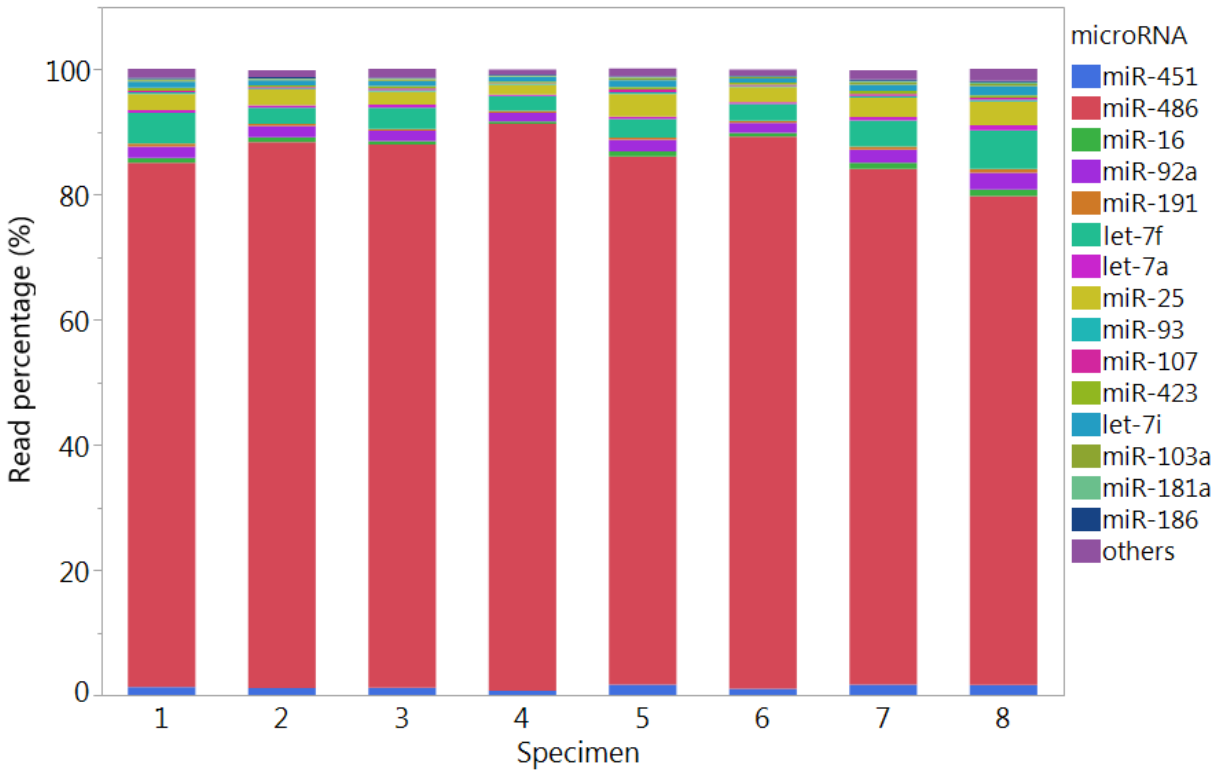

Figure 5.4: Graphical representation of the most abundant microRNAs quantified using the TruSeq Small RNA library preparation kit, in eight healthy cats.
MiR-486 is the most abundant microRNA detected across the specimens. In all specimens, miR-451 represents less than 2% of the reads.

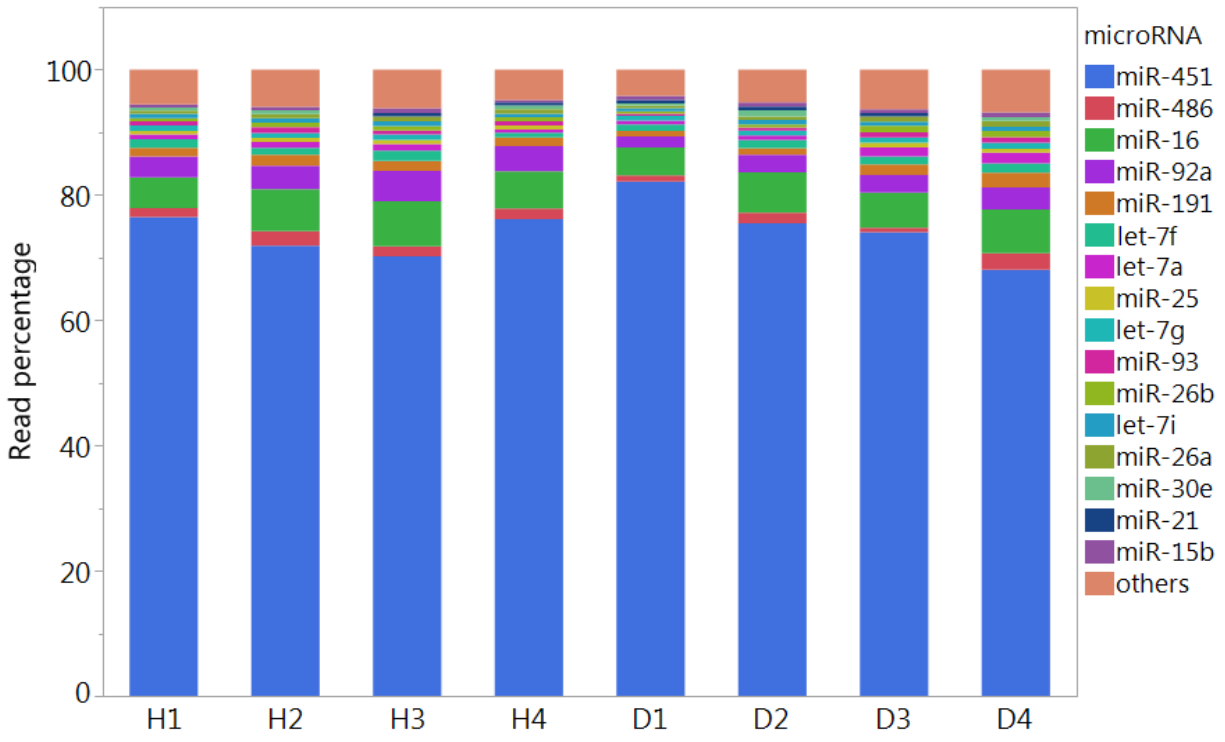

Figure 5.5: Graphical representation of the most abundant microRNAs detected in mature RBC of four healthy (H 1 to 4) and diabetic cats (D1 to 4) with the NEXTFLEX® Small RNA library preparation kit.
By far, miR-451 is the most abundant microRNA detected while miR-486 represents less than 3% of all reads.

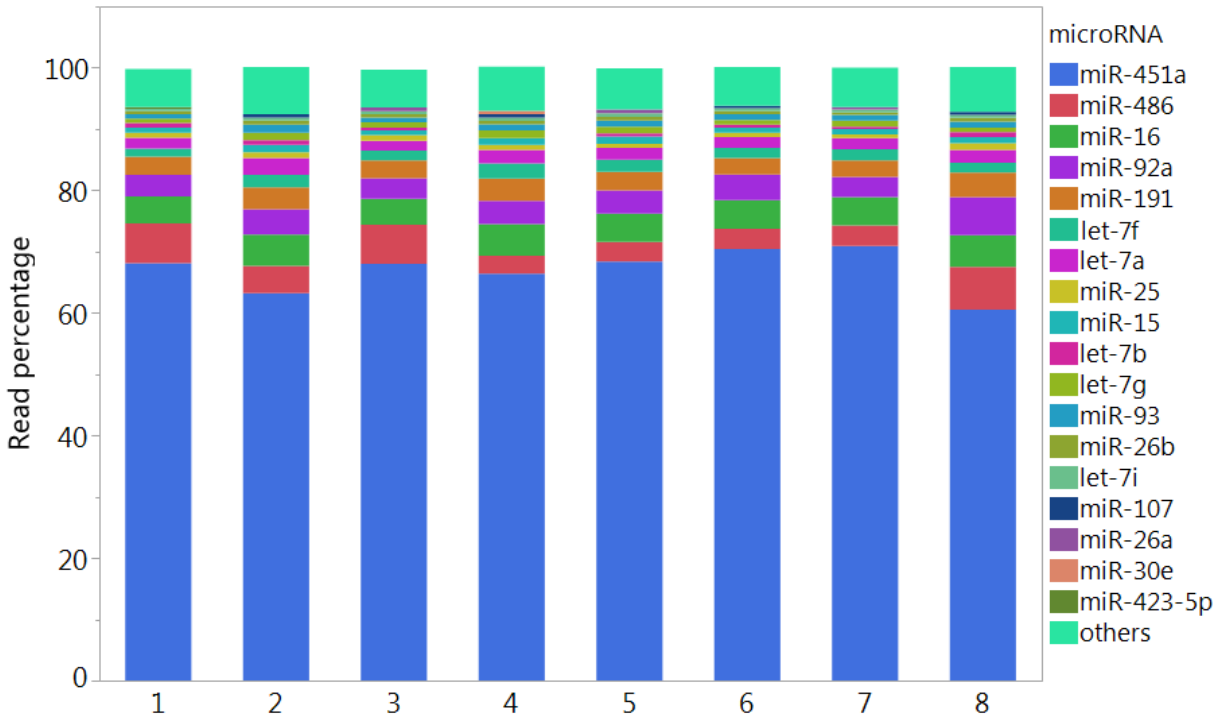

Figure 5.6: Graphical representation of the most abundant microRNAs detected with the NEXTFLEX® Small RNA library preparation kit from eight healthy cats previously quantified with the TruSeq Small RNA Library Preparation kit.
Contrary to the quantification performed on libraries prepared with the TruSeq Small RNA Library Preparation kit, miR-451 is the most abundant microRNA detected, representing more than 60% of all the reads while miR-486 accounts for less than 3% of all reads.

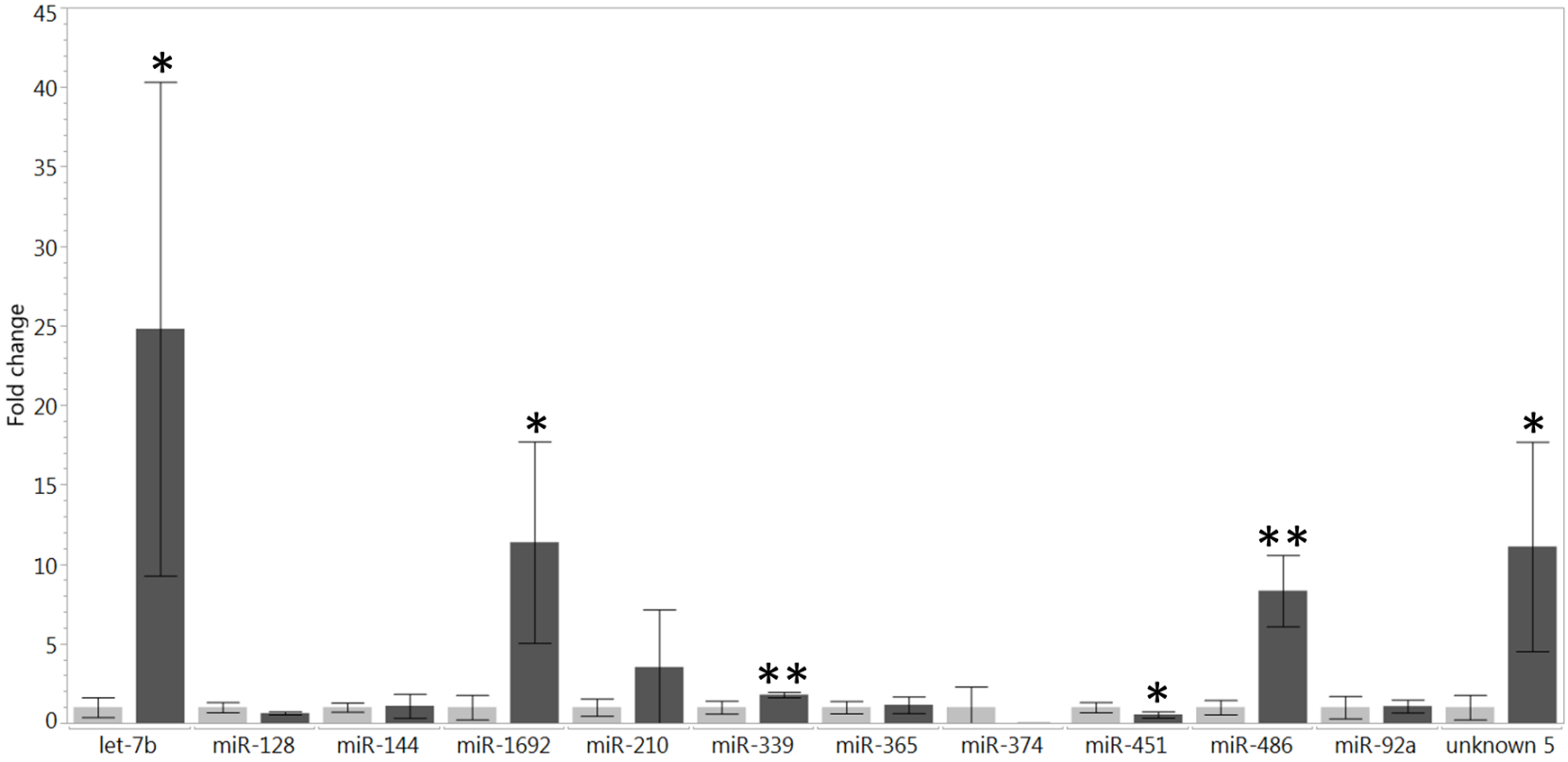

Figure 5.7: Graphic representation of microRNAs fold change determined by RT-qPCR.
Let-7b, miR-1692, miR-339, miR-486 and unknown 5 were significantly more abundant in feline mature red blood cells in comparison to RBCs of healthy control cats. miR-451 was significantly decreased in diabetic cats in comparison to healthy controls. Vertical bars represent standard error. Stars represent significance: one star represent $P < 0.1$ whereas two stars represent $P < 0.05$.

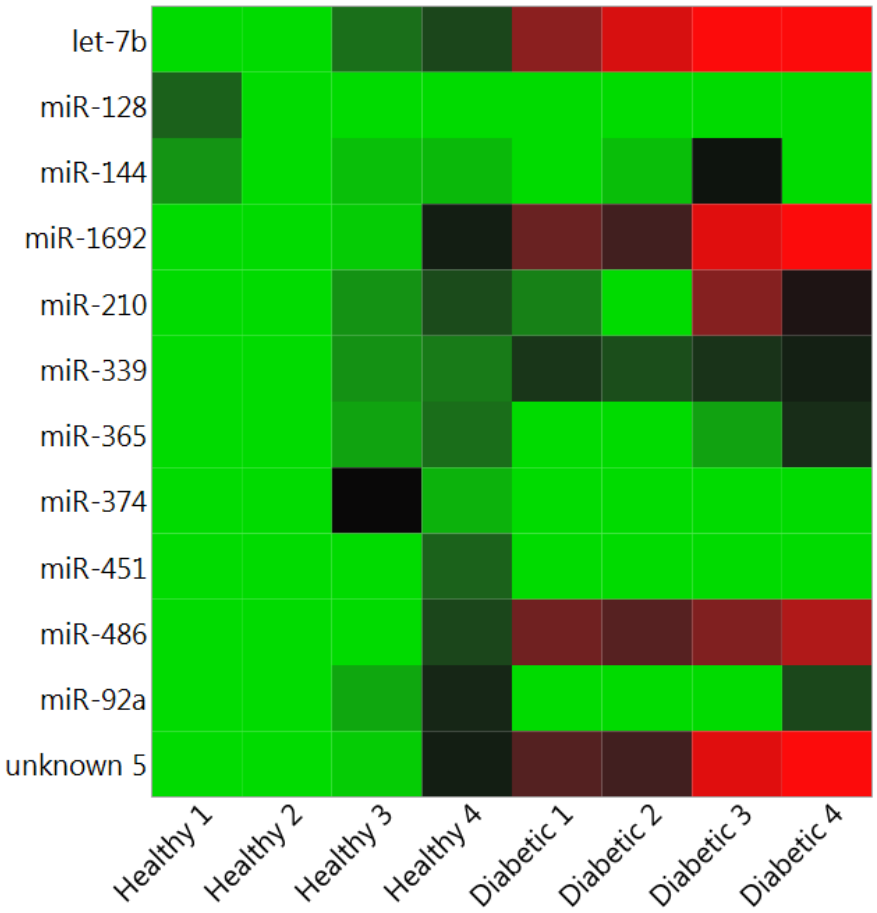

Figure 5.8: Heatmap depicting the individual stem-loop RT-qPCR results.
These results are consistent with groups RT-qPCR results with let-7b, miR-128, miR-1692, miR-486 and unknown 5 showing increased abundance in diabetic cats in comparison to healthy controls. However Healthy 4 also had a relatively abundant miR-1692 and unknown 5 similarly to diabetic cats. MiR-144 was more abundant in a single diabetic cat

CHAPTER 6. CONCLUSION

The goal of this dissertation was to identify a set of differentially abundant microRNAs in mature RBCs of felines with oxidative stress, using diabetes mellitus as an oxidative stressor. It is postulated that individual microRNAs identified in this study, may serve to generate new hypotheses for future studies, investigating the role specific microRNAs play in the development or progression of diabetes and in the oxidative damage inflicted on the red cell by this disease. Our first specific objective was to document systemic oxidative stress in diabetic cats. Secondly, we sought to isolate mature red blood cells from feline whole blood, sequence their microRNAs and evaluate changes in diabetic cats in comparison to healthy controls.

Despite an increasing interest in the role that oxidative stress plays role in various diseases[22,202,203,207,227,278], a limited number of oxidative stress assays have been properly validated for use in cats, and none assess protein carbonyls (PC). PC content testing is the most commonly performed assay for protein oxidation, since increased levels are considered an early indicator of oxidation and are relatively stable[208,209]. In the second chapter of this work, we describe and evaluate the performance of the historical 2,4-dinitrophenylhydrazine (DNPH) colorimetric protein carbonyl (PC) assay. This assay, as adapted for use in microplates by Levine *et al.* in 1990[127], was validated for determination of PC in feline plasma and serum specimens. While the DNPH assay had adequate within-run performance, the between-run variation was not acceptable. This shortcoming is likely to greatly limit the number of samples that can be included in a study, particularly when specimens are collected multiple time points and stored. Additionally, even if this test performed adequately over a wide range of PC content values, results were influenced by the presence of even slight hemolysis in samples. In contrast, lipemia did not interfere significantly

with the results. The main advantage of this test is that no standards are required, since PC content can be determined from the molar absorptivity coefficient of DNPH. However, this test is work intensive and time consuming which prompted us to develop a new PC assay.

In the third chapter of this research work, we described a new procedure to determine PC content, using a fluorophore, the 4-hydrazino-7-nitro-2,1,3-benzoxadiazole hydrazine (NBDH). NBDH becomes fluorescent only after it has reacted with carbonyls and in contrast to the DNPH colorimetric assay, this assay does not require the cumbersome and time-consuming protein washing steps to remove unreacted chromophores/fluorophores. The NBDH assay showed a low within and between-run variation, and good performances over a large range of PC content values and could be a valuable alternative to the DNPH assay. Although this assay showed significance interference from both hemoglobin and triglycerides, unlike the DNPH colorimetric assay, interferences only occurred when hemolysis or lipemia were visually moderate to marked.

Taken together, we evaluated two assays for PC content determination in feline serum and plasma. Although both tests have advantages and limitations, they are the first tests for PC content measurement in felines. In people and laboratory animals, increased PC content has been described in association with a variety of diseases including diabetes mellitus, Alzheimer's disease, inflammatory diseases or cancer[208]. The new NBDH assay for PC may serve as a useful tool to understand the role and the consequences that systemic oxidative stress play in feline disease and how to best treat or monitor treatment of these conditions.

To document oxidative stress in the four diabetic cats recruited for erythrocyte microRNA sequencing, we compared the serum and plasma PC content of these diabetic cats to healthy controls. Results can be found in chapter two and three. In chapter four, we further evaluated systemic redox status as well as that of the erythrocyte *per se*, comparing the plasma F_2-isoprostane

concentration, as a reflection of cell membrane oxidation, the serum antioxidant capacity and the intra-erythrocytic total glutathione, oxidized glutathione and the total to oxidized glutathione ratio, between diabetic and healthy control felines. Diabetic cats had higher serum and plasma PC content with both the colorimetric and fluorimetric techniques, higher plasma F_2-isoprostane concentrations as well as higher erythrocytic total glutathione concentrations. There was a trend toward higher oxidized glutathione concentrations and lower total to oxidized glutathione ratio, suggesting a red blood cell redox status trending towards oxidation. These results confirmed the presence of oxidative stress in serum, plasma and red blood cells of diabetic felines. This was expected, since all cats had Heinz bodies, erythrocytic inclusions observed on their blood smear. Heinz bodies form when hemoglobin and RBC membranes are oxidized and are considered insensitive indicators systemic oxidative stress[73]. All four diabetic cats were ketoacidotic, a relatively common complication of diabetes in cats, which is often associated with Heinz bodies[39,279]. Surprisingly, the total antioxidant capacity assay did not work in our hands, for reasons that are unknown.

In chapter five, we report a method from mature RBC isolation from whole blood in eight healthy cats. Three separate steps were used to insure the absence of other nucleated cells, platelets, and reticulocytes from the final preparations. Total RNA was extracted from these mature RBCs and library construction pursued using the TruSeq Small RNA library preparation kit; thereafter it was sequenced with sequences and annotation used to populate searchable microRNA databases. We identified 499 individual microRNA sequences, corresponding to 101 feline specific microRNAs and 398 sequences with a human or canine microRNA counterpart. Amongst these microRNAs, miR-486 was by far the most abundant sequence, representing approximately 78.2 to 90.6% of all the reads, while miR-451 accounted for only 0.7 to 1.7%. Given that miR-451 is the

most abundant microRNA identified in RBCs of humans and is believed to play an important role in erythroid homeostasis during RBC development, it was surprising to find low reads of it in the mature erythrocytes of healthy cats[189]. We repeated the same procedure to compare the mature RBC microRNA content of diabetic and healthy control cats. However, our core sequencing facility made an unannounced change in the library preparation; instead of using TruSeq, it was done with the NEXTFLEX® small RNA library preparation kit. This time, 899 individual microRNA sequences were identified, including 543 feline specific microRNAs and 356 microRNAs similar to human or canine. Interestingly, the most abundant microRNA was now miR-451, which represented 68 to 82.2% of all reads, while miR-486 represented 0.7 to 2.7%. To investigate our concern of bias in the library construction, the first eight samples from healthy cats were re-sequenced using the NEXTFLEX® small RNA library preparation kit. In the second sequencing, the most abundant microRNA in the erythrocyte of these cats was miR-451; this confirmed our suspicion that there was significant bias in the various library constructions. This phenomenon has been described in the literature; however, such discrepancies between the library construction kits was unexpected[277]. The NEXTFLEX® kit was considered most likely accurate in comparison to the TruSeq kit, given the former provided results that were similar to those reported for human erythrocytes, using a different library construction method[182]. The microRNA sequences reported in this study will populate the microRNA database, currently lacking feline sequences. This will provide essential information for future microRNA studies in cats.

A set of differentially expressed microRNAs that are present in the erythrocytes of cats with diabetes and not in healthy cats are also reported in chapter 5. Twelve differentially abundant microRNAs were identified based on RNA-Seq data, whereas six were differentially abundant on RT-qPCR. Let-7b, miR-1692, miR-339, miR-486 and a feline specific sequence, were more

abundant in RBCs of diabetic cats, while miR-451 was less abundant. Further studies are needed to elucidate the meaning of these changes. It is known that Let-7b, miR-486, miR-339 and miR-451 are needed for erythropoiesis, promoting cell proliferation, differentiation and hemoglobinization[175,178,180,183-185,272]. MiR-451 is also involved in the acquisition of antioxidant defenses in the erythroid lineage[173,254]. In light of our findings that miR-451 is decreased in diabetic cats, it may be particularly interesting to investigate it, in relation to the susceptibility of erythrocytes to oxidant damage. The role of miR-1692 and of the feline specific unidentified microRNA in erythropoiesis is unknown. In mature RBCs, these microRNAs could be by-standers and reflect the fine-tuning of erythroid cells in response to environmental changes such as hyperglycemia or increased oxidative stress in our study. As such, they may be useful biomarkers for erythropoiesis as suggested for human patients with sickle cell disease[193]. However, other researchers have suggested an active role for microRNAs in host defenses against an inhospitable microenvironment. It has been shown that microRNAs may be involved in helping to thwart malaria infection of erythrocytes. The results of one *in vitro* study, showing *Plasmodium* sp. infected RBCs release extracellular vesicles containing miR-451 bound to Argonaute 2 (AGO2), are particularly intriguing. These particles can be transferred to non-infected RBCs and provide protection against parasite infection[280]. In yet another study, it has been shown that miR-451-loaded particles from RBCs can also be transferred to endothelial cells where they change the expression of genes involved in adhesion and permeability of the endothelium. Thus, an active role for these RBC-derived microRNAs is suggested in cell-to-cell communication[197,198] and transferred microRNAs may have deleterious effect of on the vascular endothelium. These particles could, for instance, contribute to vascular disease observed in patients with malaria[198]. It is also possible that this represents a more generalized response to systemic oxidative stress; thus,

under conditions of oxidative stress, such as that experienced in a diabetic patient, RBCs may externalize microparticles. These microparticles, might play a role in cardiovascular complication associated with diabetes[197]. But is it possible that they might serve a beneficial role, such as delivering effecter molecules that promote oxidant protection? The latter hypothesis has not yet been investigated.

This research study was undertaken to evaluate changes in the expression of erythrocytic microRNAs under oxidative stress conditions, using diabetes as an oxidant stressor and to generate study hypotheses for future projects. The role of oxidative stress in disease is still not well understood. Nonetheless, the evaluation of PC content using the assay developed herein or F_2-isoprostanes may provide additional tools that can be used to better understand the effects of oxidative stress in various diseases. They could also be used to follow the effects of antioxidant treatments. However, these tests need to be validated in other domestic species and evaluated in various diseases. Another line of research might be to further study the role of microRNAs in erythropoiesis as information is sparse. Understanding their role could provide insight into the mechanisms behind erythropoiesis or stimulate the emergence of new biomarkers for bone marrow disorders or new targets for treatment. Further, the role of microRNAs in circulating mature RBCs and how they might participate in the RBC communication with their surroundings, whether beneficial or deleterious, is a ripe area for investigation.

APPENDIX A. LIST OF MATURE MICRORNA SEQUENCES IDENTIFIED IN EIGHT HEALTHY CATS

Canine or human microRNA with the same seed	Consensus mature sequence
cfa-let-7b	UGAGGUAGGAGGUUGUAUAG
cfa-let-7b	UGAGGUAGUAGAUUGUAUAG
cfa-let-7b	UGAGGUAGUAGGUUGUAUAG
cfa-let-7b	UGAGGUAGUAGGUUGUAUGG
cfa-let-7b	UGAGGUAGUAGUUUGUACAG
cfa-let-7b	UGAGGUAGUAGUUUGUGCUGU
cfa-let-7b	UGAGGUAGUAAGUUGUAU
cfa-let-7b	UGAGGUAGUAAGUUGUAUUG
cfa-miR-101	UACAGUACUGUGAUAACUGAA
cfa-miR-106a	AAAGUGCUUACAGUGCAGGUAG
cfa-miR-106a	AAAGUGCUUACAGUGCAGG
cfa-miR-106a	AAAGUGCUUACAGUGCAGGU
cfa-miR-106b	UAAAGUGCUUAUAGUGCAGGUAG
cfa-miR-106b	CAAAGUGCUGUUCGUGCAGG
cfa-miR-106b	CAAAGUGCUUACAGUGCAGGUAG
cfa-miR-106b	CAAAGUGCUUACAGUGCAGG
cfa-miR-106b	CAAAGUGCUGUUCGUGCAGGUAG
cfa-miR-107	AGCAGCAUUGUACAGGGC
cfa-miR-10a	UACCCUGUAGAUCCGAAUU
cfa-miR-10a	UACCCUGUAGAACCGAAUU
cfa-miR-1199-3p	CGCGGCCGAGCUGCCGGACCG
cfa-miR-1249	ACGCCCUUCCCCCCCUUC
cfa-miR-1249	ACGCCCUUCCCCCCCUUCU
cfa-miR-126	CAUUAUUACUUUUGGUACGCG
cfa-miR-126	CAUUAUUACUCACGGUACGAG
cfa-miR-1271	CUUGGCACCUAGUAAGCAC
cfa-miR-128	UCACAGUGAACCGGUCUC
cfa-miR-129	CUUUUUGCGGUCUGGGCUUGC
cfa-miR-1296	GUAGGGCCUAGGAAUCUGUAUU
cfa-miR-1306	CCACCUCCCCUGCAAACGUCC
cfa-miR-130b	CAGUGCAAUAGUAUUGUCAAAGC
cfa-miR-130b	CAGUGCAAUGAUAUUGUCAAAGC
cfa-miR-130b	CAGUGCAAUGAUGAAAGGGCA
cfa-miR-130b	CAGUGCAAUGUUAAAAGGGC
cfa-miR-130b	CAGUGCAAUGUUAAAAGGGCA

cfa-miR-132	UAACAGUCUACAGCCAUGGUCG
cfa-miR-1343	CUCCUGGGGCCCGCACUCUCG
cfa-miR-135b	UAUGGCUUUUCAUUCCUAUG
cfa-miR-135b	UAUGGCUUUUCAUUCCUAUGUGA
cfa-miR-138b	AGCUGGUGUUGUGAAUCAGGCCG
cfa-miR-138b	AGCUGGUGUUGUGAAUCAGGC
cfa-miR-140	ACCACAGGGUAGAACCACGGAC
cfa-miR-140	ACCACAGGGUAGAUCCACGGAA
cfa-miR-142	CCCAUAAAGUAGAAAGCAC
cfa-miR-143	UGAGAUGAAGCACUGUAGCUC
cfa-miR-146b	UGAGAACUGAAUUCCAUAGGC
cfa-miR-146b	UGAGAACUGAAUUCCAUGGGU
cfa-miR-146b	UGAGAACUGAAUUCCAUGGG
cfa-miR-148a	UCAGUGCACUACAGAACUUUG
cfa-miR-148a	UCAGUGCAUCACAGAACUUUG
cfa-miR-148a	UCAGUGCAUGACAGAACU
cfa-miR-148a	UCAGUGCAUCACAGAACUUUGU
cfa-miR-148a	UCAGUGCAUCACAGAACUUUGUC
cfa-miR-148a	UCAGUGCAUGACAGAACUUG
cfa-miR-148a	UCAGUGCAUGACAGAACUUGG
cfa-miR-148a	UCAGUGCAUGACAGAACUUGGGC
cfa-miR-150	UCUCCCAACCCUUGUACCAG
cfa-miR-150	UCUCCCAACCCUUGUACCAGUGC
cfa-miR-150	UCUCCCAACCCUUGUACCAGU
cfa-miR-151	UCGAGGAGCUCACAGUCUA
cfa-miR-151	UCGAGGAGCUCACAGUCUAG
cfa-miR-151	UCGAGGAGUUCCCCGUCU
cfa-miR-155	UUAAUGCUAAUCGUGAUAGGG
cfa-miR-15b	UAGCAGCACAUAAUGGUU
cfa-miR-15b	UAGCAGCACAUCAUGGUUUACA
cfa-miR-15b	UAGCAGCACGUAAAUAUUGGCG
cfa-miR-15b	CAGCAGCACACUGUGGUUUG
cfa-miR-15b	CAGCAGCACACUGUGGUUUGUA
cfa-miR-15b	UAGCAGCACAGAAAUAUUGGC
cfa-miR-15b	UAGCAGCACAGAAAUAUUGGCA
cfa-miR-181a	AACAUUCAACCUGUCGGUGAG
cfa-miR-181a	AACAUUCAUUGCUGUCGGUGGG
cfa-miR-181a	AACAUUCAUUGUUGUCGGUGGG
cfa-miR-181a	AACAUUCAACGCUGUCGGUGA
cfa-miR-181a	AACAUUCAACGCUGUCGGUGAG

cfa-miR-182	UUUGGCAAUGGUAGAACUCACA
cfa-miR-182	UUUGGCAAUGGUAGAACUCACAC
cfa-miR-1842	UGGCUCUGCGAGGUCGGC
cfa-miR-1842	CGGCUCUGGGAAGCACAGUGGUG
cfa-miR-1842	UGGCUCUGUCCCUCUUUCCC
cfa-miR-185	UGGAGAGAAAGGCAGUUCCUGA
cfa-miR-185	UGGAGAGAAAGGCAGUUC
cfa-miR-186	CAAAGAAUUCUCCUUUUGGGC
cfa-miR-188	CAUCCCUUGCAUGGUGGAGGG
cfa-miR-18b	UAAGGUGCAUCUAGUGCAG
cfa-miR-190b	UGAUAUGUUUGAUAUUGGGU
cfa-miR-190b	UGAUAUGUUUGAUAUUGGG
cfa-miR-190b	UGAUAUGUUUGAUAUUGGGUUG
cfa-miR-191	CAACGGAAUCCCAAAAGCAGC
cfa-miR-192	CUGACCUAUGAAUUGACAGCC
cfa-miR-192	AUGACCUAUGAACUGACAGACA
cfa-miR-192	AUGACCUAUGAACUGACAGA
cfa-miR-193a	UGGGUCUUUGCGGGCGAGA
cfa-miR-194	UGUAACAGCAACUCCAUG
cfa-miR-196b	UAGGUAGUUUCCUGUUGUUGGG
cfa-miR-196b	UAGGUAGUUUCAUGUUGUUGGG
cfa-miR-196b	UAGGUAGUUUCAUGUUGUUGGGAUU
cfa-miR-197	UUCACCACCUUCUCCACCCAG
cfa-miR-199	ACAGUAGUCUGCACAUUGG
cfa-miR-199	ACAGUAGUCUGCACAUUGGU
cfa-miR-19b	UGUGCAAAUCCAUGCAAAAC
cfa-miR-19b	UGUGCAAAUCUAUGCAAAAC
cfa-miR-200c	UAAUACUGCCGGGUAAUGAUGG
cfa-miR-21	UAGCUUAUCAGACUGAUGU
cfa-miR-21	UAGCUUAUCAGACUGAUGUUGA
cfa-miR-210	ACUGUGCGUGUGACAGCGGC
cfa-miR-22	AAGCUGCCAGUUGAAGAAC
cfa-miR-22	AAGCUGCCAGUUGAAGAACUG
cfa-miR-222	AGCUACAUUGUCUGCUGGG
cfa-miR-222	AGCUACAUCUGGCUACUGGGUCUC
cfa-miR-222	AGCUACAUUGUCUGCUGGGU
cfa-miR-23b	AUCACAUUGCCAGGGAUUACC
cfa-miR-23b	AUCACAUUGCCAGGGAUU

cfa-miR-24	UGGCUCAGUUCAGCAGGAACA
cfa-miR-24	UGGCUCAGUUCAGCAGGAAC
cfa-miR-24	UGGCUCAGUUCAGCAGGAACAG
cfa-miR-24	UGGCUCAGUUCAGCAGGAACAGG
cfa-miR-26a	UUCAAGUAAUCCAGGAUAGGC
cfa-miR-26a	UUCAAGUAAUUCAGGAUAGG
cfa-miR-27a	UUCACAGUGGCUAAGUUC
cfa-miR-28	CACUAGAUUGUGAGCUCC
cfa-miR-29b	UAGCACCAUUUGAAAUCAG
cfa-miR-29b	UAGCACCAUUUGAAAUCGGU
cfa-miR-29b	UAGCACCAUCUGAAAUCGGU
cfa-miR-29b	UAGCACCAUCUGAAAUCGG
cfa-miR-29b	UAGCACCAUUUGAAAUCGGUUAU
cfa-miR-29b	UAGCACCAUUUGAAAUCGG
cfa-miR-30d	UGUAAACAUCCCCGACUGGAAGC
cfa-miR-30d	UGUAAACAUCCUACACUCAGC
cfa-miR-30d	UGUAAACAUCCUACACUCUCAGC
cfa-miR-30d	UGUAAACAUCCUCGACUGGAAGC
cfa-miR-30d	UGUAAACAUCCUUGACUGGAAGC
cfa-miR-320	AAAAGCUGGGUUGAGAGGGCGA
cfa-miR-324	CGCAUCCCCUAGGGCAUUGG
cfa-miR-326	CCUCUGGGCCCUUCCUCCAG
cfa-miR-328	CUGGCCCUCUCUGCCCUUCCG
cfa-miR-328	CUGGCCCUCUCUGCCCUUCCGU
cfa-miR-329b	AACACACCUAUUCAAGGA
cfa-miR-335	UCAAGAGCAAUAACGAAAAA
cfa-miR-339	UCCCUGUCCUCCAGGAGCUC
cfa-miR-345	CCUGAACUAGGGGUCUGGAG
cfa-miR-361	UUAUCAGAAUCUCCAGGGG
cfa-miR-362	AAUCCUUGGAACCUAGGUGUGAG
cfa-miR-365	UAAUGCCCCUAAAAAUCC
cfa-miR-374b	AUAUAAUACAACCUGCUAAG
cfa-miR-375	UUUGUUCGUUCGGCUCGCGUGA
cfa-miR-378	ACUGGACUUGGAGUCAGAAGGC
cfa-miR-378	UCUGGACUCAGCUUUGCUGCC
cfa-miR-421	AUCAACAGACAUUAAUUGGGCG
cfa-miR-423a	UGAGGGGCAGAGAGCGAGAC
cfa-miR-423a	UGAGGGGCAGAGAGCGGGAG
cfa-miR-423a	UGAGGGGCAGAGCGGGAGAC
cfa-miR-423a	CGAGGGGCAGAGAGCGAGAG
cfa-miR-423a	UGAGGGGCAGAGCGAGAG

cfa-miR-425	AAUGACACGAUCACUCCCGU
cfa-miR-448	UUGCAUAUGUAGGAUGUCC
cfa-miR-448	UUGCAUAUGUAGGAUGUCCC
cfa-miR-450b	UUUUGCAAUAUGUUCCUGAA
cfa-miR-451	AAACCGUUACCAUUACUGAG
cfa-miR-451	GAACCGUUACCAUUACUA
cfa-miR-485	UGAGGCUGCAUCUUCCCGUC
cfa-miR-486	UCCUGUACUGAGCUGCCCCGAG
cfa-miR-486	UCCUGUACUGAGCUGCCCAGG
cfa-miR-486	UCCUGUACUGAGCUGCCCCGA
cfa-miR-499	UUAAGACUUGCAGUGAUGU
cfa-miR-500	GUGCACCUGGGCAAGGAUUC
cfa-miR-502	AAUGCACCUGGGCAAGGAUUC
cfa-miR-532	CAUGCCUUGAGUGUAGGACCG
cfa-miR-542	AGUGACAGUCAUUUGGGGC
cfa-miR-542	UGUGACAGAUUGAUAACUGA
cfa-miR-542	UGUGACAGAUUGAUAACUGAA
cfa-miR-574	CACGCUCAUGCACACACCCA
cfa-miR-574	CACGCUCAUGCACACACCCACA
cfa-miR-590	UAAUUUUAUGUAUAAGCUAG
cfa-miR-615	GGGGGUCCCCGGUGCUCGGA
cfa-miR-628	AUGCUGACAUAUUUACUAGAGG
cfa-miR-660	UACCCAUUGCAUAUCGGAGU
cfa-miR-671	UCCGGUUCUCAGGGCUCCAC
cfa-miR-671	UCCGGUUCUCAGGGCUCCACC
cfa-miR-671	UCCGGUUCUCAGGGCUCCACCUC
cfa-miR-7	UGGAAGACUAGUGAUUUUGU
cfa-miR-8804	UCCAGCACUGAGCUGCCCCG
cfa-miR-8823	UUCCUUCCUGUCGGCGGCCUGC
cfa-miR-8853	UCUGACCCUGCCCGACCCCA
cfa-miR-8853	UCUGACCCUGCCCGACCCCAG
cfa-miR-8864	UCUGAGUCAGGGCCAUGUG
cfa-miR-8868	UCCUGUGCUGAGAGGCCC
cfa-miR-8868	UCCUGUGCUGAGAGGCCCC
cfa-miR-8868	UCCUGUGCUGAGCGGCUC
cfa-miR-8868	UCCUGUGCUGGGCAGCCCCG
cfa-miR-8886	UCCCAGGAUCCGGGUGGGC
cfa-miR-8886	CCCCAGGAAGGUUCCGGACAGCG
cfa-miR-8886	UCCCAGGAUCCGGGUGGGCUG

cfa-miR-8891	UACCCAGUCACCCCUGAAGUGA
cfa-miR-8903	GCUUGGGCCGAGGGCUGAACGA
cfa-miR-8903	GCUUGGGCGGGUCGCCGGC
cfa-miR-9	UCUUUGGUUAUCUAGCUGUA
cfa-miR-9	UCUUUGGUUAUCUAGCUGUAUGA
cfa-miR-92b	UAUUGCACAUUACUAAGU
cfa-miR-92b	UAUUGCACUUGUCCCGGCCUG
cfa-miR-92b	CAUUGCACUUGUCUCGGUCUGA
cfa-miR-92b	UAUUGCACUCGUCCCGGCC
cfa-miR-92b	CAUUGCACUUGUCUCGGUC
hsa-let-7g-3p	CUGUACAGAGCUGUCCCG
hsa-miR-1180-3p	GUUCCGGCUCUUUGGCAGA
hsa-miR-1180-3p	GUUCCGGCUCUUUGGCAGAG
hsa-miR-1203	UCCGGAGCGCCGUUGGUCUCG
hsa-miR-1204	ACGUGGCCUCACCCAGGAC
hsa-miR-1205	UCUGCAGGCCUCUGGGUGGC
hsa-miR-1208	UCACUGUUCUCCCUUGCCUAGG
hsa-miR-1208	UCACUGUUCUCCCUUGCCUAG
hsa-miR-1270	UUGGAGAUGAGAAAUGCGGGUA
hsa-miR-1270	UUGGAGAUGAGAAAUGCGGGUAG
hsa-miR-1276	GAAAGAGCAGGAAGGGUCUGUA
hsa-miR-1278	CAGUACUGUUCCCGCUGC
hsa-miR-1288-5p	CCAGAUCAUUCUAAGGUGGAG
hsa-miR-1292-3p	ACGCGCCCGCCUUUCGCCCCA
hsa-miR-1292-3p	ACGCGCCCGCCUUUCGCCCCAG
hsa-miR-1292-3p	ACGCGCCCGCCUUUCGCCCCAGU
hsa-miR-1306-3p	ACGUUGGCUCUGGUGGUGA
hsa-miR-135b-3p	UUGUAGGGCUGAGGGGGGGG
hsa-miR-139-5p	UCUACAGUAGUGUUCUGUCGGC
hsa-miR-141-3p	UAACACUGUCUGGUAAAGA
hsa-miR-144-5p	GGAUAUCAUCAUAUACUGUAAG
hsa-miR-151a-3p	CUAGACUGAGGCUCCUUGAG
hsa-miR-153-5p	CCAUUUUUUGUUGUUUACUGUU
hsa-miR-153-5p	CCAUUUUUUGUUGUUUACUGU
hsa-miR-185-3p	AGGGGCUGGCUUUCCUCUGG
hsa-miR-185-3p	AGGGGCUGGCUUUCCUCUGGU
hsa-miR-18a-3p	ACUGCCCUAAGUGCUCCUUC
hsa-miR-18a-3p	ACUGCCCUGCCCACCUCACA
hsa-miR-1908-5p	GGGCGGGGAGGCGGGGCGGGGGGGC

hsa-miR-1915-3p	UCCCAGGGCCUGUCUCCUC
hsa-miR-193b-3p	AACUGGCCCACAAAGUCCCGC
hsa-miR-193b-3p	AACUGGCCUACAAAGUCCC
hsa-miR-193b-3p	AACUGGCCUACAAAGUCCCA
hsa-miR-193b-3p	AACUGGCCUACAAAGUCCCAGU
hsa-miR-210-3p	CUGUGCGUGUGACAGCGGC
hsa-miR-219a-1-3p	AGAGUUGAGUCUGGACGUCCCGA
hsa-miR-219b-3p	AGAAUUGCGUUUGGACAA
hsa-miR-2278	AAGAGCAGGAAGGGUCUGUA
hsa-miR-3064-5p	CCUGGCUGGGGAACUCAAGAACC
hsa-miR-3074-5p	GUUCCUGCUGAACUGAGCC
hsa-miR-3074-5p	GUUCCUGCUGAACUGAGCCA
hsa-miR-3074-5p	GUUCCUGCUGAACUGAGCCAG
hsa-miR-3117-3p	GUAGGACUCCAGAGCAGAGC
hsa-miR-3117-3p	GUAGGACUCCAGAGCAGAGCC
hsa-miR-3133	AAAAGAACUCACAGAACUCAC
hsa-miR-3150b-3p	AGAGGAGAAUGGAGGGAUGAG
hsa-miR-3156-3p	GUCCCACUUCGAACCCUGUC
hsa-miR-3175	AGGGGAGAAUGAACUGGUGCCU
hsa-miR-3191-5p	GUCUCUGGCUGUCUCUGCAG
hsa-miR-3192-5p	CCUGGGAGCUGUAGGGCAGCA
hsa-miR-3200-3p	CACCUUGCGCUACUCAGGUCC
hsa-miR-324-3p	UCUGCCCCUUGUUUCCUUCCAG
hsa-miR-324-3p	ACUGCCCCAGGUGCUGCUGG
hsa-miR-324-3p	ACUGCCCCAGGUGCUGCUGGG
hsa-miR-324-3p	UCUGCCCCUUGUUUCCUUCCA
hsa-miR-33a-3p	CAAUGUUUCCACAGUGCA
hsa-miR-33a-3p	CAAUGUUUCCACAGUGCAU
hsa-miR-3613-3p	ACAAAAAAAAAAAGCCCAACCC
hsa-miR-3654	GACUGGACCCCUCUCCCUGGG
hsa-miR-3661	UGACCUGGGACUCGGACAGC
hsa-miR-3661	UGACCUGGCCUCCCAUGCCC
hsa-miR-3661	UGACCUGGUUACCUCCAACAG
hsa-miR-3674	AUUGUAGAAAGACUUACUA
hsa-miR-3688-5p	UGUGGCAACCAAGCGCUCGA
hsa-miR-3688-5p	UGUGGCAACCAAGCGCUCGAUC
hsa-miR-3690	UCCUGGACUGAGCAGCCCC
hsa-miR-3690	UCCUGGACUGAUCUGCCC
hsa-miR-374b-3p	CUUAGCAGGUUGUAUUAUAU

hsa-miR-378g	CCUGGGCUCGGGAACGGAG
hsa-miR-378g	GCUGGGCUGUGUCACCGGAUCCC
hsa-miR-3914	GAGGAACCUGUGUGGCUUAGC
hsa-miR-3915	UUGAGGAAUAGCCAGUAACC
hsa-miR-3918	ACAGGGCCCUGCUGUGCGUAG
hsa-miR-3922-3p	GCUGGCCUGUAGUCUGGAAG
hsa-miR-3925-5p	GAGAGAACAGAGGGGCAGAG
hsa-miR-4298	GUGGGACAGAGAGAAAAGGAA
hsa-miR-4303	CUCUGAGCUCCAUCCCCGGC
hsa-miR-4308	ACCCUGGAGAUCCUAAUU
hsa-miR-4308	UCCCUGGAGUAUGCUACUC
hsa-miR-4325	GUGCACUUGUCUCGGCCUG
hsa-miR-4326	UGUUCCUCUUCUUCGCCACCCU
hsa-miR-4419a	UGAGGGAGUAAAAUGGAGAG
hsa-miR-4419b	GAGGCUGAGCUCUGCCCCCCUGC
hsa-miR-4425	AGUUGGGAGAGCGUUAGACUGA
hsa-miR-4433b-3p	CAGGAGUGAUGGAGCUGUCUC
hsa-miR-4433b-3p	CAGGAGUGUAAUUAUUUCAUGA
hsa-miR-4442	CCCGGACAAGUUCAAAGGCCUG
hsa-miR-4459	CCAGGAGGGCUAUCUGAGCAGC
hsa-miR-4460	UUAGUGGUAUCAUUGAAAUGACC
hsa-miR-4479	CGCGCGGCCGGGCUGCAGGGGC
hsa-miR-4479	CGCGCGGCCGGGCUGCAGGGGG
hsa-miR-4497	AUCCGGGACGAGCCCCCA
hsa-miR-4505	AGGCUGGGGGCUGAGCAGAC
hsa-miR-4512	CAGGGCCUUCUCUUCUCCCAGA
hsa-miR-4512	CAGGGCCUUCUCUUCUCCCAG
hsa-miR-4515	AGGACUGGAGGCGACAGAUGG
hsa-miR-4520-2-3p	UUUGGACAUACUAGAAAAGGA
hsa-miR-4520-2-3p	UUUGGACAUACUAGAAAAGGA
hsa-miR-4529-3p	CUUGGACUUGAAGGAGAGCG
hsa-miR-4529-3p	CUUGGACUUGAAGGAGAGCGA
hsa-miR-4529-5p	CGGCCAUCUGUCCUGCAGG
hsa-miR-4536-5p	CGUGGUAGCUGUCCUGAGCCG
hsa-miR-4648	AGUGGGACAGAGAGAAAAGGAA
hsa-miR-4653-5p	GCUCUGAGCUCCAUCCCCGG
hsa-miR-4659a-5p	UUGCCAUGAUCUGAAGAGGGAG
hsa-miR-4688	GAGGGGCAGAGAGCGAGA
hsa-miR-4688	GAGGGGCAAAGAGCGAGACA
hsa-miR-4718	UGCUGUACUGGGCUGCACAG

hsa-miR-4732-3p	UCCCUGACCUCCAGGAGCUC
hsa-miR-4733-5p	AAUCCCAAAUCUGUCAGGCC
hsa-miR-4741	CGGGCUGUGGGAGAUGAU
hsa-miR-4747-5p	UGGGAAGGAGGGAAAGGAGA
hsa-miR-4757-5p	UGGCCUCUCCUCUGCCACCG
hsa-miR-4775	GUAAUUUUAUGUAUAAGCUAG
hsa-miR-4778-5p	AAUUCUGUAGGGCGCCUGGA
hsa-miR-4790-3p	UGAAUGGUUGAGGUCAAAGAG
hsa-miR-4802-5p	CAUGGAGGUCUCUGUCUGGC
hsa-miR-4802-5p	CAUGGAGGUCUCUGGCUGGA
hsa-miR-486-3p	AGGGGCAGAGCGCGAGAA
hsa-miR-486-3p	UGGGGCAGAGCUCGCGCG
hsa-miR-486-3p	AGGGGCAGAUAGCGAGAG
hsa-miR-498	GUUCAAGCCGGGCGUCGGGC
hsa-miR-5002-3p	UGACUGCCUGUCUCUCCACCG
hsa-miR-5008-5p	UGAGGCCCAGCUCUGAGCCG
hsa-miR-504-3p	GGGAGUGCAGAGCCUGGCG
hsa-miR-505-3p	CGUCAACACUUGCUGGUUUCC
hsa-miR-5093	AGGAAAUGAGGUUUGUCUGGCU
hsa-miR-5188	CAUCGGACAACGGACUGAGUUC
hsa-miR-519b-3p	AAAGUGCACGCGCUUUGGGAC
hsa-miR-5590-3p	CAUAAAGUAGAAAGCACUAC
hsa-miR-5682	CUAGCACCAUCUGAAAUCGG
hsa-miR-5695	UCUCCAAGGAUCCCUGGCUAG
hsa-miR-5708	CUGAGCGAUUUGUAGGUCG
hsa-miR-572	UUCCGCUCAGGUCGUCAUCUCG
hsa-miR-580-3p	GUGAGAAUCUUUUGUUUGGC
hsa-miR-580-3p	GUGAGAAUCUUUUGUUUGGCUA
hsa-miR-615-3p	UCCGAGCCUGGGUCUCCCUC
hsa-miR-6165	AAGCAGGAUUUAGACUACAAUA
hsa-miR-6165	AAGCAGGAUUUAGACUACAA
hsa-miR-628-3p	UCUAGUAAGAGUGGCAGUCG
hsa-miR-630	GGUAUUCUUGUAGGGCUGACA
hsa-miR-6510-3p	CACCGACUGCUCGCUGACCC
hsa-miR-6512-3p	CUCCAGCCCCAUAGCCUCAG
hsa-miR-664a-3p	UAUUCAUUUAUCUCCCAGCCUACA
hsa-miR-671-5p	AGGAAGCCAGACACUGGCAGG
hsa-miR-6727-5p	AUCGGGGCACUGCUGCGUUC
hsa-miR-6727-5p	UUCGGGGCCUGCGUCGGGC
hsa-miR-6734-5p	GUGAGGGGCUGCGGGGCAGGGG

hsa-miR-6736-3p	CCAGCUCCCCCCCGCCUGCC
hsa-miR-6738-5p	AGAGGGGUGAGGUAGCAGC
hsa-miR-6749-3p	CUCCUCCCCAUCCGUCGUCC
hsa-miR-6749-3p	CUCCUCCCCAUCCGUCGUCCC
hsa-miR-6765-3p	GCACCUGGGCAAGGAUUCCGA
hsa-miR-6770-3p	AUGGCGGCCGCACUCUGGCC
hsa-miR-6777-3p	UCCACUCUGGCAGAUACUCCG
hsa-miR-6782-5p	UAGGGGUGGGAAGAUCUGGUC
hsa-miR-6794-3p	UUCACUCUGCAUUUCCCUCUUCC
hsa-miR-6805-3p	UUGCUCUGGCCUUCGACCCCGG
hsa-miR-6812-5p	GUGGGGUGGAGUUGGGGAGA
hsa-miR-6823-3p	UGAGCCUCAAGCAAGGGAC
hsa-miR-6832-5p	AGUAGAGAGAGUAGAGCGGCA
hsa-miR-6832-5p	AGUAGAGAGAGUAGAGCGGCAG
hsa-miR-6834-5p	GUGAGGGACUGCAAGAGCC
hsa-miR-6834-5p	GUGAGGGACUGCAAGAGCCU
hsa-miR-6835-3p	AAAAGCACGCGCUGCCGGAAG
hsa-miR-6835-3p	UAAAGCACCCGCUGUGGAAGG
hsa-miR-6835-3p	UAAAGCACCCGCUGUGGAAGGC
hsa-miR-6844	AUCUUUGUGGGUCACUGAC
hsa-miR-6850-3p	CCCGGCCGAGCUCUGUCCC
hsa-miR-6852-3p	UGUCCUCUGACCGCCCUGCC
hsa-miR-6854-5p	UAGCUCAGAGUUCUGAUGGA
hsa-miR-6867-5p	UGUGUGUGUAUGUCUGUAGC
hsa-miR-7106-5p	AGGGAGGACUGUUCUGCGGAG
hsa-miR-7106-5p	AGGGAGGACUGUUCUGCGGAGC
hsa-miR-7111-3p	UUCCUCUCACCUUCCCCGCGC
hsa-miR-7-1-3p	CAACAAAUCACAGUCUGCC
hsa-miR-7-1-3p	CAACAAAUCACAGUCUGCCAU
hsa-miR-744-5p	UGCGGGGCUAGGGCUAACAGC
hsa-miR-766-3p	ACUCCAGCCCCAUAGCCUCAGC
hsa-miR-766-3p	ACUCCAGCCCCAUAGCCUCA
hsa-miR-767-3p	CCUGCUCACUCCUGGCCAC
hsa-miR-7703	CUGCACUCAGCUGCCCCGAG
hsa-miR-7850-5p	CUUUGGACAUACUAGAAAAGGA
hsa-miR-7977	AUCCCAGCCUGGCUCUCUGC
hsa-miR-8052	UGGGACUGAGACACGGCC
hsa-miR-8057	CUGGCUCUAGCUUCCCUGC
hsa-miR-8067	UCUAGAAAAUCAGCAUAUAAG

hsa-miR-874-5p	CGGCCCCAGCCCCCACUCCC
hsa-miR-877-5p	GUAGAGGAGAUGGCGCAGGGGA
hsa-miR-877-5p	GUAGAGGAGAUGGCGCAGGG
hsa-miR-889-5p	CAUGGCUGUCUCUGUCUGGC
hsa-miR-939-3p	ACCUGGGCUCGGGAACGGAG
hsa-miR-939-3p	UCCUGGGCUUAUCUGCCCC
hsa-miR-943	CUGACUGUAAACACUGACGGCA
hsa-miR-943	CUGACUGUAAACACUGACGGC
	AAUGGCGCCACUAGGGUUG
	ACAAAGAUCUGAGGACAAGAGA
	ACUUGUUAGGAUGAGGAC
	AGACUGGGUCCUGAGGCC
	AGGUAGAUAGAACAGGUC
	AUCUCAGGUUCGUCAGCCCG
	GAGAGAUCAGAGGCGCAGAG
	UACCGCACUGUGGGUACUUGC
	UCGGGCACCUUCUCUGAUCGG
	UGAGGGGCAGAGAUGGAGA
	UUAUAAAGCAAUGAGACUGA
	UUCUCAGGUUGGACAGUCC
	UUCUGACAGUAAUAGCUC
	AGCCUGCUUUGGAUUCUGUGUC
	AGGCAGUAGGUUGUAUAG
	CUUACCAGGUUGUAUUGUAA
	UUUGCUUGCUGUCCUGGCC
	AGGACUCAGGGUGGCUCUGUGA
	CUGUGCUGAGCUGCCCCU
	UAGAGAAGUGAAAGGAAGCUC
	UCUCUGGGCCUGUGUCUUAGGC
	UGAGCAACCGAGGUGCCCG
	UUAUUACAGCUGAAAGUCCAC
	AGGCGGUAGAGCAUGAGACUC
	CGGGACGCCUGGGUAGCUCAG
	UCUCACACAGAAAUCGCACCCG
	UGUGCUAGAUAUGCUGACCC
	AGGUUGAUUUGGGUCUGGCGUC
	CCUGCUUUGGAUUCUGUGUC
	GUGAGGUUGAUUUGGGUC
	UCUGAAGCAGGCUCCAGGC
	UGGCCCCGUGACUCUGGCUC

	UGUUCCUGCUGAACUGAGCCA
	AAUUGUAGAAAGACUUACUA
	AGGACUCAGGGUGGCUCUGUG
	AGGCGACCCUGCUCUGAUGGCG
	AUACCCUGUAGAACCGAAUU
	CAAGGCUGAGGCUCCUUGAG
	CAGCAGGCUGUCAGGCUC
	CAUCUGUGACCCUGCCUC
	CAUCUGUGACCCUGCCUCUAG
	CCCCGGACAAGUUCAAAGGCC
	GAGAGCAUACCAAGCAGGC
	GCUGACUCCUAGUCCAGUGC
	UAGAGAAGUGAAAGGAAGC
	UCACUGUGAAGAAUGCUGC
	UCUGGGGCUGCAGAGGAGGAG
	UGAGCAACCGAGGUGCCCGUGC
	UGCCUCUCACCCUCUGCCCACA
	AACAAAUCACAGUCUGCCAU
	AAGGAGAGAACAGGUGAUG
	AAGUUUCUCUGAAUGUGUAGA
	AAUUGGGCAGGUAGGAGGAGAU
	ACAAAGAUCUGAGGACAAGA
	ACCUAUAGAUCAAUAACAC
	ACCUCUGAAUGCUCUGGUC
	ACCUGAGCCGAAGUCGGACAC
	AGCCCUUUGUCUGUCCUCUAG
	AGCCUGCUUUGGAUUCUGUG
	AGGCAGAUAGAACAGGUC
	AGGGCAGAGUGUGGGAUGGUUG
	AGGUGGUAGAUGGUAUAG
	AGUUUCUCUGAAUGUGUAGA
	AUGGGCACUGGUCUCUGUUC
	AUGGGCACUGGUCUCUGUUCUAC
	AUGGGUUACAGUAGACUUAGGG
	CCUGGGGCUUCUGACAGGCAC
	CGCGUACCAAAAGUAAUAA
	CUCCAGCUCAGGUCAUCUCU
	CUCCAGGCUCUGAGCUGUCACA
	CUGUGCUGAGCUGCCCUG
	CUUACCAGGUUGUAUUGUAAU
	CUUCCACUCGGGUCGUGAUCUCA

	GCAGCAGGCUGUCAGGCUC
	GUCAACACUUGCUGGUUUCC
	GUCAGAGCCCCUUGCUGCGCC
	UAAUGUAUACAUAUGCCUGUG
	UAGAAAUUAGGUCUGUAAC
	UAGAUCUGGGGUAGGGCCUAA
	UAGAUCUGGGGUAGGGCCUGG
	UAUUUGUGGACAGUUACUCAU
	UCAACACUUGCUGGUUUCCUC
	UCACUGUGUCUUUCCCCUUAGC
	UCGAGCCCCGCGUCAGGCUC
	UCGAGGAGCUCACAGUCU
	UCUCUCUUCUUCGUUGGCC
	UCUCUCUUCUUCGUUGGCCCAG
	UCUGGACCCACUCUCACC
	UCUGGACCCACUCUCACCUA
	UCUGGGGCUGCAGAGGAGGAGU
	UCUUUGUGGGUCACUGAC
	UGAGCUGCCCAGGAGUCCCUGCAUU
	UGAGGGGCAGAGAGCGAG
	UUAACCAACUGAGCCACCCAGA
	UUCUAGUAAGAGUGGCAGUCG
	UUCUGAAAGGGCAUAAUAUG
	UUGGACAUACUAGAAAAGGA
	UUGGGGGCCAGAAUAAGGAC
	UUGUGACAGAUUGAUAAC
	UUGUGACAGAUUGAUAACUGA
	UUUGCUUGCUGUCCUGGCCUGA
	AGAGGUAGUGGGUUGCAUAG

APPENDIX B. LIST OF MATURE MICRORNA SEQUENCES IDENTIFIED IN FOUR DIABETIC AND FOUR HEALTHY CATS

Canine or human microRNA with the same seed	Consensus mature sequence
cfa-miR-1	UGGAAUGUAAAGAAGUAUGUAU
cfa-miR-1	UGGAAUGUAAGGAAGUGUGUGG
cfa-miR-7	UGGAAGACUAGUGAUUUUGU
cfa-miR-7	UGGAAGACUAGUGAUUUUGUUG
hsa-miR-7-1-3p	CAACAAAUCACAGUCUGCC
cfa-miR-9	UCUUUGGUUAUCUAGCUGUA
cfa-miR-9	UCUUUGGUUAUCUAGCUGUAU
cfa-miR-21	UAGCUUAUCAGACUGAUGUUGA
cfa-miR-22	AAGCUGCCAGUUGAAGAAC
cfa-miR-22	AAGCUGCCAGUUGAAGAACUGU
cfa-miR-22	CAGCUGCCUCCUGACCACAUGA
cfa-miR-22	GAGCUGCCAGUUGAAGAAUUU
cfa-miR-24	UGGCUCAGUUCAGCAGGAACA
cfa-miR-28	CACUAGAUUGUGAGCUCC
cfa-miR-95	UUCAACGGGUAUUUAUUGAGCA
cfa-miR-101	UACAGUACUGUGAUAACUGAA
cfa-miR-101	UACAGUACUGUGAUAACUGAAG
cfa-miR-107	AGCAGCAUUGUACAGGGC
cfa-miR-107	AGCAGCAUUGUACAGGGCU
cfa-miR-107	AGCAGCAUUGUACAGGGCUAUGA
cfa-miR-107	AGCAGCAUUGUACCGGGG
cfa-miR-122	UGGAGUGUGACAAUGGUGUUU
cfa-miR-126	CAUUAUUACUUUUGGUACGCG
cfa-miR-128	UCACAGUGAACCGGUCUC
cfa-miR-128	UCACAGUGAACCGGUCUCU
cfa-miR-129	CUUUUUGCGGUCUGGGCUUG
cfa-miR-129	CUUUUUGCGGUCUGGGCUUGC
cfa-miR-132	UAACAGUCUACAGCCAUGGUCG
cfa-miR-140	ACCACAGGGUAGAACCACGGAC
cfa-miR-140	ACCACAGGGUAGAUCCACGGAA
cfa-miR-142	CCCAUAAAGUAGAAAGCAC
cfa-miR-142	CCCAUAAAGUAGAAAGCACU
cfa-miR-143	UGAGAUGAAGCACUGUAGCUC
hsa-miR-144-5p	GGAUAUCAUCAUAUACUGUAAG

cfa-miR-145	CUCCAGUUCCUCCUCGUCGGG
cfa-miR-145	GUCCAGUUUUCCCAGGAAUCCCU
cfa-miR-149	UCUGGCUCCGUGUCUUCACU
cfa-miR-150	UCUCCCAACCCUUGUACCAG
cfa-miR-150	UCUCCCAACCCUUGUACCAGUG
cfa-miR-151	UCGAGGAGCUCAAAGUCUGGU
cfa-miR-151	UCGAGGAGCUCACAGUCUAGU
cfa-miR-151	UCGAGGAGUUCCCCGUCU
cfa-miR-153	UUGCAUAGUCACAAAAGUGA
hsa-miR-153-5p	CCAUUUUUUGUUGUUUACUGUU
cfa-miR-155	UUAAUGCUAAUCGUGAUAGGG
cfa-miR-155	UUAAUGCUAAUCGUGAUAGGGGU
cfa-miR-182	UUUGGCAAUGGUAGAACUCACA
cfa-miR-183	UAUGGCACUGGUAGAAUUCACU
cfa-miR-184	CGGACGGAAGGUGGUGCGCUUCA
cfa-miR-185	UGGAGAGAAAGGCAGUUC
cfa-miR-185	UGGAGAGAAAGGCAGUUCCUGA
cfa-miR-185	UGGAGAGAGCUCACCAUCCCU
cfa-miR-186	CAAAGAAUUCUCCUUUUGGGC
cfa-miR-186	CAAAGAAUUCUCCUUUUGGGCU
cfa-miR-186	CAAAGAAUUUUCCUCUUGGG
cfa-miR-188	CAUCCCUUGCAUGGUGGAGGG
cfa-miR-188	CAUCCCUUGCAUGGUGGAGGGU
cfa-miR-191	CAACGGAAUCCCAAAAGCAGC
cfa-miR-191	CAACGGAAUCCCAAAAGCAGCU
cfa-miR-192	AUGACCUAUGAACUGACAGA
cfa-miR-192	AUGACCUAUGAACUGACAGACA
cfa-miR-192	CUGACCUAUGAAUUGACAGCC
cfa-miR-194	UGUAACAGCAACUCCAUG
cfa-miR-194	UGUAACAGCAACUCCAUGUGG
cfa-miR-197	UUCACCACCUUCUCCACCCAG
cfa-miR-211	UUCCCUUUGUCAUCCUAUGCCU
cfa-miR-211	UUCCCUUUGUCAUCCUUUGCCU
cfa-miR-212	ACCUUGGCUCUAGACUGCUUACU
cfa-miR-219-5p	UGAUUGUCACCUUUUCGAGUAGA
cfa-miR-222	AGCUACAUCUGGCUACUGGGU
cfa-miR-222	AGCUACAUCUGGCUACUGGGUC
cfa-miR-222	AGCUACAUUGUCUGCUGGG
cfa-miR-222	AGCUACAUUGUCUGCUGGGUU

cfa-miR-320	AAAAGCUGGGUUGAGAGGGCGA
cfa-miR-320	AAAAGCUGGGUUGAGGGGCG
cfa-miR-320	AAAAGCUGGGUUGAGGGGCGC
hsa-miR-324-3p	ACUGCCCCAGGUGCUGCUGG
hsa-miR-324-3p	ACUGCCCCAGGUGCUGCUGGG
cfa-miR-326	CCUCUGGGCCCUUCCUCCAG
cfa-miR-326	CCUCUGGGCCCUUCCUCCAGC
cfa-miR-328	CUGGCCCUCUCUGCCCUUCCG
cfa-miR-335	UCAAGAGCAAUAACGAAAAA
cfa-miR-335	UCAAGAGCAAUAACGAAAAAUG
cfa-miR-339	UCCCUGUCCUCCAGGAACUG
cfa-miR-339	UCCCUGUCCUCCAGGAGC
cfa-miR-339	UCCCUGUCCUCCAGGAGCU
cfa-miR-339	UCCCUGUCCUCCAGGAGCUC
cfa-miR-339	UCCCUGUCCUCCAGGAGCUCA
cfa-miR-345	CCUGAACUAGGGGUCUGGAG
cfa-miR-346	UGUCUGCCCGCAUGCCUGCCUCU
cfa-miR-350	CUCACAAAGCCCGUACACUUU
cfa-miR-361	AUAUCAGAAUCUCCUGGGG
cfa-miR-361	UUAUCAGAAUCUCCAGGGGUA
cfa-miR-362	AAUCCUUGGAACCUAGGUGUGAG
cfa-miR-362	AAUCCUUGUUGUGCAGAAGAGA
cfa-miR-365	UAAUGCCCCUAAAAAUCC
cfa-miR-365	UAAUGCCCCUAAAAAUCCUU
cfa-miR-375	UUUGUUCGUUCGGCUCGCGUGA
cfa-miR-378	ACUGGACUUGGAGUCAGAAGGC
cfa-miR-378	CCUGGACUGUAUCUGGGCC
cfa-miR-378	UCUGGACUCAGCUUUGCUGCC
cfa-miR-383	UGAUCAGAAUCUCCAGGGUU
cfa-miR-421	AUCAACAGACAUUAAUUGGGCG
cfa-miR-425	AAUGACACGAUCACUCCCGU
cfa-miR-425	AAUGACACGAUCACUCCCGUUGA
cfa-miR-448	UUGCAUAUGUAGGAUGUCC
cfa-miR-451	AAACCGUUACCAUUACUGAG
cfa-miR-451	GAACCGUUACCAUUACUA
cfa-miR-451	GAACCGUUACCAUUACUAA
cfa-miR-486	UCCUGUACUGAGCUGCCC
cfa-miR-486	UCCUGUACUGAGCUGCCCAGG
cfa-miR-486	UCCUGUACUGAGCUGCCCCGA
cfa-miR-486	UCCUGUACUGAGCUGCCCCGAG

cfa-miR-489	UUGACAUCUGGGGAAUGUAGU
cfa-miR-490	UAACCUGGGUCCCCUCCUUCA
cfa-miR-491	CUUAUGCAAGAUUCCCUUC
cfa-miR-491	CUUAUGCAAGAUUCCCUUCU
cfa-miR-499	UUAAGACUUGCAGUGAUGU
cfa-miR-499	UUAAGACUUGCAGUGAUGUUU
cfa-miR-499	UUAAGACUUGGAGUGAUG
cfa-miR-502	AAUGCACCUGGGCAAGGAUU
cfa-miR-502	AAUGCACCUGGGCAAGGAUUC
cfa-miR-504	UGACCCUGGCCCCUCCCCGCA
cfa-miR-505	UGGAGCCAGCCCCUGAGUCU
cfa-miR-532	CAUGCCUUGAGUGUAGGACCG
cfa-miR-532	CAUGCCUUGAGUGUAGGACCGU
cfa-miR-542	UGUGACAGAUUGAUAACUGA
cfa-miR-574	CACGCUCAUGCACACACCCA
cfa-miR-574	CACGCUCAUGCACACACCCACA
hsa-miR-580-3p	GUGAGAAUCUUUUGUUUGGC
cfa-miR-590	UAAUUUUAUGUAUAAGCUAG
cfa-miR-590	UAAUUUUAUGUAUAAGCUAGU
cfa-miR-615	GGGGGUCCCCGGUGCUCGGA
cfa-miR-631	CACCUGGCCCAGCGCUCCACU
cfa-miR-660	UACCCAUUGCAUAUCGGAGU
cfa-miR-660	UACCCAUUGCAUAUCGGAGUUG
cfa-miR-671	UCCGGUUCUCAGGGCUCCA
cfa-miR-671	UCCGGUUCUCAGGGCUCCAC
hsa-miR-671-5p	AGGAAGCCAGACACUGGCAGG
cfa-miR-708	AAGGAGCUCACAGUCUAUUGA
cfa-miR-761	ACAGCAGGGCCCCUGUGAGCU
hsa-miR-766-3p	ACUCCAGCCCCAUAGCCUCA
hsa-miR-766-3p	ACUCCAGCCCCAUAGCCUCAGC
cfa-miR-1199-3p	CGCGGCCGAGCUGCCGGACCG
hsa-miR-1208	UCACUGUUCUCCCUUGCCUAGG
cfa-miR-1249	ACGCCCUUCCCCCCCUUC
cfa-miR-1249	ACGCCCUUCCCCCCCUUCU
cfa-miR-1271	CUUGGCACCUAGUAAGCAC
cfa-miR-1271	CUUGGCACCUAGUAAGCACU
cfa-miR-1271	CUUGGCACCUAGUAAGCC
cfa-miR-1271	UUUGGCACUAGCACAUUUUUGCU
hsa-miR-1288-5p	CCAGAUCAUUCUAAGGUGGAG
hsa-miR-1292-3p	ACGCGCCCGCCUUUCGCCCCA

cfa-miR-1296	GUAGGGCCUAGGAAUCUGUAUU
cfa-miR-1296	UUAGGGCCCUGGCUCCAUCUC
cfa-miR-1296	UUAGGGCCCUGGCUCCAUCUCC
cfa-miR-1301	UUGCAGCUGCCUGGGAGUGA
cfa-miR-1343	CUCCUGGGACCCGCACUCU
cfa-miR-1343	CUCCUGGGGCCCGCACUCUCG
cfa-miR-1842	UGGCUCUGCGAGGUCGGC
cfa-miR-1842	UGGCUCUGCGAGGUCGGCUCA
cfa-miR-1842	UGGCUCUGUCCCUCUUUCCC
hsa-miR-3133	AAAAGAACUCACAGAACUCAC
hsa-miR-3613-3p	ACAAAAAAAAAAGCCCAACCC
hsa-miR-3922-3p	GCUGGCCUGUAGUCUGGAAG
hsa-miR-3925-5p	GAGAGAACAGAGGGGCAGAG
hsa-miR-4298	GUGGGACAGAGAGAAAAGGAA
hsa-miR-4308	ACCCUGGAGAUCCUAAUU
hsa-miR-4505	AGGCUGGGGGCUGAGCAGAC
hsa-miR-4512	CAGGGCCUUCUCUUCUCCCAGA
hsa-miR-4529-3p	CUUGGACUUGAAGGAGAGCGA
hsa-miR-4733-5p	AAUCCCAAAUCUGUCAGGCC
hsa-miR-4741	CGGGCUGUGGGAGAUGAU
hsa-miR-4802-5p	CAUGGAGGUCUCUGGCUGGA
hsa-miR-4802-5p	CAUGGAGGUCUCUGUCUGGC
hsa-miR-5682	CUAGCACCAUCUGAAAUCGG
cfa-miR-6516	AUUGCAGUUGUCCAGGCA
hsa-miR-6770-3p	AUGGCGGCCGCACUCUGGCC
hsa-miR-6777-3p	UCCACUCUGGCAGAUACUCCG
hsa-miR-6832-5p	AGUAGAGAGAGUAGAGCGGCA
hsa-miR-6834-5p	GUGAGGGACUGCAAGAGCC
hsa-miR-6835-3p	AAAAGCACGCGCUGCCGGAAG
hsa-miR-6844	AUCUUUGUGGGUCACUGAC
hsa-miR-7106-5p	AGGGAGGACUGUUCUGCGGAG
hsa-miR-7106-5p	AGGGAGGACUGUUCUGCGGAGC
hsa-miR-7850-5p	CUUUGGACAUACUAGAAAAGGA
hsa-miR-7977	AUCCCAGCCUGGCUCUCUGC
cfa-miR-8789	UUCAGGCAUGUGUCUCUUCU
cfa-miR-8789	UUCAGGCAUGUGUCUCUUCUUGC
cfa-miR-8801	UGGACAGUGGCUAAGUUCUG
cfa-miR-8804	UCCAGCACGGGCCCCUGAGU
cfa-miR-8807	UCUGUGUGGCAAAGAGGGUGG

cfa-miR-8827	UCCUCCUCGUCGGCCUCUUCG
cfa-miR-8827	UCCUCCUCUCCCCUCGCCCGGC
cfa-miR-8836	UGGAAAGGAAUAAACAGAACA
cfa-miR-8846	UGGGACAGAGAGAAAAGGAAAC
cfa-miR-8851	UGACCUCAGGUGCCCGGUGGAUGA
cfa-miR-8853	UCUGACCCUGCCCGACCCC
cfa-miR-8853	UCUGACCCUGCCCGACCCCAG
cfa-miR-8868	UCCUGUGCAGAGAGAGAGAC
cfa-miR-8868	UCCUGUGCUGAGAGGCCC
cfa-miR-8868	UCCUGUGCUGAGCGGCUC
cfa-miR-8868	UCCUGUGCUGGGCAGCCCCG
cfa-miR-8874	CACUUCUCAGGAAAAGCCAGUU
cfa-miR-8876	CUGCCUCUUCCCUGCCCUAGG
cfa-miR-8884	UUUGAUGGCUGUUCCUCUCAC
cfa-miR-8886	CCCCAGGAAGGUUCCGGACAGCG
cfa-miR-8886	UCCCAGGAUCCGGGUGGGC
cfa-miR-8891	UACCCAGUCACCCCUGAAGUGA
cfa-miR-8903	GCUUGGGCCGAGGGCUGAACGA
cfa-miR-8903	GCUUGGGCGGGUCGCCGGC
cfa-miR-106a	AAAGUGCUUACAGUGCAGGUAG
cfa-miR-106b	CAAAGUGCUGUUCGUGCAGG
cfa-miR-106b	CAAAGUGCUGUUCGUGCAGGUAG
cfa-miR-106b	CAAAGUGCUUACAGUGCAGGUAG
cfa-miR-106b	CAAAGUGCUUACAGUGCAGGUAGU
cfa-miR-106b	GAAAGUGCUGUUUGUGCAG
cfa-miR-106b	UAAAGUGCUGACAGUGCAGA
cfa-miR-106b	UAAAGUGCUUAUAGUGCAGGUAG
cfa-miR-10a	UACCCUGUAGAACCGAAUU
cfa-miR-10a	UACCCUGUAGAACCGAAUUUG
cfa-miR-10a	UACCCUGUAGAUCCGAAUU
cfa-miR-10a	UACCCUGUAGAUCCGAAUUUG
cfa-miR-125b	CCCCUGAGGCUCAGUCGGC
cfa-miR-125b	UCCCUGAGACCCUAACUUGUGA
cfa-miR-130b	CAGUGCAAUAGUAUUGUCAAAGC
cfa-miR-130b	CAGUGCAAUGAUAUUGUCAAAG
cfa-miR-130b	CAGUGCAAUGAUAUUGUCAAAGC
cfa-miR-130b	CAGUGCAAUGAUGAAAGGGCA
cfa-miR-130b	CAGUGCAAUGUUAAAAGGGC
cfa-miR-130b	CAGUGCAAUGUUAAAAGGGCA
cfa-miR-130b	UAGUGCAAUAUUGCUUAUAGGGU

cfa-miR-133b	UUUGGUCCCCUUCAACCAGCU
cfa-miR-133c	UUGGUCCCCUUCAACCAGCUGU
cfa-miR-135b	UAUGGCUUUUCAUUCCUAUG
cfa-miR-135b	UAUGGCUUUUCAUUCCUAUGUGA
cfa-miR-135b	UAUGGCUUUUUAUUCCUAUGUGA
cfa-miR-138b	AGCUGGUGUUGUGAAUCAGGCCG
cfa-miR-146b	UGAGAACUCUCCUGGGGAA
cfa-miR-146b	UGAGAACUGAAUUCCAUAGGC
cfa-miR-146b	UGAGAACUGAAUUCCAUAGGCU
cfa-miR-146b	UGAGAACUGAAUUCCAUGGGU
cfa-miR-146b	UGAGAACUGAAUUCCAUGGGUU
cfa-miR-148a	UCAGUGCACUACAGAACUUUG
cfa-miR-148a	UCAGUGCAUCACAGAACUUUG
cfa-miR-148a	UCAGUGCAUGACAGAACU
cfa-miR-148a	UCAGUGCAUGACAGAACUUGGG
hsa-miR-151a-3p	CUAGACUGAGGCUCCUUGAG
cfa-miR-15b	CAGCAGCACACUGUGGUUUG
cfa-miR-15b	UAGCAGCACAGAAAUAUUGGC
cfa-miR-15b	UAGCAGCACAUAAUGGUU
cfa-miR-15b	UAGCAGCACAUAAUGGUUUGU
cfa-miR-15b	UAGCAGCACAUCAUGGUUUACA
cfa-miR-15b	UAGCAGCACGUAAAUAUUGGCG
cfa-miR-181a	AACAUUCAACCUGUCGGUGAG
cfa-miR-181a	AACAUUCAACGCUGUCGGUGA
cfa-miR-181a	AACAUUCAACGCUGUCGGUGAG
cfa-miR-181a	AACAUUCAUUGCUGUCGGUGGG
cfa-miR-181a	AACAUUCAUUGUUGUCGGUGGG
cfa-miR-181a	AACAUUCAUUGUUGUCGGUGGGU
hsa-miR-18a-3p	ACUGCCCUAAGUGCUCCUUC
cfa-miR-18b	UAAGGUGCAUCUAGUGCAG
cfa-miR-18b	UAAGGUGCAUCUAGUGCAGA
cfa-miR-190b	UGAUAUGUUUGAUAUUGGGU
cfa-miR-190b	UGAUAUGUUUGAUAUUGGGUUG
cfa-miR-193a	UGGGUCUUGGGGAGGUUAAGGAA
cfa-miR-193a	UGGGUCUUUGCGGGCGAGAUG
hsa-miR-193b-3p	AACUGGCCCACAAAGUCCCGC
hsa-miR-193b-3p	AACUGGCCUACAAAGUCCCAGU

cfa-miR-196b	UAGGUAGUUUCAUGUUGUUGGG
cfa-miR-196b	UAGGUAGUUUCAUGUUGUUGGGAUU
cfa-miR-196b	UAGGUAGUUUCAUGUUGUUGGGC
cfa-miR-196b	UAGGUAGUUUCCUGUUGUUGGG
cfa-miR-196b	UAGGUAGUUUCCUGUUGUUGGGA
cfa-miR-19b	UGUGCAAAUCCAUGCAAAAC
cfa-miR-19b	UGUGCAAAUCCAUGCAAAACUGA
cfa-miR-19b	UGUGCAAAUCUAUGCAAAAC
cfa-miR-19b	UGUGCAAAUCUAUGCAAAACUGA
cfa-miR-200c	UAAUACUGCCGGGUAAUGAUGG
cfa-miR-200c	UAAUACUGCCGGGUAAUGAUGGA
cfa-miR-216b	GAAUCUCUACGGGUAAGUGU
hsa-miR-219a-1-3p	AGAGUUGAGUCUGGACGUCCCGA
cfa-miR-23b	AUCACAUUGCCAGGGAUU
cfa-miR-23b	AUCACAUUGCCAGGGAUUU
cfa-miR-26a	UUCAAGUAAUCCAGGAUAGGC
cfa-miR-26a	UUCAAGUAAUCCAGGAUAGGCU
cfa-miR-26a	UUCAAGUAAUUCAGGAUAGG
cfa-miR-27a	UUCACAGUGGCUAAGUUC
cfa-miR-27a	UUCACAGUGGCUAAGUUCCG
cfa-miR-27a	UUCACAGUGGCUAAGUUCUG
cfa-miR-27a	UUCACAGUGGUUAAGUUCCC
cfa-miR-29b	UAGCACCAUCUGAAAUCGGUU
cfa-miR-29b	UAGCACCAUUUGAAAUCAG
cfa-miR-29b	UAGCACCAUUUGAAAUCAGU
cfa-miR-29b	UAGCACCAUUUGAAAUCGGU
cfa-miR-29b	UAGCACCAUUUGAAAUCGGUU
cfa-miR-30d	UGUAAACAUCCCCGACUGGAAG
cfa-miR-30d	UGUAAACAUCCCCGACUGGAAGC
cfa-miR-30d	UGUAAACAUCCUACACUCAGC
cfa-miR-30d	UGUAAACAUCCUACACUCAGCU
cfa-miR-30d	UGUAAACAUCCUACACUCUCAGC
cfa-miR-30d	UGUAAACAUCCUACACUCUCAGCU
cfa-miR-30d	UGUAAACAUCCUCGACUGGAAGC
cfa-miR-30d	UGUAAACAUCCUCGACUGGAAGCU
cfa-miR-30d	UGUAAACAUCCUUGACUGGAAGC
cfa-miR-30d	UGUAAACAUCCUUGACUGGAAGCU
hsa-miR-3150b-3p	AGAGGAGAAUGGAGGGAUGAG

hsa-miR-33a-3p	CAAUGUUUCCACAGUGCAU
cfa-miR-34c	UGGCAGUGUCUUAGCUGGUUGU
cfa-miR-374b	AUAUAAUACAACCUGCUAAG
cfa-miR-374b	AUAUAAUACAACCUGCUAAGU
cfa-miR-374b	UUAUAAUACAACCUGAUAAGU
cfa-miR-423a	AGAGGGGCAGAGCGAGAC
cfa-miR-423a	UGAGGGGCAGAGAGCGAGAC
cfa-miR-423a	UGAGGGGCAGAGAGCGAGACU
cfa-miR-423a	UGAGGGGCAGAGAGCGGG
cfa-miR-423a	UGAGGGGCAGAGAGCGGGA
cfa-miR-423a	UGAGGGGCAGAGAGCGGGAG
cfa-miR-423a	UGAGGGGCAGAGCGGGAGAC
cfa-miR-423a	UGAGGGGCGAGAGCGAGA
cfa-miR-450b	UUUUGCAAUAUGUUCCUGAA
cfa-miR-450b	UUUUGCAAUAUGUUCCUGAAU
cfa-miR-508a	AACUUGAGCACCUAACAAUG
hsa-miR-519b-3p	AAAGUGCACGCGCUUUGGGAC
hsa-miR-664a-3p	UAUUCAUUUAUCUCCCAGCCUACA
cfa-let-7b	AGAGGUAGUGGGUUGCAUAG
cfa-let-7b	AGAGGUAGUGGGUUGCAUAGU
cfa-let-7b	GGAGGUAGUAAAUUGUCUA
cfa-let-7b	UGAGGUAGGAGGUUGUAUAG
cfa-let-7b	UGAGGUAGGAGGUUGUAUAGUUG
cfa-let-7b	UGAGGUAGUAAGUAAUAU
cfa-let-7b	UGAGGUAGUAAGUAAUAUU
cfa-let-7b	UGAGGUAGUAAGUUGUAU
cfa-let-7b	UGAGGUAGUAAGUUGUAUUGU
cfa-let-7b	UGAGGUAGUAGAUUGUAUAG
cfa-let-7b	UGAGGUAGUAGAUUGUAUAGU
cfa-let-7b	UGAGGUAGUAGGUAUUAUAG
cfa-let-7b	UGAGGUAGUAGGUUGUAU
cfa-let-7b	UGAGGUAGUAGGUUGUAUAG
cfa-let-7b	UGAGGUAGUAGGUUGUAUAGU
cfa-let-7b	UGAGGUAGUAGGUUGUAUGG
cfa-let-7b	UGAGGUAGUAGUUUGUACAG
cfa-let-7b	UGAGGUAGUAGUUUGUACAGU
cfa-let-7b	UGAGGUAGUAGUUUGUGCUGU
cfa-let-7b	UGAGGUAGUAGUUUGUGCUGUU
cfa-miR-8834a	GGCCGGGCGUGUGGAGUGCUGUG

cfa-miR-92b	AAUUGCACGGUAUCCAUC
cfa-miR-92b	AAUUGCACGGUAUCCAUCUG
cfa-miR-92b	CAUUGCACUUGUCUCGGUCUGA
cfa-miR-92b	UAUUGCACAUUACUAAGU
cfa-miR-92b	UAUUGCACAUUACUAAGUUG
cfa-miR-92b	UAUUGCACUUGUCCCGGCCUG
cfa-miR-92b	UAUUGCACUUGUCCCGGCCUGU
cfa-miR-99a	AACCCGUAGAUCCGAACUUGUG
cfa-miR-99a	AACCCGUAGAUCCGAUCUUGU
	AAAACAUGAAUUGCUGCUGCA
	AAAAGAAAUCAUUAAUGAGUAG
	AAAAGCACGCGCUGCCGGAAGUGA
	AAAAGGAAUUCAAAUUGGUA
	AAACAAUGGGCCCUGCUAAGC
	AAACCCAGGUGUCAGGCUCGCU
	AAACCCCUUACACUCUCCAGG
	AAAGAAUUCUCCUUGUGGGA
	AAAGAGGAGCUGGAGUUGGA
	AAAGCACUUUGAAGAGAG
	AAAGCAGACUGAGGGAGGUG
	AAAGCAGACUGAGGGAGGUGG
	AAAGGAAUUCAAAUUGGUAAG
	AAAUAAUUCUCCUUUUGGGGU
	AACAUGUCCUUGGGUCUGCAGA
	AACCAUCCUGACCCUGUCUGU
	AACUCCCAGGGACACCGUUCA
	AACUCCCUCUCCUUUCAGUAGCU
	AACUCGUUAGAAAGGUAGA
	AACUCGUUAGAAAGGUAGAC
	AACUGAUUCCCAUACUGACU
	AACUGAUUCCCAUACUGACUUG
	AACUGGCCCACAAAGUCCCGCU
	AAGAACAUUUGUUCACAAGAGUGU
	AAGCAGGAUUUAGACUACAAUAU
	AAGCAGUAGGCCUGGACC
	AAGCAGUAGGCCUGGACCUCA
	AAGCUGUGAGAUCAUGACCUGA
	AAGGAAUUCAAAUUGGUAAGU
	AAGGAGAGAACAGGUGAUG
	AAGGAGAGAACAGGUGAUGUGG

	AAGGCAGUAGGUUGUAUAGU
	AAGUAGAGGCAAAUGUGGUAA
	AAUAACUGAUGGACCAAAGAAG
	AAUAGCUCAGAAUGUCACU
	AAUCCCAAAUCUGUCAGGCCU
	AAUCUCGGCAUCCCUGGUCACG
	AAUGGCGCCACUAGGGUUG
	AAUGGCGCCACUAGGGUUGUGC
	AAUGUAGUGUGAAUGGUGCCC
	AAUGUGAAUUCUUCUCCCGUGGU
	AAUUGAAGGAAUAUGGGGUUC
	AAUUGAAGGAAUAUGGGGUUCG
	AAUUGGGCAGGUAGGAGGAGA
	AAUUGUAGAAAGACUUACUA
	AAUUGUAGAAAGACUUACUAUG
	AAUUGUGUGACCCUGAAAAUG
	ACAAAGAUCUGAGGACAAGA
	ACAAAGAUCUGAGGACAAGAGA
	ACAAAUCCACGGAGUCCCUG
	ACAAGGGGUCACUCACUGUGA
	ACACACACACACACACACACA
	ACACCCAACCGACUGAGCCA
	ACACGCAUGGCACACCUGAG
	ACACUGGGAACCACUGCUCUU
	ACAGCGGCCUCUUCACUCACA
	ACCACAGUGUGGUUUGGACG
	ACCCAGCCAGGCUCCCUAGCA
	ACCCCAGGGUAGAACCACUG
	ACCCCCCGUCUGUACCGUGAGA
	ACCGAGCAUCCCAAGCAGGCU
	ACCGCCAGUAGUGACUAGGGA
	ACCUAUAGAUCAAUAACAC
	ACCUAUAGAUCAAUAACACU
	ACCUCAGUCCUGAGCAAACUGG
	ACCUCUCCCACUCCCAUCCAGG
	ACCUCUGAAUGCUCUGGUCU
	ACCUGAGCCGAAGUCGGACGC
	ACCUGGGCUCGGGAACGGA
	ACGAUGGUAGAUUUGGAAGUC
	ACGAUGGUAGAUUUGGAAGUCA
	ACGUUGUGCCCGUUUCCCUGA

	ACUAAAACAUGGAAGCACUU
	ACUCGUGACCUUAUCCUGCAG
	ACUCUCCCGGGACUUGGAGCG
	ACUUCAAAGCCGAGCUCUCU
	ACUUGUUACAGGUGUAGAAUC
	ACUUGUUACAGGUGUAGAAUCU
	ACUUGUUAGGAUGAGGAC
	ACUUGUUAGGAUGAGGACUCU
	ACUUUUUGUCAGAUACUGCAG
	AGAAUCCUCACUCCUGCCGCC
	AGAAUUAUAGUGAAAUGAACAU
	AGACGCCGCGUUUCUGACCAG
	AGACUGGGUCCUGAGGCC
	AGACUGUUCAUUUCUCCC
	AGACUGUUCAUUUCUCCCUCU
	AGACUUCAUGGGCUCUGCCUUGU
	AGAGAGAAUCCCAAACAGGCU
	AGAGCAGGUGACAAUAAAGUGA
	AGAGGACAUGCCCCAGACCUAG
	AGAGGCAGCAGCUAGGAUUCU
	AGAGUCAUGGGAAAACCGAGA
	AGAGUUGAGUCUGGACGUCC
	AGAUCACCGGUCCCCGAUCU
	AGAUGUCCAGCCACAAUUCUCG
	AGCAAACGGGUGUCUUCUGUG
	AGCAUGUGACUCUUAAUC
	AGCCCAAGCUGUCUCUGGUU
	AGCCCUUUGUCUGUCCUCUAGG
	AGCCUACCCCUUCUCCUUUUG
	AGCCUGCUUUGGAUUCUGUG
	AGCCUGCUUUGGAUUCUGUGUC
	AGCUAUGUCCUGGGUUAGGAGA
	AGCUCAUGUCCAACACCUAGA
	AGCUGCCCAGGAGUCCCUGCA
	AGGAAGAAUGGAGGUGGAAUUU
	AGGACUCAGGGUGGCUCUGUGA
	AGGCAGAUAGAACAGGUC
	AGGCAGUAGGUUGUAUAG
	AGGCGACCCUGCUCUGAUGGCG
	AGGGACUGUGACUGGGUGUCA
	AGGGCACACAGGGACAGAG

	AGGGCACACAGGGACAGAGCUG
	AGGGGCGCCUGGGUAGCUCAG
	AGGGGCGCCUGGGUAGCUCAGU
	AGGUAGAUAGAACAGGUC
	AGGUGGUAGAUGGUAUAG
	AGUAAGGGCUCUGUAAGUAUU
	AGUCACUGUUGUCACAUUGC
	AGUCACUGUUGUCACAUUGCU
	AGUCUGGAGCGCUUGGGUGACU
	AGUGCCUCGGCAGUGCAGCCC
	AGUGCUGCAGGAAGCCUGAAGCG
	AGUGGGCUGCAGGUGUGUGGU
	AGUGGGCUGCAGGUGUGUGGUU
	AGUGGUGACAAUGAGACCUGU
	AGUUCCGCCAUGGCCUCCGAGGA
	AGUUCCGGCUCUUUGGCAGA
	AGUUUCUCUGAAUGUGUAGAGU
	AUCCACGGUGUUUGCAGUCUUG
	AUCCCACCUCUGCCACCA
	AUCCCGGACGAGCCCCCC
	AUCCGAGCAGGAAGGGACCA
	AUCGGGGCACUGCUGCGUU
	AUCGUUACCAGACAGUGUUAGA
	AUCUAAAGGUCCCUGGUUCG
	AUCUCAGGUUCGUCAGCCCG
	AUCUCAGGUUCGUCAGCCCGUG
	AUCUCUGCCUCUCUCCCCUCA
	AUCUUCGUGGGUCACUGCCU
	AUCUUUGUGGGUCACUGACU
	AUGAUGGUUAGAGAUAAAGACU
	AUGCCCCGGAGGCAGGUCUGA
	AUGCGUGCACGUGUUUGUG
	AUGGCGGCCGCACUCUGGCCUGC
	AUGGGUUACAGUAGACUUAGGG
	AUUAGCUAGUUGGUGAGGUA
	AUUCAGACUACUCUCCCCCGUCC
	AUUGAAACUCAUGCAUAUCAGA
	AUUGGGACUGAGACACGGCC
	CAACAUGCCUGGGUCCCACUCU
	CAAGGCUGAGGCUCCUUGAG

	CACAGCCUGCCCACCCUG
	CACAGGAUCUGAAAUGGGC
	CACCGCGUGGGCUUCUGGGCGA
	CACCUUGCGCUACUCAGGUCCU
	CACUCACCCUACCUCUGGCAG
	CAGAAACGCGGCGUCUCAGA
	CAGAACCUCCUGGUGCCCUGGA
	CAGAGGGGAGGACACAUUCAGA
	CAGCACUGUCCGGUAAGA
	CAGCCCCGGGCCUGGAGGA
	CAGCCUGCCCACCCUGGA
	CAGCGGGUUCAGAUCUCUUCU
	CAGCUCUUUCUGCGCGACCUA
	CAGUACUGUUCCCGCUGCUAGGG
	CAGUCGGUAGAGCAUGGG
	CAUCUGGUCCCCUCUUUCCU
	CAUCUGGUCCCCUCUUUCCUGCA
	CAUCUGUGACCCUGCCUC
	CAUCUGUGACCCUGCCUCUAG
	CAUGGAGGUCUCUGUCUGGCU
	CAUUGAACUUGUCUCUGU
	CAUUUGUCACUUCCUGCUUCU
	CCAGAUCAUUCUAAGGUGGAGC
	CCAGGGAAAGAUGAAAAGGA
	CCAUUUUUUGUUGUUUACUGUUU
	CCCCGGACAAGUUCAAAGGCC
	CCCCGGACAAGUUCAAAGGCCUG
	CCCCGUCCUUGGCCUCCA
	CCCCUGUCCUCCAGGAGCUUA
	CCCGCCCGGACCUGGCUCACC
	CCCUCCCAGCAUCCACGAGCGA
	CCGGCCAGACUUCCUCCCUAU
	CCGGUGCUGAGCUGCCCC
	CCUGCUCACUCCUGGCCACU
	CCUGCUGUUUCUCACCUGACA
	CCUGCUUUGGAUUCUGUGUC
	CCUGUCCUGAGAUGCCCC
	CGAGGUGCUCACAGUCUAGU
	CGCCCAUCCUCUCUCCUCCCUGA

	CGCCCCUUUCUGCUCUCCAGC
	CGGGACGCCUGGGUAGCUCAG
	CGGGGCGCCUGGGUGGCUCAG
	CGUCAACACUUGCUGGUUU
	CGUUUUGUGUUCUUUUUAUUGCU
	CUCCCACUGUGGUCGCCA
	CUCCCGGGGUCGAAGGCCAGA
	CUCCCGGUGUGGGAACCA
	CUCUUCAUCAGGUGUAAAUGG
	CUCUUCAUCAGGUGUAAAUGGA
	CUGACCGUCCUGUGCCCACA
	CUGACUGUAAACACUGACGGCA
	CUGCCUGGACCCCUGCUCA
	CUGCCUGGACCCCUGCUCACC
	CUGCGUUGGAUUCUGCGUC
	CUGCUGUUUCCCUCUAUUAGUUU
	CUGGGUCCCAGGAGAGUCUGA
	CUGUGCAUGCUGAGAGCC
	CUGUGCAUGCUGAGAGCCU
	CUGUGCUGAGCUGCCCCU
	CUUACCAGGUUGUAUUGUAA
	CUUAGCAGGUUGUAUUAUA
	CUUCCACUCAGGUCAUGCUCU
	CUUCCACUCAGGUCAUGCUCUCG
	CUUCGGACACCCAACCCUGA
	CUUGGCUCUGAGGGCUGGGCA
	CUUUCACUCAGGUCAUCAUCU
	GAAAUUAGGUCUGUAACUUA
	GAACAGCCCCUCUCUGGCCCCACA
	GAACAUCCUGCAUAGUGCUGCCA
	GAACGAAAUCCAAGCGCAGCUGG
	GAAGUGGGGCAAGACUGGGUGG
	GAAUAGAACAUAGGUGGCU
	GACAAUGUCUACAAGCUGCAGU
	GACACUACCGAGGCCCUGGAGA
	GACAGUCGGGGGCAGCAG
	GACCUUCUGUCUGCCCGGCAGA
	GAGAGAAUCCCAAGCAGGCU
	GAGAGAUCAGAGGCGCAGAG

	GAGAGAUCAGAGGCGCAGAGU
	GAGAGCAUACCAAGCAGGC
	GAGGAACCUGUGUGGCUUAG
	GAGGGCCCCCCCCAAUCCUGU
	GAGGGGCAGAGCACGAGA
	GAUCUGAGUCAGGGCCAUGUG
	GAUCUGAGUCAGGGCCAUGUGU
	GAUGUGGCGACGAAUGUCU
	GAUUAUUCCAGUGUGCAGCC
	GCACGGAAGUUUUAUUCUCUUG
	GCAGCAGGCUGUCAGGCUCU
	GCCACCGGGGGCCUGUCGCU
	GCCAGAUGCUGAUCUCAUGGGA
	GCCCUGCGCUCUCUGCUCCAGG
	GCUCAGCCGGAGGUAGGG
	GCUGACUCCUAGUCCAGUGCU
	GGAUAUCAUCAUAUACUGUAAGU
	GGCCCCGUCCUUGGCCUCCA
	GGCGGGACCGUCUGUCCGGGU
	GGCUAGCUCAGUCGGUAG
	GGGGAUGUAGCUCAGUGGUAGA
	GGGGGACCUGUGUGGCUUAG
	GGUGGAGAGGGGCUGAAAGUC
	GGUGGAGAGGGGCUGAAAGUCU
	GUAGCACCAGAAACAGCUGUG
	GUCCCACUUCGAACCCUGUCAUU
	GUGAGGGUGAAGAAAACC
	GUGAGGGUGAAGAAAACCUGUGU
	GUGAGGUUGAUUUGGGUC
	GUGCAUUGCUGUUGCAUUGC
	GUGCUCUUGUCUUUCUCUCAGA
	GUGUCAUUUAUACUGUAUUCU
	GUGUGUGUGUGUGUGUGUGUG
	GUUCCUGCUGAACUGAGCCAGU
	GUUUUGUGUUCUUUUUAUUGCU
	UAAAAAUGGCUGACUCCUGUU
	UAAAACAUGGAAGCACUUAC
	UAAAACAUGGAAGCACUUACU
	UAAAAGGCUGUUAAAUGGUGA
	UAAAGCACCCGCUGUGGAAG

	UAACACUGUCUGGUAAAGAUG
	UAACUCCCCUCCGCCCCAGCU
	UAAGAAGAUGGGGGCACUUGGG
	UAAGAGGCUAACACAGAAGGGU
	UAAGGGCUCGUCGUCAGGGU
	UAAGGGCUCGUCGUCAGGGUU
	UAAUGUAUACAUAUGCCUGUG
	UAAUGUAUACAUAUGCCUGUGU
	UACAGUAGUCUGCACAUUGGU
	UACCACAGGGUAGAACCACGGA
	UACCCAGAUGUCCCUUUGUGCA
	UACCGCACUGUGGGUACUUGC
	UACGUAGAUAUAUAUGUAUUU
	UACUCACGCGCUUGUUUGU
	UACUUAUUGGAUGAGAUAGU
	UAGAAAAGAGGUUGAAGAUAGA
	UAGAAAAUCAGCAUAUAAGACA
	UAGAAACGGAUGGAAGACUUG
	UAGAAACGGAUGGAAGACUUGC
	UAGAAAUUAGGUCUGUAAC
	UAGAAGCUCCCCAUGUUU
	UAGAGAAGUGAAAGGAAGCU
	UAGAGAAGUGAAAGGAAGCUC
	UAGAUCUGGGGUAGGGCC
	UAGAUCUGGGGUAGGGCCUGA
	UAGAUCUGGGGUAGGGCCUGGG
	UAGCAGAUGCUCAUAAUAUG
	UAGCAUGCAGCUCUUGAUCUCA
	UAGCAUUGGACAACGGACUGAGU
	UAGCUCAGAGUUCUGAUGGAU
	UAGGCCGCAAGAGACACCAGGG
	UAGGGGAUGAUUGUAGAGGAGA
	UAUAGGUCAGGGCUCAAGGGCA
	UAUCAAUGGUGGCUUUAAAUGU
	UAUCAGGAAGAAAGGGAGAG
	UAUCAGGAAGAAAGGGAGAGA
	UAUCCUCAGUGCCUAGUGAC
	UAUGACUACAGAGGCUGUGUU
	UAUGGAGUGUGACCUGGGCA
	UAUGGAGUGUGACCUGGGCAAC
	UAUUCAUUUAUCUCCCAGCCU

	UAUUUGUGGACAGUUACUCAU
	UAUUUGUGGACAGUUACUCAUU
	UCAAUGGCGCCUCUUGGACU
	UCACACAGCCUUUGAGAAU
	UCACCCAAGCGCUCCAGACU
	UCACGCUCUGGGUUGGUCU
	UCACUAAACCUGUCUGAGCCA
	UCACUAAACCUGUCUGAGCCAGU
	UCACUGUGAAGAAUGCUGC
	UCAGACCCGGCCCUACUCCCU
	UCAGCCUGCUGCAUCCCUGCCU
	UCAGGCUCAGUCCCCUCCCGA
	UCAUCGCUCCUUUCUUCCAGCA
	UCCAAGGACCUCAGCGGCA
	UCCACCUCUGCUCCCGGCCCAGG
	UCCACUCUGGCAGAUACUCCGU
	UCCAGAGCUCUCUCAGCCA
	UCCCACCGCGUGUUCCAGAGU
	UCCCACCGCGUGUUCCAGAGUGC
	UCCCAUAAUGUAGUAGAAAUCG
	UCCCCCAAAACGACCUCUCACU
	UCCCGGAUAGCUCAGUCG
	UCCCGGUGAGACUCACCUUCC
	UCCCUACCCUCUCACCUCUGCC
	UCCCUUCUUCACUUUUCCCAGG
	UCCGAGAAUCCCAAGCAGGCU
	UCCGAGCCUGGGUCUCCCUCU
	UCCGCCUGUGAGAGGGACACG
	UCCGCUCCGGCUGUGACACGGGU
	UCCUGCAGGUGGGAUAGGCCGG
	UCCUGCCCUUCCCCGGCGACG
	UCCUGGACUCCUCUGACCCGUU
	UCCUGGACUGAUCUGCCC
	UCCUUUACUGGUCUGCCCC
	UCGAGGAGCUCACAGUCUA
	UCGCUAUGCAGGUGCGGAAG
	UCGCUCAGCUGCUAACCCGG
	UCGGAGGAGGAAGGGUGCCGCG
	UCGGGCACCUUCUCUGAUCGGC

	UCGUACCGUGAGUAAUAAUGCG
	UCGUCCCGGGCUACUUGCUU
	UCUACAGUGCACGUGUCUCCA
	UCUACAGUGCACGUGUCUCCAG
	UCUAGGUAUGGUCCCAGGGAU
	UCUAGUAAGAGUGGCAGUCG
	UCUCACACAGAAAUCGCACCCG
	UCUCACACAGAAAUCGCACCCGU
	UCUCAGCUCUGCCACCUCU
	UCUCAUUUUAUAAGUCCUAGCU
	UCUCCAAGGAUCCCUGGCUAG
	UCUCCCGCAUUGGACUGAAACUG
	UCUCCGCGACUCCCUGGCUCG
	UCUCUCUUCUUCGUUGGCC
	UCUCUCUUCUUCGUUGGCCCAGA
	UCUCUGGGCCUGUGUCUUAGGC
	UCUCUGGGCCUGUGUCUUAGGCU
	UCUGAAGCAGGCUCCAGGC
	UCUGAAGCAGGCUCCAGGCU
	UCUGACCACCCACCCUUGCC
	UCUGCAGGCCUCUGGGUGGC
	UCUGCAGGCCUCUGGGUGGCU
	UCUGCUGCCGUGGUGACUGGCA
	UCUGGCUUCCUCUUCCUGUC
	UCUGGCUUCCUCUUCCUGUCU
	UCUGGGAGUCCUCAUGCAU
	UCUGGGGCUGCAGAGGAGGAG
	UCUGGGGCUGCAGAGGAGGAGU
	UCUUCACUCACGAAGAGCUCUG
	UCUUCAGCUCACAUUUGGAAU
	UCUUCCCAUCUAGGCUGCC
	UCUUGUCCUCAGAUCUUUGUGU
	UGAAAAAGCGGCCACCUGAGU
	UGAAACUGAAGGACAACGAGA
	UGAAAGGGUAGCACUCAUGAGA
	UGAAGUCAGUGAUCGGAGAGCA
	UGAAUGAAUGAAUGAUGAGUGA
	UGAAUGGUUGAGGUCAAAGAGU
	UGAAUUAACUUUUAUGUAGA

	UGACCUAUGAAUUGACAGCCAGU
	UGACCUGGGACUCGGACAGC
	UGACCUGGGACUCGGACAGCU
	UGACCUGGUUACCUCCAACA
	UGACGUCAUCACGCCCGCGCUGC
	UGACUCUGCCUUCUGAGGCU
	UGACUCUGCCUUCUGAGGCUC
	UGACUGCCUGUCUCUCCACCG
	UGAGAAUCUUUUGUUUGGCU
	UGAGCAACCGAGGUGCCCG
	UGAGCAACCGAGGUGCCCGUGC
	UGAGCCUCAAGCAAGGGAC
	UGAGCUCAUGUCCAACACCU
	UGAGGAUAAGGGACACUGUAG
	UGAGGGACAGAGAGCGAG
	UGAGGGGCAGAGAGCGAG
	UGAGGGGCAGAGAUGGAGA
	UGAGGGGCAGAGCGAGAG
	UGAGGUUCGCGGUGGCUGCU
	UGAGUCACCCAGGCACGUCU
	UGAUAAUACAACCUGAUAAGU
	UGCAAAGAACAAGAAAAAUAUU
	UGCACAGAGAGUGUCCACUGGC
	UGCACGAACCCCGGCUGGGU
	UGCACGCUUCUCCCCUUCCG
	UGCACUGAACAAGACCAAAU
	UGCAGAAGGAUCUGGAAGAGGA
	UGCCCGCCACCUGGUCUCUGUG
	UGCCCUUGAAUUCAUUCUCUUU
	UGCCGUCUGGGUUUCUGUCCC
	UGCCGUCUGGGUUUCUGUCCCA
	UGCCUCUCACCCUCUGCCCACA
	UGCCUGUAAGCCUACUCUG
	UGCCUGUAAGCCUACUCUGC
	UGCGAAGAACAAGAAAAAUAUU
	UGCGACAGCUUGUAGACCAGCG
	UGCGGCUCAGGUCAUUAUCU
	UGCGGGGCUAGGGCUAACAGC
	UGCUCGGCCCUGCUUCCUUG

	UGCUCUGCCGUGUCCCCAGA
	UGCUGACAGUCACCGCUCGU
	UGCUGGUAGAGAUAUGUGUGA
	UGCUUAUCCACUCUUGCCC
	UGGAAACAUUUCUGCACAAACU
	UGGAAAGAAAAGGAUGGCA
	UGGAGACAGGGCAGGACUG
	UGGCACCAGCACUGGCGGUG
	UGGCACGCCUCUUCCGACACUG
	UGGCAGAACCCACGCAGUCU
	UGGCCCCGUGACUCUGGCU
	UGGCCCCGUGACUCUGGCUC
	UGGCCGGAGCGAGCCUACCUGGA
	UGGGGCACCUGAUUGGUUCA
	UGGGGCAGAGCUCGCGCG
	UGUACGCGUGACUCGAGUUC
	UGUACUCUAGAGCCAAGCUGC
	UGUACUCUAGAGCCAAGCUGCC
	UGUAUCCUCAGUGCCUAGUGA
	UGUCCUCUGACCGCCCUGCC
	UGUCUCUACAACUCUGCCAC
	UGUCUUACGUGGGUACGUGU
	UGUGCUAGAUAUGCUGACCC
	UGUGCUAGAUAUGCUGACCCUCG
	UGUGGCAACCAAGCGCUCGA
	UGUGUGGGGGUGUGUAUGU
	UGUGUGUGUAUGUCUGUAGC
	UGUGUGUGUAUGUCUGUAGCU
	UGUGUGUGUGUGUGUGUGUGU
	UGUUCCUCUUCUUCGCCACCCU
	UGUUCCUGCUGAACUGAGCCA
	UGUUGUACUUUUUUGUUUGUUU
	UGUUGUACUUUUUUUUUUGUU
	UGUUUCUAAGUAACUGAUAGA
	UUAACCAACUGAGCCACCCAGA
	UUACAGCGGAAUAAGGGAAU
	UUACUACUUAUAGGAUAUGCA
	UUACUCUAGGACAUUUGCUGUGU
	UUAGGGGCAGAGAGCAAGA

	UUAUAAAGCAAUGAGACUGA
	UUAUAAAGCAAUGAGACUGAUU
	UUAUGGCCCUUCGGUAAUU
	UUAUUACAGCUGAAAGUCCAC
	UUAUUACAGCUGAAAGUCCACU
	UUAUUUAUUGUUUUGGAGAGA
	UUCAGCCAGAUCAGGAUCUCACG
	UUCAGCUCAGGUCAUGAUC
	UUCAGCUCAGGUCAUGAUCUCA
	UUCAGGGACUCAGAGAUAAA
	UUCAUUUUGAUCCCACAGCCU
	UUCCAAAUGUGAGCUCAAGA
	UUCCCACGUCUUAUGCCCCAGU
	UUCCCCGUCCGCCUGGUAGG
	UUCCGGACCUUGAGAGAGAC
	UUCCGUAACCAGUAAUUAUAGA
	UUCCUGCCGUGCCUGCUCUAG
	UUCCUGCCGUGCCUGCUCUAGU
	UUCCUGUGACUGUGAGGC
	UUCCUGUGACUGUGAGGCUU
	UUCCUUGCCCCAACCCCCCAGG
	UUCCUUUCUGCAGCUACCGCGU
	UUCGUCAGUUUCCUAGGGAGA
	UUCUACUUGUCUCCCUCACAGA
	UUCUCAGGUUGGACAGUCC
	UUCUCAGGUUGGACAGUCCUGG
	UUCUCAUUGGUUUCAUGUCCUGU
	UUCUCCCCUUCCCUGCCCACA
	UUCUCGUCCUUCUCGCCUGCA
	UUCUCUGGAGGGCUGCGGUGA
	UUCUGAAAGGGCAUAAUAUG
	UUCUGAAAGGGCAUAAUAUGUGA
	UUCUGACAGUAAUAGCUC
	UUCUGACAGUAAUAGCUCU
	UUCUUGGUCAUCCUGGGGUGU
	UUCUUGUCGCCCGUCUUCCAGG
	UUGAAUGAAGGCAACUGGCU
	UUGACCUACUGAGCCACCCA
	UUGAGCUCAUGAAUUGUGAGA

	UUGAGUAGCUCACAGUCUAG
	UUGCAAGCAACACUCUGUGUCA
	UUGCUCAGAUUCCACCUACA
	UUGGAGACAGGGCAGGACUGA
	UUGGAGAUGAGAAAUGCGGGUA
	UUGGAGAUGAGAAAUGCGGGUAG
	UUGGAGGUAAAUUAGCAGCAUGG
	UUGGCCUACAGAAAUGACAGA
	UUGGGAUUGUGCCUGUUUUGA
	UUGGGGGCAGUUCCUGCUGAG
	UUGGGGUGUGGAUACUGGAGUCA
	UUGUAUAUUGUAAAGGAGAGUG
	UUGUGACAGAUUGAUAAC
	UUGUGACCGCACUCUCUUUUGU
	UUUACUGGUUUGGGAAAGACA
	UUUAGUGGUAUCAUUGAAAUGA
	UUUCCUGAUGGUGCUUCACG
	UUUCCUGGGGACCAGCACUGU
	UUUCCUUGCUCUCUGCCUCCA
	UUUCUUUCUUUCUUUCUUUCU
	UUUGAUGACUGUUCCUCCUAUU
	UUUGCACCUCUGAGAGUGGAGU
	UUUGCCUCCCACUGACUCA
	UUUGCUGGUGCUGAAGAC
	UUUGCUGGUGCUGAAGACUGA
	UUUGCUUGCUGUCCUGGCC
	UUUGCUUGCUGUCCUGGCCUGA
	UUUGGACAUACUAGAAAAGGA
	UUUGGAGAGGUCCACUGAGGGA
	UUUGGGAAGUGGUAGUAAAGG
	UUUGGUAAAUGAAGUAUGUGC
	UUUGGUAAAUGAAGUAUGUGCA
	UUUGUGCUCUCCCCCUUC
	UUUUCUAGUUGUGUGACCUUU
	UUUUGCGAUGUGUUCCUAAUA
	UUUUUCCUUGAUUCUCACAGC
	UUUUUCUUGAUUCUAUGG

REFERENCES

1. Gilor C, Niessen SJ, Furrow E, et al. What's in a Name? Classification of Diabetes Mellitus in Veterinary Medicine and Why It Matters. J Vet Intern Med 2016;30:927-940.

2. American Diabetes A. Diagnosis and classification of diabetes mellitus. Diabetes Care 2013;36 Suppl 1:S67-74.

3. Root MV, Johnson KH, Allen WT, et al. Diabetes mellitus associated with pancreatic endocrine insufficiency in a kitten. J Small Anim Pract 1995;36:416-420.

4. Thoresen SI, Bjerkas E, Aleksandersen M, et al. Diabetes mellitus and bilateral cataracts in a kitten. J Feline Med Surg 2002;4:115-122.

5. Prahl A, Guptill L, Glickman NW, et al. Time trends and risk factors for diabetes mellitus in cats presented to veterinary teaching hospitals. J Feline Med Surg 2007;9:351-358.

6. Farrow HA, Rand JS, Morton JM, et al. Effect of dietary carbohydrate, fat, and protein on postprandial glycemia and energy intake in cats. J Vet Intern Med 2013;27:1121-1135.

7. Ohlund M, Fall T, Strom Holst B, et al. Incidence of Diabetes Mellitus in Insured Swedish Cats in Relation to Age, Breed and Sex. J Vet Intern Med 2015;29:1342-1347.

8. O'Leary CA, Duffy DL, Gething MA, et al. Investigation of diabetes mellitus in Burmese cats as an inherited trait: a preliminary study. N Z Vet J 2013;61:354-358.

9. Yaribeygi H, Farrokhi FR, Butler AE, et al. Insulin resistance: Review of the underlying molecular mechanisms. J Cell Physiol 2018.

10. Nolan CJ, Prentki M. The islet beta-cell: fuel responsive and vulnerable. Trends Endocrinol Metab 2008;19:285-291.

11. Appleton DJ, Rand JS, Sunvold GD. Insulin sensitivity decreases with obesity, and lean cats with low insulin sensitivity are at greatest risk of glucose intolerance with weight gain. J Feline Med Surg 2001;3:211-228.

12. Hoenig M, Thomaseth K, Waldron M, et al. Insulin sensitivity, fat distribution, and adipocytokine response to different diets in lean and obese cats before and after weight loss. Am J Physiol Regul Integr Comp Physiol 2007;292:R227-234.

13. Appleton DJ, Rand JS, Sunvold GD. Plasma leptin concentrations in cats: reference range, effect of weight gain and relationship with adiposity as measured by dual energy X-ray absorptiometry. J Feline Med Surg 2000;2:191-199.

14. Hoenig M, Pach N, Thomaseth K, et al. Cats differ from other species in their cytokine and antioxidant enzyme response when developing obesity. Obesity (Silver Spring, Md) 2013;21:E407-414.

15. Jaso-Friedmann L, Leary JH, 3rd, Praveen K, et al. The effects of obesity and fatty acids on the feline immune system. Vet Immunol Immunopathol 2008;122:146-152.

16. Hoenig M, Pach N, Thomaseth K, et al. Evaluation of long-term glucose homeostasis in lean and obese cats by use of continuous glucose monitoring. Am J Vet Res 2012;73:1100-1106.

17. Ahren B, Pacini G. Islet adaptation to insulin resistance: mechanisms and implications for intervention. Diabetes Obes Metab 2005;7:2-8.

18. Maedler K, Spinas GA, Lehmann R, et al. Glucose induces beta-cell apoptosis via upregulation of the Fas receptor in human islets. Diabetes 2001;50:1683-1690.

19. Zini E, Osto M, Franchini M, et al. Hyperglycaemia but not hyperlipidaemia causes beta cell dysfunction and beta cell loss in the domestic cat. Diabetologia 2009;52:336-346.

20. Back SH, Kang SW, Han J, et al. Endoplasmic reticulum stress in the beta-cell pathogenesis of type 2 diabetes. Exp Diabetes Res 2012;2012:618396.

21. Brownlee M. A radical explanation for glucose-induced beta cell dysfunction. J Clin Invest 2003;112:1788-1790.

22. Herndon AM, Breshears MA, McFarlane D. Oxidative modification, inflammation and amyloid in the normal and diabetic cat pancreas. J Comp Pathol 2014;151:352-362.

23. Fehmann HC, Weber V, Goke R, et al. Cosecretion of amylin and insulin from isolated rat pancreas. FEBS Lett 1990;262:279-281.

24. Mirzabekov TA, Lin MC, Kagan BL. Pore formation by the cytotoxic islet amyloid peptide amylin. J Biol Chem 1996;271:1988-1992.

25. Weise K, Radovan D, Gohlke A, et al. Interaction of hIAPP with model raft membranes and pancreatic beta-cells: cytotoxicity of hIAPP oligomers. Chembiochem 2010;11:1280-1290.

26. Lutz TA, Ainscow J, Rand JS. Frequency of pancreatic amyloid deposition in cats from south-eastern Queensland. Aust Vet J 1994;71:254-256.

27. Zini E, Lunardi F, Zanetti R, et al. Endocrine Pancreas in Cats With Diabetes Mellitus. Vet Pathol 2016;53:136-144.

28. Radin MJ, Sharkey LC, Holycross BJ. Adipokines: a review of biological and analytical principles and an update in dogs, cats, and horses. Vet Clin Pathol 2009;38:136-156.

29. Larsen CM, Faulenbach M, Vaag A, et al. Sustained effects of interleukin-1 receptor antagonist treatment in type 2 diabetes. Diabetes Care 2009;32:1663-1668.

30. Prentki M, Nolan CJ. Islet beta cell failure in type 2 diabetes. J Clin Invest 2006;116:1802-1812.

31. Boden G. Gluconeogenesis and glycogenolysis in health and diabetes. J Investig Med 2004;52:375-378.

32. Basu R, Chandramouli V, Dicke B, et al. Obesity and Type 2 Diabetes Impair Insulin-Induced Suppression of Glycogenolysis as Well as Gluconeogenesis. Diabetes 2005;54:1942-1948.

33. Nelson RW. Diabetes Mellitus. In: Ettinger SJ, Feldman EC, eds. Textbook of Veterinary Internal Medicine, Elsevier Saunders ed. Saint Louis, Missouri: Elsevier Saunders; 2005:1563-1591.

34. Henson MS, O'Brien TD. Feline models of type 2 diabetes mellitus. ILAR J 2006;47:234-242.

35. Singh VP, Bali A, Singh N, et al. Advanced glycation end products and diabetic complications. Korean J Physiol Pharmacol 2014;18:1-14.

36. Link KR, Rand JS. Changes in blood glucose concentration are associated with relatively rapid changes in circulating fructosamine concentrations in cats. J Feline Med Surg 2008;10:583-592.

37. Lutz TA, Rand JS, Ryan E. Fructosamine concentrations in hyperglycemic cats. The Canadian Veterinary Journal 1995;36:155-159.

38. Adams LG, Hardy RM, Weiss DJ, et al. Hypophosphatemia and hemolytic anemia associated with diabetes mellitus and hepatic lipidosis in cats. J Vet Intern Med 1993;7:266-271.

39. Christopher MM. Relation of endogenous Heinz bodies to disease and anemia in cats: 120 cases (1978-1987). J Am Vet Med Assoc 1989;194:1089-1095.

40. Christopher MM, Broussard JD, Peterson ME. Heinz body formation associated with ketoacidosis in diabetic cats. J Vet Intern Med 1995;9:24-31.

41. Christopher MM, Broussard JD, Peterson ME. Heinz Body Formation Associated With Ketoacidosis in Diabetic Cats. J Vet Intern Med 1995;9:24-31.

42. Gomberg M. An instance of trivalent carbon triphenylmethyl. J Am Chem Soc 1900;22:757-771.

43. Commoner B, Townsend J, Pake GE. Free radicals in biological materials. Nature 1954;174:689-691.

44. Babior BM, Curnutte JT, Kipnes RS. Biological defense mechanisms. Evidence for the participation of superoxide in bacterial killing by xanthine oxidase. J Lab Clin Med 1975;85:235-244.

45. Babior BM, Kipnes RS, Curnutte JT. Biological defense mechanisms. The production by leukocytes of superoxide, a potential bactericidal agent. J Clin Invest 1973;52:741-744.

46. Palmer RM, Ferrige AG, Moncada S. Nitric oxide release accounts for the biological activity of endothelium-derived relaxing factor. Nature 1987;327:524-526.

47. Boveris A, Chance B. The mitochondrial generation of hydrogen peroxide. General properties and effect of hyperbaric oxygen. Biochem J 1973;134:707-716.

48. Mann T, Keilin D. Haemocuprein and Hepatocuprein, Copper-Protein Compounds of Blood and Liver in Mammals1938;303-315.

49. Markowitz H, Cartwright GE, Wintrobe MM. Studies on copper metabolism. XXVII. The isolation and properties of an erythrocyte cuproprotein (erythrocuprein). J Biol Chem 1959;234:40-45.

50. Kimmel JR, Markowitz H, Brown DM. Some chemical and physical properties of erythrocuprein. J Biol Chem 1959;234:46-50.

51. McCord JM, Fridovich I. Superoxide dismutase. An enzymic function for erythrocuprein (hemocuprein). J Biol Chem 1969;244:6049-6055.

52. Sies H. Oxidative stress: from basic research to clinical application. Am J Med 1991;91:31S-38S.

53. Drose S, Brandt U. Molecular mechanisms of superoxide production by the mitochondrial respiratory chain. Adv Exp Med Biol 2012;748:145-169.

54. Niedowicz DM, Daleke DL. The role of oxidative stress in diabetic complications. Cell Biochem Biophys 2005;43:289-330.

55. Du XL, Edelstein D, Dimmeler S, et al. Hyperglycemia inhibits endothelial nitric oxide synthase activity by posttranslational modification at the Akt site. J Clin Invest 2001;108:1341-1348.

56. Brownlee M. Biochemistry and molecular cell biology of diabetic complications. Nature 2001;414:813-820.

57. Hunt JV, Dean RT, Wolff SP. Hydroxyl radical production and autoxidative glycosylation. Glucose autoxidation as the cause of protein damage in the experimental glycation model of diabetes mellitus and ageing. Biochem J 1988;256:205-212.

58. Wolff SP, Dean RT. Glucose autoxidation and protein modification. The potential role of 'autoxidative glycosylation' in diabetes. Biochem J 1987;245:243-250.

59. Litwinoff E, Hurtado Del Pozo C, Ramasamy R, et al. Emerging Targets for Therapeutic Development in Diabetes and Its Complications: The RAGE Signaling Pathway. Clin Pharmacol Ther 2015;98:135-144.

60. Rossi F, Zatti M. Effect of phagocytosis on the carbohydrate metabolism of polymorphonuclear leucocytes. Biochim Biophys Acta 1966;121:110-119.

61. Weaver J, Taylor-Fishwick DA. Relationship of NADPH Oxidase-1 expression to beta cell dysfunction induced by inflammatory cytokines. Biochem Biophys Res Commun 2017;485:290-294.

62. Quagliaro L, Piconi L, Assaloni R, et al. Intermittent high glucose enhances apoptosis related to oxidative stress in human umbilical vein endothelial cells: the role of protein kinase C and NAD(P)H-oxidase activation. Diabetes 2003;52:2795-2804.

63. Cosentino F, Eto M, De Paolis P, et al. High Glucose Causes Upregulation of Cyclooxygenase-2 and Alters Prostanoid Profile in Human Endothelial Cells. Circulation 2003;107:1017-1023.

64. Lassegue B, Clempus RE. Vascular NAD(P)H oxidases: specific features, expression, and regulation. Am J Physiol Regul Integr Comp Physiol 2003;285:R277-297.

65. Blaser H, Dostert C, Mak TW, et al. TNF and ROS Crosstalk in Inflammation. Trends Cell Biol 2016;26:249-261.

66. Gorin Y, Block K. Nox as a target for diabetic complications. Clin Sci (Lond) 2013;125:361-382.

67. Butler R, Morris AD, Belch JJ, et al. Allopurinol normalizes endothelial dysfunction in type 2 diabetics with mild hypertension. Hypertension 2000;35:746-751.

68. Desco MC, Asensi M, Marquez R, et al. Xanthine oxidase is involved in free radical production in type 1 diabetes: protection by allopurinol. Diabetes 2002;51:1118-1124.

69. Wang Z, Hall SD, Maya JF, et al. Diabetes mellitus increases the in vivo activity of cytochrome P450 2E1 in humans. Br J Clin Pharmacol 2003;55:77-85.

70. White RE, Coon MJ. Oxygen activation by cytochrome P-450. Annu Rev Biochem 1980;49:315-356.

71. Zangar RC, Novak RF. Effects of fatty acids and ketone bodies on cytochromes P450 2B, 4A, and 2E1 expression in primary cultured rat hepatocytes. Arch Biochem Biophys 1997;337:217-224.

72. Kaplowitz N. The importance and regulation of hepatic glutathione. The Yale Journal of Biology and Medicine 1981;54:497-502.

73. Harvey JW. Chapter 7 - The Erythrocyte: Physiology, Metabolism, and Biochemical Disorders. In: Bruss JJKWHL, ed. Clinical Biochemistry of Domestic Animals (Sixth Edition). San Diego: Academic Press; 2008:173-240.

74. Whillier S, Raftos JE, Kuchel PW. Glutathione synthesis by red blood cells in type 2 diabetes mellitus. Redox Rep 2008;13:277-282.

75. Livingstone C, Davis J. Review: Targeting therapeutics against glutathione depletion in diabetes and its complications. The British Journal of Diabetes & Vascular Disease 2007;7:258-265.

76. Zhang H, Forman HJ, Choi J. Gamma-glutamyl transpeptidase in glutathione biosynthesis. Methods Enzymol 2005;401:468-483.

77. Kondo T, Dale GL, Beutler E. Glutathione transport by inside-out vesicles from human erythrocytes. Proc Natl Acad Sci U S A 1980;77:6359-6362.

78. Kondo T, Murao M, Taniguchi N. Glutathione S-conjugate transport using inside-out vesicles from human erythrocytes. Eur J Biochem 1982;125:551-554.

79. Sundaram RK, Bhaskar A, Vijayalingam S, et al. Antioxidant status and lipid peroxidation in type II diabetes mellitus with and without complications. Clin Sci (Lond) 1996;90:255-260.

80. Murakami K, Kondo T, Ohtsuka Y, et al. Impairment of glutathione metabolism in erythrocytes from patients with diabetes mellitus. Metabolism 1989;38:753-758.

81. Sailaja YR, Baskar R, Saralakumari D. The antioxidant status during maturation of reticulocytes to erythrocytes in type 2 diabetics. Free Radic Biol Med 2003;35:133-139.

82. van Dam PS, van Asbeck BS, Van Oirschot JF, et al. Glutathione and alpha-lipoate in diabetic rats: nerve function, blood flow and oxidative state. Eur J Clin Invest 2001;31:417-424.

83. Hamilton JS, Powell LA, McMaster C, et al. Interaction of glucose and long chain fatty acids (C18) on antioxidant defences and free radical damage in porcine vascular smooth muscle cells in vitro. Diabetologia 2003;46:106-114.

84. Obrosova IG, Fathallah L, Liu E, et al. Early oxidative stress in the diabetic kidney: effect of DL-alpha-lipoic acid. Free Radic Biol Med 2003;34:186-195.

85. Aragno M, Parola S, Brignardello E, et al. Oxidative stress and eicosanoids in the kidneys of hyperglycemic rats treated with dehydroepiandrosterone. Free Radic Biol Med 2001;31:935-942.

86. Tagami S, Kondo T, Yoshida K, et al. Effect of insulin on impaired antioxidant activities in aortic endothelial cells from diabetic rabbits. Metabolism 1992;41:1053-1058.

87. Zelko IN, Mariani TJ, Folz RJ. Superoxide dismutase multigene family: a comparison of the CuZn-SOD (SOD1), Mn-SOD (SOD2), and EC-SOD (SOD3) gene structures, evolution, and expression. Free Radic Biol Med 2002;33:337-349.

88. Karasu C. Increased activity of H2O2 in aorta isolated from chronically streptozotocin-diabetic rats: effects of antioxidant enzymes and enzymes inhibitors. Free Radic Biol Med 1999;27:16-27.

89. Memisogullari R, Taysi S, Bakan E, et al. Antioxidant status and lipid peroxidation in type II diabetes mellitus. Cell Biochem Funct 2003;21:291-296.

90. Jachec W, Tomasik A, Tarnawski R, et al. Evidence of oxidative stress in the renal cortex of diabetic rats: favourable effect of vitamin E. Scand J Clin Lab Invest 2002;62:81-88.

91. Wohaieb SA, Godin DV. Alterations in free radical tissue-defense mechanisms in streptozocin-induced diabetes in rat. Effects of insulin treatment. Diabetes 1987;36:1014-1018.

92. Martín-Gallán P, Carrascosa A, Gussinyé M, et al. Biomarkers of diabetes-associated oxidative stress and antioxidant status in young diabetic patients with or without subclinical complications. Free Radic Biol Med 2003;34:1563-1574.

93. Goth L, Eaton JW. Hereditary catalase deficiencies and increased risk of diabetes. The Lancet 2000;356:1820-1821.

94. Goth L, Lenkey A, Bigler WN. Blood Catalase Deficiency and Diabetes in Hungary. Diabetes Care 2001;24:1839-1840.

95. Goth L, Nagy T. Acatalasemia and diabetes mellitus. Arch Biochem Biophys 2012;525:195-200.

96. Lu J, Holmgren A. The thioredoxin antioxidant system. Free Radic Biol Med 2014;66:75-87.

97. Stroher E, Millar AH. The biological roles of glutaredoxins. Biochem J 2012;446:333-348.

98. Poynton RA, Hampton MB. Peroxiredoxins as biomarkers of oxidative stress. Biochim Biophys Acta 2014;1840:906-912.

99. Paula FM, Ferreira SM, Boschero AC, et al. Modulation of the peroxiredoxin system by cytokines in insulin-producing RINm5F cells: down-regulation of PRDX6 increases susceptibility of beta cells to oxidative stress. Mol Cell Endocrinol 2013;374:56-64.

100. Wolf G, Aumann N, Michalska M, et al. Peroxiredoxin III protects pancreatic ss cells from apoptosis. J Endocrinol 2010;207:163-175.

101. Petry SF, Sharifpanah F, Sauer H, et al. Differential expression of islet glutaredoxin 1 and 5 with high reactive oxygen species production in a mouse model of diabesity. PLoS One 2017;12:e0176267.

102. Shalev A. Minireview: Thioredoxin-Interacting Protein: Regulation and Function in the Pancreatic β-Cell. Mol Endocrinol 2014;28:1211-1220.

103. Xu G, Chen J, Jing G, et al. Preventing β-Cell Loss and Diabetes With Calcium Channel Blockers. Diabetes 2012;61:848-856.

104. Ayala A, Munoz MF, Arguelles S. Lipid peroxidation: production, metabolism, and signaling mechanisms of malondialdehyde and 4-hydroxy-2-nonenal. Oxid Med Cell Longev 2014;2014:360438.

105. Yin H, Xu L, Porter NA. Free radical lipid peroxidation: mechanisms and analysis. Chem Rev 2011;111:5944-5972.

106. May JM. Ascorbate function and metabolism in the human erythrocyte. Front Biosci 1998;3:d1-10.

107. Mendiratta S, Qu ZC, May JM. Erythrocyte ascorbate recycling: antioxidant effects in blood. Free Radic Biol Med 1998;24:789-797.

108. Nourooz-Zadeh J, Rahimi A, Tajaddini-Sarmadi J, et al. Relationships between plasma measures of oxidative stress and metabolic control in NIDDM. Diabetologia 1997;40:647-653.

109. Davison GW, George L, Jackson SK, et al. Exercise, free radicals, and lipid peroxidation in type 1 diabetes mellitus. Free Radic Biol Med 2002;33:1543-1551.

110. Jain SK, Palmer M, Chen Y. Effect of vitamin E and N-acetylcysteine on phosphatidylserine externalization and induction of coagulation by high-glucose-treated human erythrocytes. Metabolism 1999;48:957-959.

111. Kashiba M, Oka J, Ichikawa R, et al. Impaired ascorbic acid metabolism in streptozotocin-induced diabetic rats. Free Radic Biol Med 2002;33:1221-1230.

112. Kohen R, Nyska A. Oxidation of biological systems: oxidative stress phenomena, antioxidants, redox reactions, and methods for their quantification. Toxicol Pathol 2002;30:620-650.

113. Amano F, Noda T. Improved detection of nitric oxide radical (NO.) production in an activated macrophage culture with a radical scavenger, carboxy PTIO and Griess reagent. FEBS Lett 1995;368:425-428.

114. Han JY, Hong JT, Oh KW. In vivo electron spin resonance: An effective new tool for reactive oxygen species/reactive nitrogen species measurement. Arch Pharm Res 2010;33:1293-1299.

115. Collins AR. Measuring oxidative damage to DNA and its repair with the comet assay. Biochim Biophys Acta 2014;1840:794-800.

116. Nikitaki Z, Hellweg CE, Georgakilas AG, et al. Stress-induced DNA damage biomarkers: applications and limitations. Frontiers in chemistry 2015;3:35.

117. Breton J, Sichel F, Abbas A, et al. Simultaneous use of DGGE and DHPLC to screen TP53 mutations in cancers of the esophagus and cardia from a European high incidence area (Lower Normandy, France). Mutagenesis 2003;18:299-306.

118. McMillan RM, MacIntyre DE, Booth A, et al. Malonaldehyde formation in intact platelets is catalysed by thromboxane synthase. Biochem J 1978;176:595-598.

119. Milne GL, Dai Q, Roberts LJ, 2nd. The isoprostanes-25 years later. Biochim Biophys Acta 2015;1851:433-445.

120. Moore K, Roberts LJ, 2nd. Measurement of lipid peroxidation. Free Radic Res 1998;28:659-671.

121. Cracowski J-L, Durand T, Bessard G. Isoprostanes as a biomarker of lipid peroxidation in humans: physiology, pharmacology and clinical implications. Trends Pharmacol Sci 2002;23:360-366.

122. Soffler C, Campbell VL, Hassel DM. Measurement of urinary F2-isoprostanes as markers of in vivo lipid peroxidation: a comparison of enzyme immunoassays with gas chromatography-mass spectrometry in domestic animal species. J Vet Diagn Invest 2010;22:200-209.

123. Milne GL, Gao B, Terry ES, et al. Measurement of F2- isoprostanes and isofurans using gas chromatography-mass spectrometry. Free Radic Biol Med 2013;59:36-44.

124. Halliwell B, Lee CY. Using isoprostanes as biomarkers of oxidative stress: some rarely considered issues. Antioxid Redox Signal 2010;13:145-156.

125. Semchyshyn HM. Reactive carbonyl species in vivo: generation and dual biological effects. The Scientific World Journal 2014;2014:417842.

126. Georgiou CD, Zisimopoulos D, Argyropoulou V, et al. Protein carbonyl determination by a rhodamine B hydrazide-based fluorometric assay. Redox Biology 2018;17:236-245.

127. Levine RL, Garland D, Oliver CN, et al. Determination of carbonyl content in oxidatively modified proteins. Methods Enzymol 1990;186:464-478.

128. Buss H, Chan TP, Sluis KB, et al. Protein carbonyl measurement by a sensitive ELISA method. Free Radic Biol Med 1997;23:361-366.

129. Augustyniak E, Adam A, Wojdyla K, et al. Validation of protein carbonyl measurement: a multi-centre study. Redox Biol 2015;4:149-157.

130. Yan LJ, Forster MJ. Chemical probes for analysis of carbonylated proteins: a review. J Chromatogr B Analyt Technol Biomed Life Sci 2011;879:1308-1315.

131. Mohanty JG, Bhamidipaty S, Evans MK, et al. A fluorimetric semi-microplate format assay of protein carbonyls in blood plasma. Anal Biochem 2010;400:289-294.

132. Stocker P, Ricquebourg E, Vidal N, et al. Fluorimetric screening assay for protein carbonyl evaluation in biological samples. Anal Biochem 2015;482:55-61.

133. Lushchak VI. Free radicals, reactive oxygen species, oxidative stress and its classification. Chem Biol Interact 2014;224C:164-175.

134. Cutler RG, Plummer J, Chowdhury K, et al. Oxidative stress profiling: part II. Theory, technology, and practice. Ann N Y Acad Sci 2005;1055:136-158.

135. McMichael MA. Oxidative stress, antioxidants, and assessment of oxidative stress in dogs and cats. J Am Vet Med Assoc 2007;231:714-720.

136. Bartosz G. Non-enzymatic antioxidant capacity assays: Limitations of use in biomedicine. Free Radic Res 2010;44:711-720.

137. MacKinnon KL, Molnar Z, Lowe D, et al. Measures of total free radical activity in critically ill patients. Clin Biochem 1999;32:263-268.

138. Lee Y, Jeon K, Lee JT, et al. MicroRNA maturation: stepwise processing and subcellular localization. EMBO J 2002;21:4663-4670.

139. Cai X, Hagedorn CH, Cullen BR. Human microRNAs are processed from capped, polyadenylated transcripts that can also function as mRNAs. RNA 2004;10:1957-1966.

140. Lee Y, Kim M, Han J, et al. MicroRNA genes are transcribed by RNA polymerase II. EMBO J 2004;23:4051-4060.

141. Landthaler M, Yalcin A, Tuschl T. The human DiGeorge syndrome critical region gene 8 and Its D. melanogaster homolog are required for miRNA biogenesis. Curr Biol 2004;14:2162-2167.

142. Denli AM, Tops BB, Plasterk RH, et al. Processing of primary microRNAs by the Microprocessor complex. Nature 2004;432:231-235.

143. Auyeung VC, Ulitsky I, McGeary SE, et al. Beyond secondary structure: primary-sequence determinants license pri-miRNA hairpins for processing. Cell 2013;152:844-858.

144. Zeng Y, Yi R, Cullen BR. Recognition and cleavage of primary microRNA precursors by the nuclear processing enzyme Drosha. EMBO J 2005;24:138-148.

145. Han J, Lee Y, Yeom KH, et al. Molecular basis for the recognition of primary microRNAs by the Drosha-DGCR8 complex. Cell 2006;125:887-901.

146. Bohnsack MT, Czaplinski K, Gorlich D. Exportin 5 is a RanGTP-dependent dsRNA-binding protein that mediates nuclear export of pre-miRNAs. RNA 2004;10:185-191.

147. Yi R, Qin Y, Macara IG, et al. Exportin-5 mediates the nuclear export of pre-microRNAs and short hairpin RNAs. Genes Dev 2003;17:3011-3016.

148. Zhang H, Kolb FA, Jaskiewicz L, et al. Single processing center models for human Dicer and bacterial RNase III. Cell 2004;118:57-68.

149. Elkayam E, Kuhn CD, Tocilj A, et al. The structure of human argonaute-2 in complex with miR-20a. Cell 2012;150:100-110.

150. Iwasaki S, Kobayashi M, Yoda M, et al. Hsc70/Hsp90 chaperone machinery mediates ATP-dependent RISC loading of small RNA duplexes. Mol Cell 2010;39:292-299.

151. Czech B, Zhou R, Erlich Y, et al. Hierarchical rules for Argonaute loading in Drosophila. Mol Cell 2009;36:445-456.

152. Hu HY, Yan Z, Xu Y, et al. Sequence features associated with microRNA strand selection in humans and flies. BMC Genomics 2009;10:413.

153. Ha M, Kim VN. Regulation of microRNA biogenesis. Nat Rev Mol Cell Biol 2014;15:509-524.

154. Jee D, Yang JS, Park SM, et al. Dual Strategies for Argonaute2-Mediated Biogenesis of Erythroid miRNAs Underlie Conserved Requirements for Slicing in Mammals. Mol Cell 2018;69:265-278 e266.

155. Filipowicz W, Bhattacharyya SN, Sonenberg N. Mechanisms of post-transcriptional regulation by microRNAs: are the answers in sight? Nat Rev Genet 2008;9:102-114.

156. Standart N, Weil D. P-Bodies: Cytosolic Droplets for Coordinated mRNA Storage. Trends Genet 2018;34:612-626.

157. Klingmuller U. The role of tyrosine phosphorylation in proliferation and maturation of erythroid progenitor cells--signals emanating from the erythropoietin receptor. Eur J Biochem 1997;249:637-647.

158. Ohneda K, Yamamoto M. Roles of hematopoietic transcription factors GATA-1 and GATA-2 in the development of red blood cell lineage. Acta Haematol 2002;108:237-245.

159. Munugalavadla V, Kapur R. Role of c-Kit and erythropoietin receptor in erythropoiesis. Crit Rev Oncol Hematol 2005;54:63-75.

160. Nocka K, Majumder S, Chabot B, et al. Expression of c-kit gene products in known cellular targets of W mutations in normal and W mutant mice--evidence for an impaired c-kit kinase in mutant mice. Genes Dev 1989;3:816-826.

161. Wang Q, Huang Z, Xue H, et al. MicroRNA miR-24 inhibits erythropoiesis by targeting activin type I receptor ALK4. Blood 2008;111:588-595.

162. Huang X, Gschweng E, Van Handel B, et al. Regulated expression of microRNAs-126/126* inhibits erythropoiesis from human embryonic stem cells. Blood 2011;117:2157-2165.

163. Grabher C, Payne EM, Johnston AB, et al. Zebrafish microRNA-126 determines hematopoietic cell fate through c-Myb. Leukemia 2011;25:506-514.

164. Lu J, Guo S, Ebert BL, et al. MicroRNA-mediated control of cell fate in megakaryocyte-erythrocyte progenitors. Dev Cell 2008;14:843-853.

165. Zhao H, Kalota A, Jin S, et al. The c-myb proto-oncogene and microRNA-15a comprise an active autoregulatory feedback loop in human hematopoietic cells. Blood 2009;113:505-516.

166. Siwaponanan P, Fucharoen S, Sirankapracha P, et al. Elevated levels of miR-210 correlate with anemia in beta-thalassemia/HbE patients. Int J Hematol 2016;104:338-343.

167. Melotti P, Calabretta B. Induction of hematopoietic commitment and erythromyeloid differentiation in embryonal stem cells constitutively expressing c-myb. Blood 1996;87:2221-2234.

168. Vegiopoulos A, Garcia P, Emambokus N, et al. Coordination of erythropoiesis by the transcription factor c-Myb. Blood 2006;107:4703-4710.

169. Bianchi E, Zini R, Salati S, et al. c-myb supports erythropoiesis through the transactivation of KLF1 and LMO2 expression. Blood 2010;116:e99-110.

170. Warren AJ, Colledge WH, Carlton MB, et al. The oncogenic cysteine-rich LIM domain protein rbtn2 is essential for erythroid development. Cell 1994;78:45-57.

171. Felli N, Pedini F, Romania P, et al. MicroRNA 223-dependent expression of LMO2 regulates normal erythropoiesis. Haematologica 2009;94:479-486.

172. Pase L, Layton JE, Kloosterman WP, et al. miR-451 regulates zebrafish erythroid maturation in vivo via its target gata2. Blood 2009;113:1794-1804.

173. Patrick DM, Zhang CC, Tao Y, et al. Defective erythroid differentiation in miR-451 mutant mice mediated by 14-3-3zeta. Genes Dev 2010;24:1614-1619.

174. Yu D, dos Santos CO, Zhao G, et al. miR-451 protects against erythroid oxidant stress by repressing 14-3-3zeta. Genes Dev 2010;24:1620-1633.

175. Listowski MA, Heger E, Boguslawska DM, et al. microRNAs: fine tuning of erythropoiesis. Cell Mol Biol Lett 2013;18:34-46.

176. Klotz LO, Sanchez-Ramos C, Prieto-Arroyo I, et al. Redox regulation of FoxO transcription factors. Redox Biol 2015;6:51-72.

177. Sangokoya C, Telen MJ, Chi JT. microRNA miR-144 modulates oxidative stress tolerance and associates with anemia severity in sickle cell disease. Blood 2010;116:4338-4348.

178. Bianchi E, Bulgarelli J, Ruberti S, et al. MYB controls erythroid versus megakaryocyte lineage fate decision through the miR-486-3p-mediated downregulation of MAF. Cell Death Differ 2015;22:1906-1921.

179. Shi XF, Wang H, Kong FX, et al. Exosomal miR-486 regulates hypoxia-induced erythroid differentiation of erythroleukemia cells through targeting Sirt1. Exp Cell Res 2017;351:74-81.

180. Wang LS, Li L, Li L, et al. MicroRNA-486 regulates normal erythropoiesis and enhances growth and modulates drug response in CML progenitors. Blood 2015;125:1302-1313.

181. Sankaran VG, Menne TF, Scepanovic D, et al. MicroRNA-15a and -16-1 act via MYB to elevate fetal hemoglobin expression in human trisomy 13. Proc Natl Acad Sci U S A 2011;108:1519-1524.

182. Azzouzi I, Moest H, Winkler J, et al. MicroRNA-96 directly inhibits gamma-globin expression in human erythropoiesis. PLoS One 2011;6:e22838.

183. Lee YT, de Vasconcellos JF, Byrnes C, et al. Erythroid-Specific Expression of LIN28A Is Sufficient for Robust Gamma-Globin Gene and Protein Expression in Adult Erythroblasts. PLoS One 2015;10:e0144977.

184. Bruchova-Votavova H, Yoon D, Prchal JT. miR-451 enhances erythroid differentiation in K562 cells. Leuk Lymphoma 2010;51:686-693.

185. Noh SJ, Miller SH, Lee YT, et al. Let-7 microRNAs are developmentally regulated in circulating human erythroid cells. J Transl Med 2009;7:98.

186. Andolfo I, De Falco L, Asci R, et al. Regulation of divalent metal transporter 1 (DMT1) non-IRE isoform by the microRNA Let-7d in erythroid cells. Haematologica 2010;95:1244-1252.

187. Rogers HM, Yu X, Wen J, et al. Hypoxia alters progression of the erythroid program. Exp Hematol 2008;36:17-27.

188. Ji P, Murata-Hori M, Lodish HF. Formation of mammalian erythrocytes: chromatin condensation and enucleation. Trends Cell Biol 2011;21:409-415.

189. Azzouzi I, Moest H, Wollscheid B, et al. Deep sequencing and proteomic analysis of the microRNA-induced silencing complex in human red blood cells. Exp Hematol 2015;43:382-392.

190. Mayr B, Mueller EE, Schafer C, et al. Pitfalls of analysis of circulating miRNA: role of hematocrit. Clin Chem Lab Med 2017;55:622-625.

191. Pritchard CC, Kroh E, Wood B, et al. Blood cell origin of circulating microRNAs: a cautionary note for cancer biomarker studies. Cancer Prev Res (Phila) 2012;5:492-497.

192. Kirschner MB, Edelman JJB, Kao SCH, et al. The Impact of Hemolysis on Cell-Free microRNA Biomarkers. Frontiers in Genetics 2013;4.

193. Chen SY, Wang Y, Telen MJ, et al. The genomic analysis of erythrocyte microRNA expression in sickle cell diseases. PLoS One 2008;3:e2360.

194. Sun L, Fan F, Li R, et al. Different Erythrocyte MicroRNA Profiles in Low- and High-Altitude Individuals. Front Physiol 2018;9:1099.

195. Hamilton AJ. MicroRNA in erythrocytes. Biochem Soc Trans 2010;38:229-231.

196. Wang Z, Xi J, Hao X, et al. Red blood cells release microparticles containing human argonaute 2 and miRNAs to target genes of Plasmodium falciparum. Emerg Microbes Infect 2017;6:e75.

197. Vu L, Ragupathy V, Kulkarni S, et al. Analysis of Argonaute 2-microRNA complexes in ex vivo stored red blood cells. Transfusion 2017;57:2995-3000.

198. Mantel PY, Hjelmqvist D, Walch M, et al. Infected erythrocyte-derived extracellular vesicles alter vascular function via regulatory Ago2-miRNA complexes in malaria. Nat Commun 2016;7:12727.

199. Bayraktar R, Van Roosbroeck K, Calin GA. Cell-to-cell communication: microRNAs as hormones. Mol Oncol 2017;11:1673-1686.

200. Webb CB, Falkowski L. Oxidative stress and innate immunity in feline patients with diabetes mellitus: the role of nutrition. J Feline Med Surg 2009;11:271-276.

201. Keegan RF, Webb CB. Oxidative stress and neutrophil function in cats with chronic renal failure. J Vet Intern Med 2010;24:514-519.

202. Valle E, Prola L, Vergnano D, et al. Investigation of hallmarks of carbonyl stress and formation of end products in feline chronic kidney disease as markers of uraemic toxins. J Feline Med Surg 2018:1098612X18783858.

203. Whitehouse W, Quimby J, Wan S, et al. Urinary F2 -Isoprostanes in Cats with International Renal Interest Society Stage 1-4 Chronic Kidney Disease. J Vet Intern Med 2017;31:449-456.

204. Webb C, Lehman T, McCord K, et al. Oxidative stress during acute FIV infection in cats. Vet Immunol Immunopathol 2008;122:16-24.

205. Branter E, Drescher N, Padilla M, et al. Antioxidant status in hyperthyroid cats before and after radioiodine treatment. J Vet Intern Med 2012;26:582-588.

206. Christiansen LB, Dela F, Koch J, et al. Impaired cardiac mitochondrial oxidative phosphorylation and enhanced mitochondrial oxidative stress in feline hypertrophic cardiomyopathy. Am J Physiol Heart Circ Physiol 2015;308:H1237-1247.

207. Tecles F, Caldin M, Tvarijonaviciute A, et al. Serum biomarkers of oxidative stress in cats with feline infectious peritonitis. Res Vet Sci 2015;100:12-17.

208. Dalle-Donne I, Giustarini D, Colombo R, et al. Protein carbonylation in human diseases. Trends Mol Med 2003;9:169-176.

209. Griffiths HR, Moller L, Bartosz G, et al. Biomarkers. Mol Aspects Med 2002;23:101-208.

210. Hoyumpa Vogt A, Rodan I, Brown M, et al. AAFP-AAHA: feline life stage guidelines. J Feline Med Surg 2010;12:43-54.

211. Shrivastava A, Gupta V. Methods for the determination of limit of detection and limit of quantitation of the analytical methods. Chronicles of Young Scientists 2011;2.

212. Hoenig M. The cat as a model for human obesity and diabetes. J Diabetes Sci Technol 2012;6:525-533.

213. Vulcano LA, Confalonieri O, Franci R, et al. Efficacy of free glutathione and niosomal glutathione in the treatment of acetaminophen-induced hepatotoxicity in cats. Open veterinary journal 2013;3:56-63.

214. Weber D, Davies MJ, Grune T. Determination of protein carbonyls in plasma, cell extracts, tissue homogenates, isolated proteins: Focus on sample preparation and derivatization conditions. Redox Biol 2015;5:367-380.

215. Passing H, Bablok. A new biometrical procedure for testing the equality of measurements from two different analytical methods. Application of linear regression procedures for method comparison studies in clinical chemistry, Part I. J Clin Chem Clin Biochem 1983;21:709-720.

216. Bland JM, Altman DG. Statistical methods for assessing agreement between two methods of clinical measurement. Lancet 1986;1:307-310.

217. Giavarina D. Understanding Bland Altman analysis. Biochem Med (Zagreb) 2015;25:141-151.

218. Jensen AL, Kjelgaard-Hansen M. Method comparison in the clinical laboratory. Vet Clin Pathol 2006;35:276-286.

219. Weber D, Stuetz W, Toussaint O, et al. Associations between Specific Redox Biomarkers and Age in a Large European Cohort: The MARK-AGE Project. Oxid Med Cell Longev 2017;2017:1401452.

220. Madisetty MK, Kumaraswami K, Katkam S, et al. Assessment of Oxidative Stress Markers and Carotid Artery Intima-Media Thickness in Elderly Patients Without and with Coronary Artery Disease. Indian J Clin Biochem 2016;31:278-285.

221. Munoz ME, Galan AI, Palacios E, et al. Effect of an antioxidant functional food beverage on exercise-induced oxidative stress: a long-term and large-scale clinical intervention study. Toxicology 2010;278:101-111.

222. Cockell KA, Belonje B. The carbonyl content of specific plasma proteins is decreased by dietary copper deficiency in rats. J Nutr 2002;132:2514-2518.

223. Estevez M, Luna C. Dietary protein oxidation: A silent threat to human health? Crit Rev Food Sci Nutr 2017;57:3781-3793.

224. Pastore A, Federici G, Bertini E, et al. Analysis of glutathione: implication in redox and detoxification. Clin Chim Acta 2003;333:19-39.

225. Yilmaz O, Ozkan Y, Yildirim M, et al. Effects of alpha lipoic acid, ascorbic acid-6-palmitate, and fish oil on the glutathione, malonaldehyde, and fatty acids levels in erythrocytes of streptozotocin induced diabetic male rats. J Cell Biochem 2002;86:530-539.

226. Kampa M, Nistikaki A, Tsaousis V, et al. A new automated method for the determination of the Total Antioxidant Capacity (TAC) of human plasma, based on the crocin bleaching assay. BMC Clin Pathol 2002;2:3.

227. Vilhena H, Figueiredo M, Ceron JJ, et al. Acute phase proteins and antioxidant responses in queens with pyometra. Theriogenology 2018;115:30-37.

228. Krofic Zel M, Tozon N, Nemec Svete A. Plasma and erythrocyte glutathione peroxidase activity, serum selenium concentration, and plasma total antioxidant capacity in cats with IRIS stages I-IV chronic kidney disease. J Vet Intern Med 2014;28:130-136.

229. Viviano KR, Lavergne SN, Goodman L, et al. Glutathione, cysteine, and ascorbate concentrations in clinically ill dogs and cats. J Vet Intern Med 2009;23:250-257.

230. Huntzinger E, Izaurralde E. Gene silencing by microRNAs: contributions of translational repression and mRNA decay. Nat Rev Genet 2011;12:99-110.

231. Bartel DP. MicroRNAs: target recognition and regulatory functions. Cell 2009;136:215-233.

232. Martin HC, Wani S, Steptoe AL, et al. Imperfect centered miRNA binding sites are common and can mediate repression of target mRNAs. Genome Biol 2014;15:R51.

233. Zhou SS, Jin JP, Wang JQ, et al. miRNAS in cardiovascular diseases: potential biomarkers, therapeutic targets and challenges. Acta Pharmacol Sin 2018;39:1073-1084.

234. Tian J, An X, Niu L. Role of microRNAs in cardiac development and disease. Exp Ther Med 2017;13:3-8.

235. do Amaral AE, Cisilotto J, Creczynski-Pasa TB, et al. Circulating miRNAs in nontumoral liver diseases. Pharmacol Res 2018;128:274-287.

236. Miao C, Xie Z, Chang J. Critical Roles of microRNAs in the Pathogenesis of Fatty Liver: New Advances, Challenges, and Potential Directions. Biochem Genet 2018;56:423-449.

237. Mukhadi S, Hull R, Mbita Z, et al. The Role of MicroRNAs in Kidney Disease. Noncoding RNA 2015;1:192-221.

238. Moghaddas Sani H, Hejazian M, Hosseinian Khatibi SM, et al. Long non-coding RNAs: An essential emerging field in kidney pathogenesis. Biomed Pharmacother 2018;99:755-765.

239. Ichii O, Horino T. MicroRNAs associated with the development of kidney diseases in humans and animals. J Toxicol Pathol 2018;31:23-34.

240. Yaribeygi H, Katsiki N, Behnam B, et al. MicroRNAs and type 2 diabetes mellitus: Molecular mechanisms and the effect of antidiabetic drug treatment. Metabolism 2018;87:48-55.

241. Assmann TS, Recamonde-Mendoza M, de Souza BM, et al. MicroRNAs and diabetic kidney disease: Systematic review and bioinformatic analysis. Mol Cell Endocrinol 2018;477:90-102.

242. Zhang Y, Sun X, Icli B, et al. Emerging Roles for MicroRNAs in Diabetic Microvascular Disease: Novel Targets for Therapy. Endocr Rev 2017;38:145-168.

243. Croce CM. Causes and consequences of microRNA dysregulation in cancer. Nat Rev Genet 2009;10:704-714.

244. Kluiver J, Kroesen BJ, Poppema S, et al. The role of microRNAs in normal hematopoiesis and hematopoietic malignancies. Leukemia 2006;20:1931-1936.

245. Bissels U, Bosio A, Wagner W. MicroRNAs are shaping the hematopoietic landscape. Haematologica 2012;97:160-167.

246. O'Connell RM, Zhao JL, Rao DS. MicroRNA function in myeloid biology. Blood 2011;118:2960-2969.

247. Byon JC, Papayannopoulou T. MicroRNAs: Allies or foes in erythropoiesis? J Cell Physiol 2012;227:7-13.

248. Zhang L, Sankaran VG, Lodish HF. MicroRNAs in erythroid and megakaryocytic differentiation and megakaryocyte-erythroid progenitor lineage commitment. Leukemia 2012;26:2310-2316.

249. Lawrie CH. microRNA expression in erythropoiesis and erythroid disorders. Br J Haematol 2010;150:144-151.

250. Bousquet M, Quelen C, Rosati R, et al. Myeloid cell differentiation arrest by miR-125b-1 in myelodysplastic syndrome and acute myeloid leukemia with the t(2;11)(p21;q23) translocation. J Exp Med 2008;205:2499-2506.

251. Guglielmelli P, Tozzi L, Bogani C, et al. Overexpression of microRNA-16-2 contributes to the abnormal erythropoiesis in polycythemia vera. Blood 2011;117:6923-6927.

252. Bruchova H, Yoon D, Agarwal AM, et al. Regulated expression of microRNAs in normal and polycythemia vera erythropoiesis. Exp Hematol 2007;35:1657-1667.

253. Shaham L, Vendramini E, Ge Y, et al. MicroRNA-486-5p is an erythroid oncomiR of the myeloid leukemias of Down syndrome. Blood 2015;125:1292-1301.

254. Rasmussen KD, Simmini S, Abreu-Goodger C, et al. The miR-144/451 locus is required for erythroid homeostasis. The Journal of Experimental Medicine 2010;207:1351-1358.

255. Doss JF, Corcoran DL, Jima DD, et al. A comprehensive joint analysis of the long and short RNA transcriptomes of human erythrocytes. BMC Genomics 2015;16:952.

256. Freeman LM, Rush JE, Stern JA, et al. Feline Hypertrophic Cardiomyopathy: A Spontaneous Large Animal Model of Human HCM. Cardiol Res 2017;8:139-142.

257. Chambers JK, Tokuda T, Uchida K, et al. The domestic cat as a natural animal model of Alzheimer's disease. Acta Neuropathol Commun 2015;3:78.

258. O'Brien SJ, Menotti-Raymond M, Murphy WJ, et al. The Feline Genome Project. Annu Rev Genet 2002;36:657-686.

259. Yamamoto J, Sanou M, Abbott J, et al. Feline Immunodeficiency Virus Model for Designing HIV/AIDS Vaccines. Current HIV Research 2010;8:14-25.

260. Westropp JL, Buffington CA. In vivo models of interstitial cystitis. J Urol 2002;167:694-702.

261. Rand JS. Pathogenesis of feline diabetes. Vet Clin North Am Small Anim Pract 2013;43:221-231.

262. Tamazian G, Simonov S, Dobrynin P, et al. Annotated features of domestic cat - Felis catus genome. GigaScience 2014;3:13.

263. Lagana A, Dirksen WP, Supsavhad W, et al. Discovery and characterization of the feline miRNAome. Sci Rep 2017;7:9263.

264. Cong W, Zhang XX, He JJ, et al. Global miRNA expression profiling of domestic cat livers following acute Toxoplasma gondii infection. Oncotarget 2017;8:25599-25611.

265. Ichii O, Otsuka S, Ohta H, et al. MicroRNA expression profiling of cat and dog kidneys. Res Vet Sci 2014;96:299-303.

266. Bricker NK, Raskin RE, Densmore CL. Cytochemical and immunocytochemical characterization of blood cells and immunohistochemical analysis of spleen cells from 2 species of frog, Rana (Aquarana) catesbeiana and Xenopus laevis. Vet Clin Pathol 2012;41:353-361.

267. Martin M. Cutadapt removes adapter sequences from high-thoughput sequencing reads. EMBnetjournal 2011;17:10-12.

268. Friedlander MR, Mackowiak SD, Li N, et al. miRDeep2 accurately identifies known and hundreds of novel microRNA genes in seven animal clades. Nucleic Acids Res 2012;40:37-52.

269. Love MI, Huber W, Anders S. Moderated estimation of fold change and dispersion for RNA-seq data with DESeq2. Genome Biol 2014;15:550.

270. Livak KJ, Schmittgen TD. Analysis of relative gene expression data using real-time quantitative PCR and the 2(-Delta Delta C(T)) Method. Methods 2001;25:402-408.

271. Li Y, Vecchiarelli-Federico LM, Li YJ, et al. The miR-17-92 cluster expands multipotent hematopoietic progenitors whereas imbalanced expression of its individual oncogenic miRNAs promotes leukemia in mice. Blood 2012;119:4486-4498.

272. Sarakul O, Vattanaviboon P, Tanaka Y, et al. Enhanced erythroid cell differentiation in hypoxic condition is in part contributed by miR-210. Blood Cells Mol Dis 2013;51:98-103.

273. Grebien F, Kerenyi MA, Kovacic B, et al. Stat5 activation enables erythropoiesis in the absence of EpoR and Jak2. Blood 2008;111:4511-4522.

274. Kerenyi MA, Grebien F, Gehart H, et al. Stat5 regulates cellular iron uptake of erythroid cells via IRP-2 and TfR-1. Blood 2008;112:3878-3888.

275. Tissot J-D, Canellini G, Rubin O, et al. Blood microvesicles: From proteomics to physiology. Translational Proteomics 2013;1:38-52.

276. D'Alessandro A, Kriebardis AG, Rinalducci S, et al. An update on red blood cell storage lesions, as gleaned through biochemistry and omics technologies. Transfusion 2015;55:205-219.

277. Baran-Gale J, Kurtz CL, Erdos MR, et al. Addressing Bias in Small RNA Library Preparation for Sequencing: A New Protocol Recovers MicroRNAs that Evade Capture by Current Methods. Frontiers in genetics 2015;6:352-352.

278. Castillo C, Pereira V, Abuelo A, et al. Preliminary results in the redox balance in healthy cats: influence of age and gender. J Feline Med Surg 2013;15:328-332.

279. Christopher MM, White JG, Eaton JW. Erythrocyte pathology and mechanisms of Heinz body-mediated hemolysis in cats. Vet Pathol 1990;27:299-310.

280. Wang W, Hang C, Zhang Y, et al. Dietary miR-451 protects erythroid cells from oxidative stress via increasing the activity of Foxo3 pathway. Oncotarget 2017;8:107109-107124.